sciendo

Journal of Environmental Geography 14 (3–4), 1–13.

DOI: 10.2478/jengeo-2021-0007
ISSN 2060-467X

SENSITIVITY ANALYSIS FOR EFFECT OF CHANGES IN INPUT DATA ON HYDROLOGICAL PARAMETERS AND WATER BALANCE COMPONENTS IN THE CATCHMENT AREA OF HUNGARIAN LOWLAND

Hop Quang Tran[1*,2]

[1]Department of Geoinformatics, Physical and Environmental Geography, University of Szeged, Egyetem u. 2-6, 6722 Szeged, Hungary
[2]Hanoi University of Natural Resources and Environment, Faculty of Water Resources, Hanoi, Vietnam
*Corresponding author, email: hoptran@geo.u-szeged.hu, Tel.: +36 30 179 9296

Research article, received 1 April 2021, accepted 7 September 2021

Abstract

Extreme weather and climate changes are emerging more frequently in Central Europe, Hungary, and in the near future the increase in prolonged droughts, high-intensity precipitation events and the temporal variations of precipitation are expected, which may increase the magnitude of local water damages (OVF, 2016). As a result of climate change, these extreme weather events will be more frequent, however it is difficult to predict them, as until now insufficient amount of observations are available on smaller watercourses and on refined territorial water balances. For the future assessment of the environmental and economic impacts of climate change, it is essential to explore the integrated relationship of evapotranspiration, runoff, infiltration, surface and subsurface waters, and other hydrological processes, which can fundamentally describe regionally the water management conditions.

In this research, an earlier study (DHI Hungary 2019) on the catchment area of the main canal of the Dong-ér Brook is pursued to continue the development of the MIKE SHE model in a more complex manner. Within the frame of the present study, the relationship between the individual hydrological parameters, the water balance components and extreme precipitation events (drought, heavy rainfall events) for the entire drainage basin have been examined, besides, the expected effects of the predicted temperature rise on the water balance is evaluated. Using data from 2018 as reference, the sensitivity of the changes in daily precipitation and daily mean temperature has been assessed to estimate the effects of the future climate change on hydrological parameters and water balance components.

Keywords: Dong-ér Brook, MIKE SHE, sensitivity analysis, water balance

INTRODUCTION

Water management is playing an increasingly important role in mitigating the effects of the extreme climate changes. Based on Lower Tisza District Water Directorate (ATIVIZIG) data in Hungary nearly 1100 settlements over about 42000 km^2 area occasionally struggle with severe inland water problems (ATIVIZIG, 2016). General Directorate of Water management (OVF) emphasizes that as result of climate change, extreme weather events are becoming more frequent in Hungary, and soon an increase in the regularity of high-intensity precipitation events should be expected, which may increase the magnitude of local water damages (OVF, 2016).

Extreme climatic events are also reflected in the phenomenon of drought, with a longer degree, intensity and duration. According to the survey results in South Hungary by Ladányi et al. (2014) water shortage was more damaging than inland water. Consequently, the changing climatic effects have a direct impact on agriculture, causing greater damages mainly due to the droughts and directly affect the sustainable development of agriculture and food security (Singh, 2014, Ladányi, 2010). Due to climate change, precipitation has decreased by at least 12% in recent decades in Hungary, with perhaps the most significant consequences on the Danube–Tisza Interfluve (Ladányi, 2009), where the study area is located. According to the experiences, harmful water scarcity occurs in an average of 4 years per decade in Hungary. At the same time varying amounts of excess water occurs in most years, while it is not even uncommon for the two extremes to occur in the same year, such as between the Danube and the Tisza in 2000 (Rakonczai et al., 2014). An integrated approach is necessary to evaluate the complex interrelationships of hydrological processes and changes in water balance from many aspects, thus provide effective solutions for the complex modelling challenges in the presence of both inland excess water and drought. The topic is well introduced by the Tisza River Basin Management Plan (KÖTIVIZIG, 2015).

As a result of the developments in the information technology, the application of the geographical information system (GIS) and various mathematical- and physical-based hydrological modelling software has also become feasible for related research. Among the many models, the MIKE SHE model emerges as a tool capable of implementing integrated water resources management. The model tends to effectively simulate the interaction between surface water and groundwater (Graham and

Butts, 2005). The research group of Lu et al. (2006) also had positive comments about the effectiveness of the model in simulating temporal flow dynamics in the whole basin. MIKE SHE is widely used in studies such as calculating the effect of land use changes on components of water balance in the unsaturated zone (UZ) and saturated zone (SZ) (Asadusjjaman and Farnaz, 2014). Some studies apply MIKE SHE and GIS to simulate hydrological processes for several basins (Paparrizos and Maris, 2015; Právetz et al., 2015) and assessing the effects of land change and climate change on groundwater and ecosystem by Keilholz et al. (2015). Among the hydrological models that have been verified on the catchment area of the Fehértó-majsa Canal, which is located next to the Dong-er catchment to the south by Benyhe et al. (2015) include BUDYKO, HEC-RAS and MIKE SHE and concluded that the MIKE SHE model was more efficient than the other two. The process of modelling inland excess water with MIKE SHE and using satellite imagery for validation by van Leeuwen et al. (2016) is another example showing the effectiveness of the MIKE SHE model to predict the extent, location and duration of inland excess water. The research team of Nagy et al. (2019) built a MIKE SHE model to simulate the accumulation processes of excess water, water storage, and excess water maps for Dong-ér catchment and have very remarkable results. However, the above studies also have shown a disadvantage of this model is that it requires many good quality input data. In Dong-ér catchment, the data is not continuously measured, there is no data for water level and discharge in the open channels, and many parameters are not validated (e.g. LAI, root depth. hydraulic conductivity). Nagy et al. (2019) has calibrated the model focused on the groundwater levels for 2015 and 2018-years' springtime. The comparison between the modelled and measured groundwater level is 45 cm, which is very relevant considering the lack of input parameters and the uncertainties. This result shows that the integrated MIKE SHE model built for the Dong-ér catchment has been relatively calibrated and can be inherited to calculate and analyse many other aspects of hydrology in the relationship between surface water and groundwater.

In such areas where inland excess water and drought are both affects the landscape heavily, understanding the state of the water balance becomes even more imperative. Importance of management, planning and optimal consumption of water resources more effectively and sustainably is even more crucial (EU Water Framework Directive, 2000; OVF, 2009). Sipos and Právecz (2014) stated that only the local water balance models can be considered reliable in order to make efficient and economically sustainable water use options in the dry season and water retention in the rainy season.

One of the advantages of MIKE SHE is that it includes a comprehensive, integrated water balance tool for the complete local and entire catchment water balance for any time interval. Water balance output can include area flows, storage changes and water balance changes (DHI, 2017). The total water balance change value is calculated for the entire model catchment. In addition, there are water balance changes for each hydrologic component. However, within the scope of this study, only the variation of total water balance change under different climatic conditions are considered, analyzed and evaluated. The value of these parameters plays an important role as the foundation for assessing the water balance in the Dong-ér catchment. It is useful for integrating, mapping and plotting water flow processes between water balance components (Graham and Butts, 2005). There are many factors that affect directly and indirectly on the water balance of a basin, the first of which is precipitation and temperature. They are the two main forces that operate the hydrologic cycle and have a major impact on water balance. The question is how changes in inputs due to climate change affect the outputs of hydrological parameters and water balance components. According to the studies of Hamby (1994) and Lenhart et al. (2002) the variation in the input data causes effects on the model results and it is necessary to consider the sensitivity of the input data and apply the sensitivity analysis method to determine which inputs have the greatest influence on the outputs. Ibarra et al. (2016) confirmed that setting up sensitivity analysis is necessary to improve the accuracy and optimize the calibration process. Besides, the sensitivity analysis enables the estimation of the parameters and explains the response of the model for the variation of the input data.

The objective of the study is to simulate different climate conditions and use sensitivity analysis to evaluate the influence of input parameters on hydrological parameters and water balance components. However, to perform these integration tasks, MIKE SHE needs a lot of hydrological and meteorological data input (van Leeuwen et al., 2016) and especially difficult for areas with few data such as Dong-ér catchment. Deterministic models have uncertainties, these include reasons such as measurement errors, variation of parameters on the sub-grid scale and incorrect initial, boundary conditions (Graham and Butts, 2005). Bahremnad and De Smedt (2007) also highlighted sensitivity analysis as a valuable tool to identify influential model parameters and thereby make the model structure more stable. There are many methods of sensitivity analysis that have been used in the international literature, most of them are very complex and the simplest approach to conceptualize is the one-at-a-time method where sensitivity measures are determined by varying each parameter independently while keeping all other parameters do not change. The disadvantage that it can only do local sensitivity analysis at a certain selected point and not for the entire parameter distribution (Hamby, 1994). However, with the flexible simulation framework on spatial and temporal scale of the MIKE SHE model, this disadvantage can be improved and gives us an integrated view and more comprehensive. To understand the hydrological phenomena that will occur in the future, this study inherits the MIKE SHE data tree built by Nagy et al. (2019). However, to apply the one-at-a-time method, the variable parameters and the water calculation module has been developed and used by author to simulate and evaluate with an integrated approach which manifestation of climate change has the greater impact to the outputs of the hydrological parameters and water balance components. To achieve

these objectives, it is necessary to 1) review the suitability, determining the advantages and disadvantages of the MIKE SHE model for Dong-ér catchment, 2) simulate hydrological and complex water balance processes under different input variable conditions, 3) simulation results are compared to see which factors are most affected and most sensitive to variations in input data. Based on this result, evaluate the effects of climate change on hydrological parameters and water balance components in the future.

STUDY AREA

The inland water system of the Dong-ér brook is in the middle part of the sand ridge region of the Danube-Tisza Interfluve, about 50 km from the southern border of Hungary (Fig. 1). The total area of the catchment is 2127 km^2, and it is characterized by a small relative relief (<2m/km^2).

In the initial section of the Dong-ér Brook the surface water transport is minimal, the occasionally drying riverbed is revealed only by the vegetation of wetlands. Therefore, water resources of this area are not suitable for utilization, rather the use of groundwater resources comes to the fore (Kozák, 2020). The system of small brooks collects and carries excess water into the main Dong-ér Brook and then flows into the Tisza River near the settlement of Baks. The gravitational flow terminates only in the case of the formation of an extreme Tisza flood wave. The discharge of the Dong-ér Brook is 2-3 m^3/s during the normal period, meanwhile in times of spring inland excess water it can excess 20-30 m^3/s. However, in extremely dry summer days, the brooks dry out completely (K&K Mérnöki Iroda Kft, 2013). Prevailing wind direction NW, average wind speed about 2-3 m/s. The surface-forming activity of the wind shaped the topography. The topography of the area basically defines the water networks. The flow direction of the Dong-ér is SW-NE, while the flow direction of the tributaries is NW-SE, typically follows natural deflationary depressions. In rainy years, groundwater can appear in the deflation hollows, forming temporarily inundated areas (Sipos and Právecz, 2014).

Based on studies conducted by the Hungarian Meteorological Service (2018) with two regional climate models and two scenarios, the average temperature in Hungary may increase by 3-4˚C by the end of the century and the 2˚C threshold is expected to reach earlier. Dong-ér catchment is one of the warmest and driest areas. Therefore, the drought hazard is high in the area (Sipos and Právecz, 2014). The area under investigation is dry continental temperate climate. According to the data from Hungarian Meteorological Service (OMSZ) and from 25 available meteorological stations between 2010 and 2018, the average annual rainfall in the area over the period is 611 mm, but in extreme cases it can reach as high values as 842 mm (in 2014) or as low as 203 mm (2000). During the period between 2000 and 2018, the lowest monthly mean temperature was -5.2°C measured in February 2012 and January 2017, the highest was +24.5°C measured in August 2018. The average thickness of the snow cover in winter is about 18-22 cm. The most frequently mentioned feature of climate change is rising temperatures. According to the climate models adopted by the Intergovernmental Panel on Climate Change (IPCC, 2018), the average temperature of the Earth could reach an increase of 1.5˚C in 2030-2052.

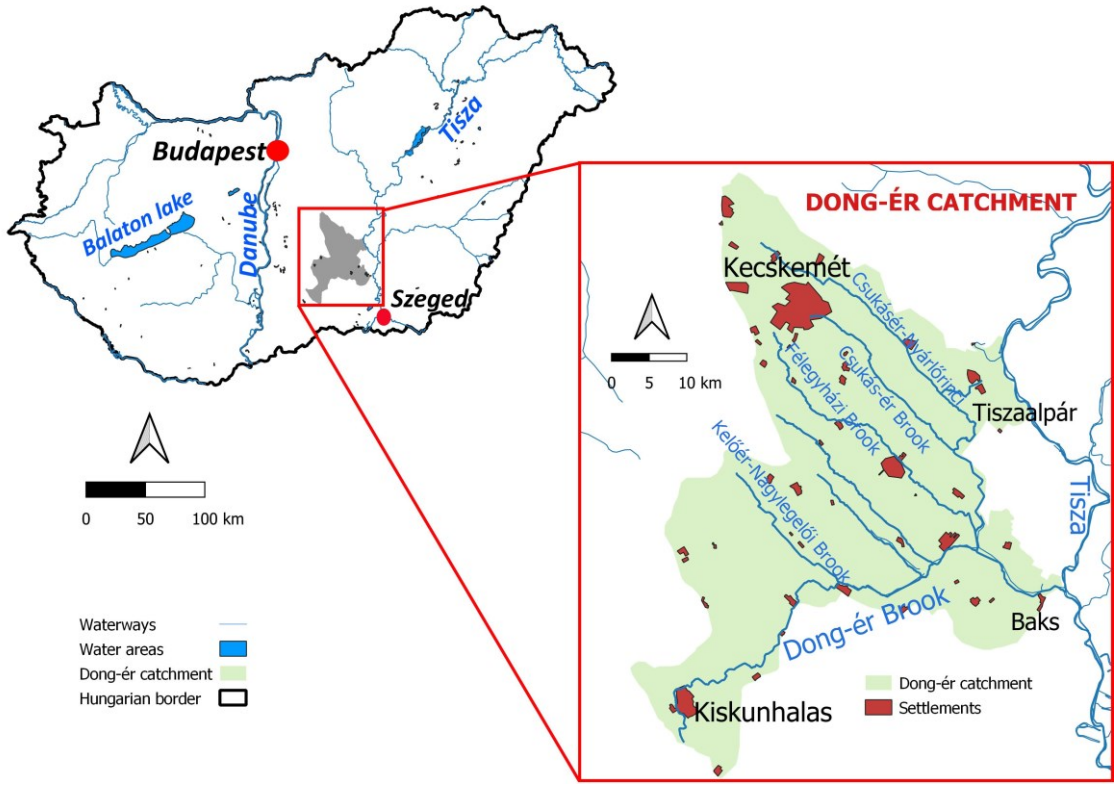

Fig. 1 The study area

Non-irrigated arable land dominates the area by ~41%, followed by pastures ~13%, by broad-leaved forest ~10% of the total study site, the rest are various small land uses, like transitional woodland-shrub, complex cultivation patterns, discontinuous urban fabric. Based on the available agrotopographic map, the soils in the area are extremely heterogeneous. The most typical soil types are blown sand, humid sand, sandy soils, chernozem and saline soils. These soils have the potential to infiltrate. Since the late 1970s, the decreasing trend of the precipitation induced significant decrease of the groundwater level in the Danube–Tisza Interfluve, which exceeds 2 meters on average (Fehér, 2019). Afterwards, in the periods of persistent precipitation, water shortages in the lower parts of the sand ridge have been restored; in fact, sometimes the groundwater level has risen to harmful level, causing surface overflows (Szatmári and van Leeuwen, 2013).

DATA AND METHODS

Input data used in the model

Meteorological data

The most important meteorological data in a hydrological cycle are precipitation, temperature and evapotranspiration. For the observed precipitation in study area, the daily data of 25 meteorological stations was available in the period 2010-2018 from ATIVIZIG. According to this, the average monthly precipitation of the study area varies around 46 mm. According to the OMSZ (2018a) database, in the drought year of 2000, about half of the average monthly precipitation (29 mm) was measurable in Szeged, but some extreme years, such as the 2014 rainy year, also occurred in 89 mm in the study area. Snow storage is a physical state of precipitation and differs from the rainfall form in the time of accumulation, so participate more slowly in the water cycle. Temperature is a factor that can accelerate water accumulation through melting. Temperature also affects directly (e.g., pond water evaporation, soil evaporation) and indirectly (transpiration by vegetation) on evapotranspiration. As a result of temperature fluctuations, several important climatic elements change, and these greatly affect the water balance of the area. Temperature data for 2014 and 2018 are taken from the European Climate Assessment and Dataset (ECAD) database for the period 2010-2018 by Nagy et al. (2019). Daily average temperature data for the year 2000 are obtained from the OMSZ (2018a) database by author.
Evapotranspiration is the most difficult parameter to determine and there are no data in the study area. To calculate the amount of evapotranspiration the Food and Agriculture Organization of the United Nations (FAO) recommends a combination of the FAO-56 Penman-Monteith equations (Allen et al., 1998). Due to the lack of input data, the use of the FAO-56 Penman-Monteith equation is limited. The potential evapotranspiration (ETP) can still be estimated more easily and simply by the function for different temperature (T) values, to which the following exponential function describes the relationship well (Fiala et al., 2018):

$$ET_P = ET_{ref} = e^{0.07T} \quad (1)$$

Land cover data

The current modelling framework identified 23 different land use classes. Each class has different characteristics of canopy interception, transpiration, soil evaporation, flow formation, and different water retention ability by roots. The research is based on the Corine Land Cover (EEA, 2018), the de facto standard for land use and land cover monitoring at the pan-European level (Feranec, 2016; Aune-Lundberg and Geir-Harald, 2020). The Leaf Area Index (LAI) is determined by the combination of MODIS images (Myneni et al., 2015) and root depth values are referenced from the results of scientific studies for CORINE categories (Nagy et al., 2019).

Soil data

Exact determination of subsurface conditions (water content of unsaturated and saturated soils) is crucial in our model building scenario, since both Rakonczai et al. (2011) and Farsang (2014) indicated significant interrelationship between the soil and the water balance of the site. The current model is based on the 250 m resolution 3D Soil Hydraulic Database of Europe (Tóth et al., 2017). Since there is no reliable data source available deeper than 2 meters for the study site (nor even Hungary), the current research is based on the 2 m depth soil layer of the database. The author has updated the following parameters of the original model: saturated water content, saturated hydraulic conductivity, and moisture retention curve. The parameters of deeper geological layers were spatially estimated based on 13 borehole records provided by ATIVZIG.

Topography

Since topographical conditions determine overland and underground flows significantly, an accurate digital elevation model is crucial for a successful modelling scenario. The present study is based on a 10 x 10 m resolution DEM. To run the MIKE SHE model, it is necessary to convert the DEM data into a spatial distribution grid point file (.dfs2). Point file was created using ArcGIS and could be converted to a .dfs2 file using the MIKE Zero Toolbox (DHI, 2017). The resulted spatial distribution grid can be used as input data.

Water flows

Surface channels provide unobstructed gravitational flow paths for the water into its recipient reservoir, thus proper knowledge of the geometry of the channels and surface depressions can significantly improve the model reliability. In the current framework, the water network geometry is provided by ATIVIZIG, and it can be classified into two main groups. The first class includes

brooks from the previous epoch, whereby paths are provided, cross-sectional data are measured, and data is set up as 3D GIS points. Other types of brooks are managed by ATIVIZIG. In this case the pathlines are provided as a polyline shapefile, the cross-section data is defined by longitudinal profile and different cross-section data. These data are set up in the specialized MIKE Hydro hydraulic module. The module enables complex dynamic river network modelling and can be linked to MIKE SHE to comprehensively simulate hydrologic modelling of the catchment under investigation.

Groundwater data

Groundwater has more stable water level and is less affected by external factors than the unsaturated zone or the channels. The groundwater series provided by ATIVIZIG includes 33 groundwater measurement stations with specific coordinates from 2010 to 2018. The groundwater level changes according to topography and all flows into the Tisza River and seasonal variation greatly affects groundwater change. Based on the measured data in the period 2010-2018, the highest groundwater level in the study area usually occurs in April-May, the lowest in October-December. However, there are different rainfall and temperature conditions at some measurement points, so the difference is up to 2-3 months of the year.

Computational layers

To simulate the flow processes occurring in the saturated zone it is necessary to define computational layers. In the MIKE SHE model the numerical vertical discretization is defined by explicitly defining the lower level of each calculation layer. The spatial distribution of lower level is uniform, the value of aquifer lower level is -75 m. To make corrections to the elevations layers, the minimum layer thickness is applied with a value of 2 m, this is to prevent zero-thickness or very thin layers. To define outer boundary conditions this model applies a fixed head type, based on a spatially distributed and time-varying dfs2 file, extracted from the specified groundwater table. Specified groundwater table is established based on daily groundwater elevation data from 2010 to 2018. Specified groundwater table is divided into 200 m x 200 m grid cells. MIKE SHE then interpolates in both time and space from the .dfs2 file to the local head boundary at each local time step (DHI, 2017).

Calibration data

The MIKE SHE model built for Dong-ér catchment lacks a lot of data such as brook water-level and discharges to be fully calibrated and validated. The current model has only been calibrated focused on groundwater data for 2018-years' springtime by Nagy et al. (2019). Comparing simulation results and measured data, the variance is about 45 cm, which is very suitable considering the lack of input parameters and uncertainties (such as topographic maps, vegetation features and soil characteristics). There are many parameters that need calibration to make the model more complete, for example a saturated hydraulic conductivity for unsaturated flow calibration and hydraulic conductivity, specific yield, specific storage for groundwater flow calibration. However, due to the lack of data and not the objective of the study, it was not mentioned.

MIKE SHE output results

The output results obtained from the MIKE SHE simulation depend on the selected modelling sequence. According to the MIKE SHE User guide (2017), the model saves the results in three groups of files, these are 1) ASCII files, which is a catalogue of all output files (.sheres) of the simulation; 2) a binary output file containing all the static information of the simulation (.frf); 3) the simpler, timeseries-generated dfs0, 2-dimensionally defined dfs2, and 3-dimensional dfs3 files (.dfs).

In this study only the results in .sheres format and the time series results (dfs0, dfs2, and dfs3) for the water balance are examined (Table 2). The water balance simulation can be performed with a separate module, Water balance calculation, which delivers results of a post-processing of the data stored in the .sheres file.

The common understanding which states that all water flows into system are positive and all outflows or loss of water is negative. The storages of water system are positive in case of storage increase. Positive water balance change means that the change in storage plus the total outflows is less than the total inflows (ΔStorage + Outflow < Inflow).

Among several hydrological parameters and water balance components, the following were examined in Table 1-2.

Modelling

In the first stage of the sensitivity analysis, the input data can be divided into two groups, according to their temporal variability. The first type is constant in long timespan, including the topography, water networks (rivers and lakes), soil properties, geological features. This phenomenon has negligible changes or remains unchanged in the long run without human activities. The other group consists of data that change rapidly, whether minute by minute, hour/day, or seasonally. Such features are daily precipitation, daily mean temperature, reference evapotranspiration, and land cover (including vegetation).

Thereafter the one at a time type sensitivity analysis was elaborated by five MIKE SHE simulation scenarios, including base simulation (BS), SIM1, SIM2, SIM3 and SIM4 simulations (Fig. 2). Base simulation (BS) is used to simulate integrated hydrological processes and water balance in Dong-ér catchment in 2018. The following factors supported the reason 2018 was chosen to run the base model: 1) The model has been calibrated by Nagy et al. (2019) according to the groundwater level measured in 2018. 2) The land cover data of the year 2018 used from Corine Land Cover. 3) The latest van Genuchten parameters of the moisture retention and hydraulic conductivity have just been updated by the author from the 3D Soil Hydraulic Database in the previous year (Tóth et al., 2017). 4) The precipitation measured in 2018

Table 1 Output hydrological parameters used for research (Source: DHI, 2017)

Parameters	Units	Notes
Actual evapotranspiration (ActualET)	mm/d	Actual evapotranspiration is depending on water availability at root depth and Leaf area index (LAI)
Actual transpiration (T_{act})	mm/d	Evaporation of water is mostly through the pores of the leaves.
Actual soil evaporation	mm/d	Actual soil evaporation is depending on factors such as soil characteristics, land use, vegetation.
Depth of overland water	m	It is the amount of water at the surface.
Overland flow in x- and y-direction	m^3/s	Flow on the horizontal and vertical axis
Infiltration to unsaturated zone (UZ)	mm/d	Just like overland flow in y-direction, the vertical downward flows will be positive.
Unsaturated zone (UZ) deficit	mm	Unsaturated zone deficit is the amount of air in the unsaturated zone. Thus, a decreasing deficit means that the more air has been pushed out by the water, the soil gradually becomes wetter.
Average water content in the root zone	-	It is depending on precipitation, soil features, groundwater flow and vegetation features.
Water content in unsaturated zone (UZ)	-	Contrast to unsaturated zone (UZ) deficit
Groundwater flow in x- and y-direction	m^3/s	Groundwater flow is in the horizontal and vertical axis.

Table 2 Output water balance components used for research (Source: DHI, 2017)

Name of components and in parentheses are abbreviations		Units
Precipitation		mm
Evapotranspiration	Evapotranspiration (Evapotrans), Infiltration includes evapotranspiration (Infilt.incl.ET). Exfiltration includes evapotranspiration (Exfilt.incl.ET)	mm
Flows	Overland boundary outflow (OL Bou.Outflow). Overland boundary inflow (OL Bou.Inflow). Overland flow to river (OL->River/MOUSE). Subsurface boundary inflow (SubSurf.Bou.Inflow). Subsurface boundary outflow (SubSurf.Bou.Outflow). Baseflow to river. Baseflow from river	mm
Storages	Canopy storage change (CanopyStor.Change). Snow storage change (SnowStor.Change). Overland storage change (OL Stor.Change). Subsurface storage change (SubSurfStor.Change) includes both unsaturated (UZ Stor.change)- and saturated zone storage changes (SZ Stor.change),	mm
Water balance change		mm

is much closer to the multi-annual average compared to the other years under investigation. Thereafter the base simulation running for 2018 has been considered suitable to perform one-at-a-time sensitivity analysis and the outcomes were used as reference values to compare with the other simulation scenarios.

The precipitation sensitivity analysis focused on the years with extreme precipitation (drought, rainy) and the

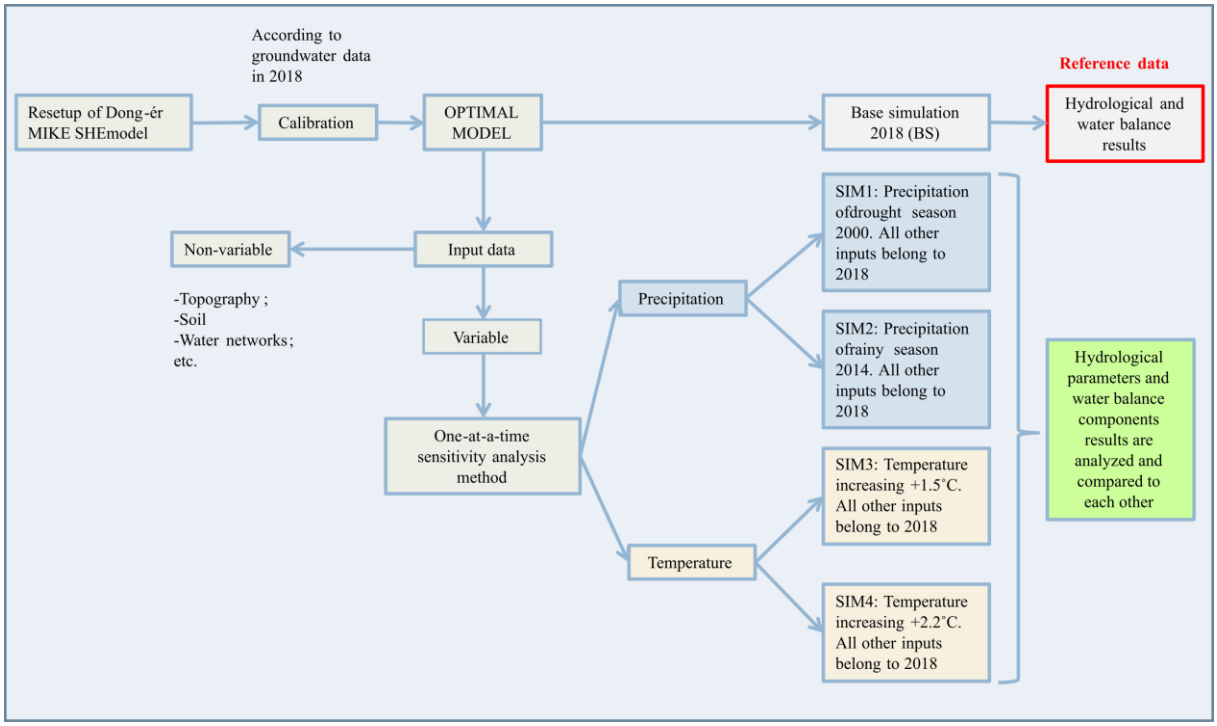

Fig. 2 Research workflow

year with average precipitation. In this part of the research, the precipitation data of the (BS) model was replaced by the drought season 2000 (SIM1), rainy season 2014 (SIM2), while keeping the other parameters of 2018 fixed. Thereafter the differences of the three models have been compared to each other.

The temperature sensitivity analysis focused on the effect of temperature increases on changes in results of hydrological parameters and water balance components. Based on the results of the IPCC (2018) and OMSZ (2018b) climate models, the temperature data of 2018 (BS) reference model was increased by +1.5˚C (SIM3) and +2.2˚C (SIM4), while the other parameters left unchanged. Thereafter the differences of the three models have been evaluated.

RESULTS

Due to time and hardware constraints, hydrological results were only extracted from cells near the settlement of Tiszaalpár, rather than from whole catchments.

The area near the settlement of Tiszaalpár has a low elevation, so it is more susceptible to groundwater level rises by extreme precipitation events or flood wave of Tisza. However, the simulation results in Figure 3 show the opposite, specifically on September 13, 2014, with 49.8 mm of precipitation, but the depth of overland water component gave a low value from 0.74 mm-0.77 mm, so there is no significant change for heavy rain events. There is a direct correlation between the precipitation events and infiltration because the top surface soil has a high permeability, most of the precipitation when reaching the surface is mostly absorbed into the soil.

The amount of infiltration into the soil is 20.6 mm, the unsaturated zone deficit is 14.8 mm. The water leaving the system through evapotranspiration, whose rate is from 1.1 mm/day to 4.1 mm/day on the 13 September of analysis years. However, the water content (~16.5 mm) infiltrates to unsaturated zone does not appear yet in the unsaturated zone (water content in unsaturated zone is 0.5 mm) and in the root zone (0.4 mm). This can be explained as a quantity of infiltrated water which is clinging to the dry soil particles, thus temporarily stored in the upper soil layer and infiltrates very slowly to the unsaturated zone because the leakage coefficient of sand is very small, about 10^{-5} m/s. Thus, it can be affirmed that even in years with high precipitation conditions like 2014, the rainfall shows no significant correlation with surface water and groundwater. Among the hydrological parameters related to the precipitation events, the unsaturated zone deficit and infiltration are found to be the most sensitive.

To explore the relationship and correlation between water balance components for the entire catchment can be performed with a *Water balance calculation* module of the MIKE modelling environment (Figs. 4-5).

Based on the values of the accumulated water balance components in the whole test years, it can be concluded that the components of subsurface boundary inflow, overland boundary outflow, evapotranspiration and precipitation have a high impact on the entire catchment water balance. The precipitation will supplement the overland storage change (12 mm and 19 mm) in some deflationary depressions and low permeable topsoil, the overland flow (-5 mm and -10 mm) direct addition to brooks (Fig. 4). However, these amounts are not much compared to the amount of precipitation and of overland boundary outflow.

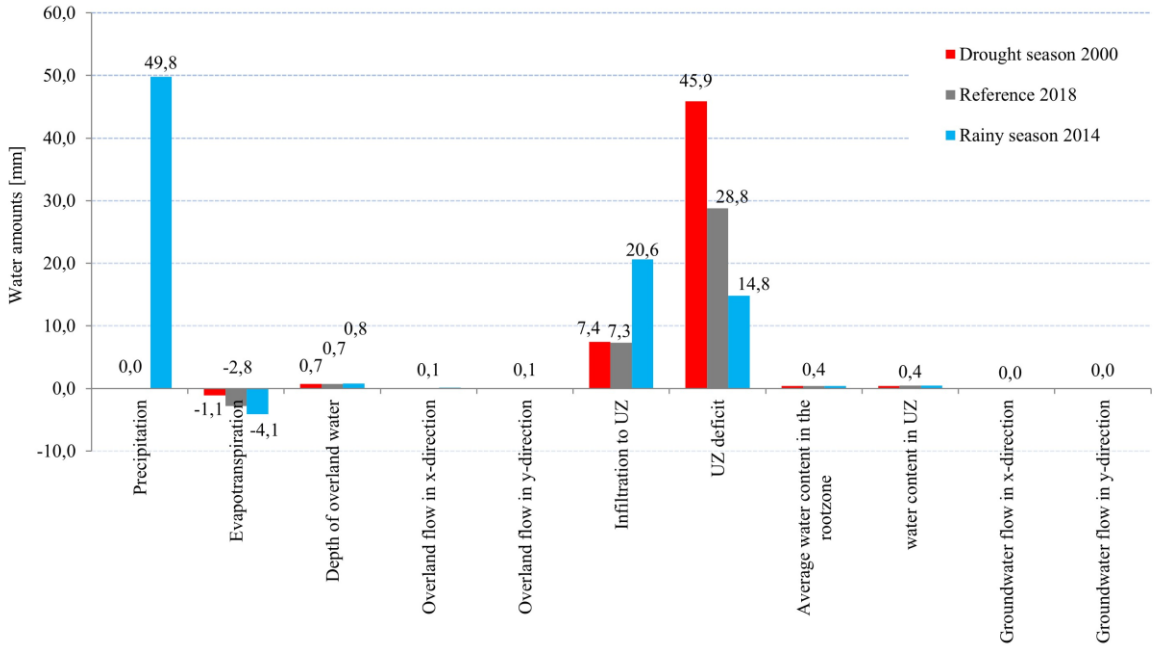

Fig. 3 Temporal changes simulated up to 13 September as a result of precipitation events in the reference year 2018, drought events of 2000 and the rainy year of 2014

According to the results shown in Figure 5 can see that as precipitation increases, the infiltration also increases from 32 mm in 2000 to 138 mm in 2014 (increased rate is 331%). In all three years, the amount of water lost through evapotranspiration was more than precipitation, with the rate of 154% more in 2000, 7.7% more in 2014 and 35% more in 2018. The year 2000 has the largest difference rate, this further aggravates the dehydration of the topsoil. Thus, it can be confirmed that evapotranspiration includes direct evaporation and indirect transpiration through vegetation which has caused a large amount of water loss from surface- and groundwater. The change in unsaturated water storage (from 2000 to 2014 increased by 166 mm) is much larger than that in saturated (increased by 35 mm), which again shows that most of the water infiltration into the soil is stored in the topsoil layer. Overland boundary outflow values were higher for precipitation and evapotranspiration in all three study years. Based on these results, the above statement is confirmed that the source of overland flow in the Dong-ér catchment is not primarily the precipitation or the overland boundary inflow. The question is where does overland boundary outflow (surface water of brooks) get its water? The watercourse nature of Dong-ér can rather be observed close to the inner area of Kiskunhalas. From this point, the water supply of the brook is gained from three sources. First, the subsurface boundary inflow source from high elevation

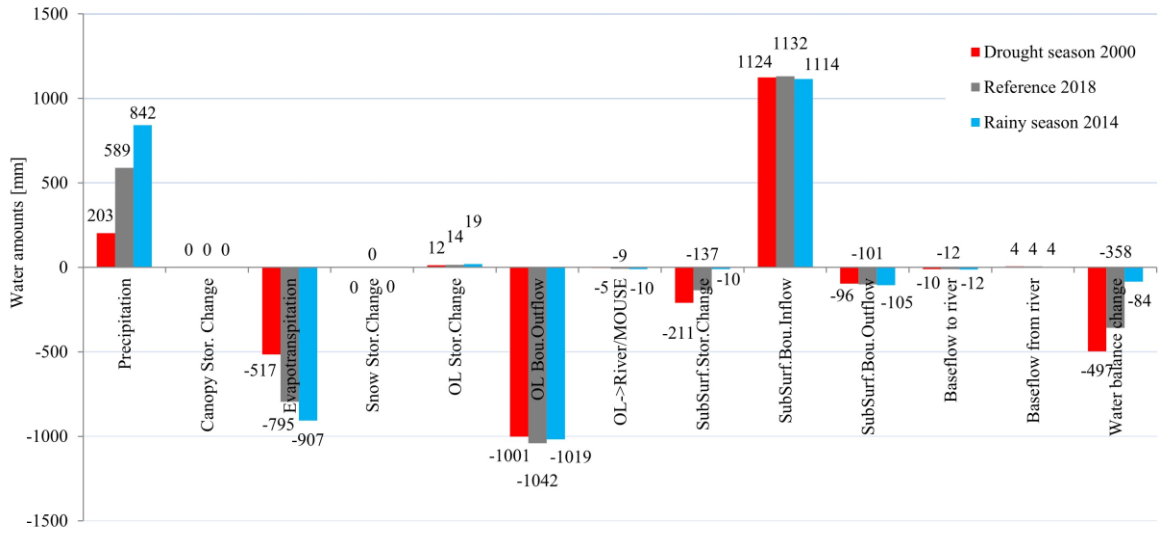

Fig. 4 Water balance values accumulated from the beginning to the end of the study years

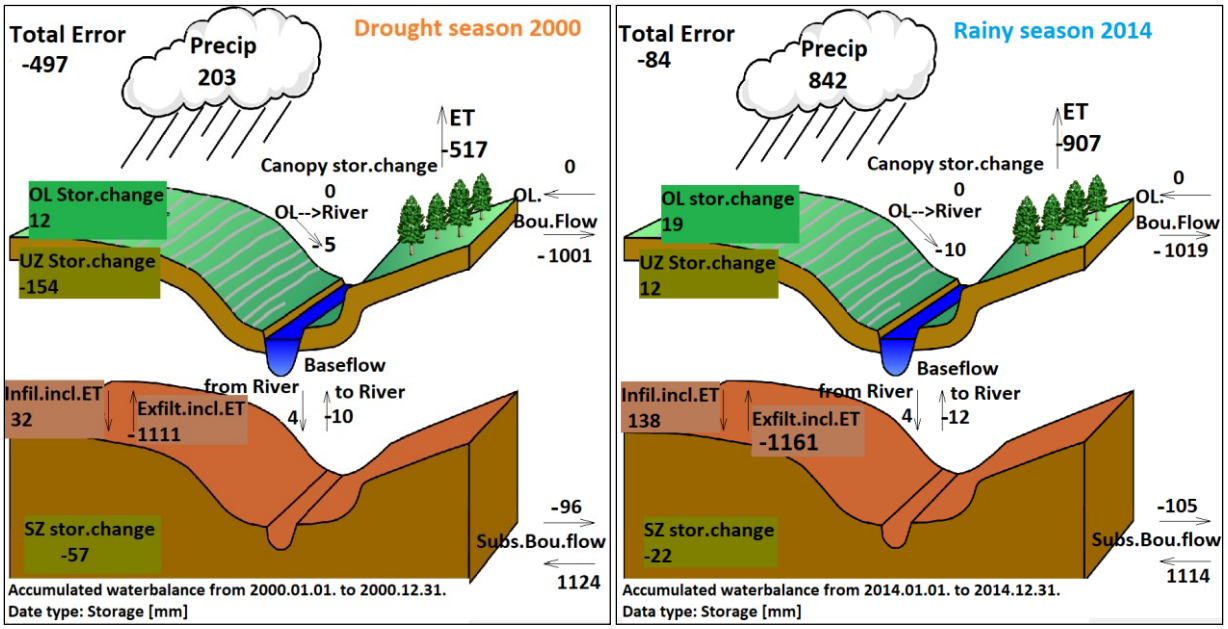

Fig. 5 Water balances for the 2000 drought and 2014 rainy years (Modified after DHI, 2017)

areas flows to the surface water in the lower area under the influence of gravity. Figure 6 shows the elevation of the groundwater level measurement stations and the elevation of the terrain.

According to Figure 6 and to the principle of communicating vessels, subsurface boundary inflow will continuously supply the surface waters from the NW, SW and W directions. On this basis, it can be concluded that the surface and groundwater dividing lines are unlikely to fall into one. In the process of water moving underground, an amount of water from 10 mm and 211 mm is stored at the subsurface storage and shows an increasing trend for

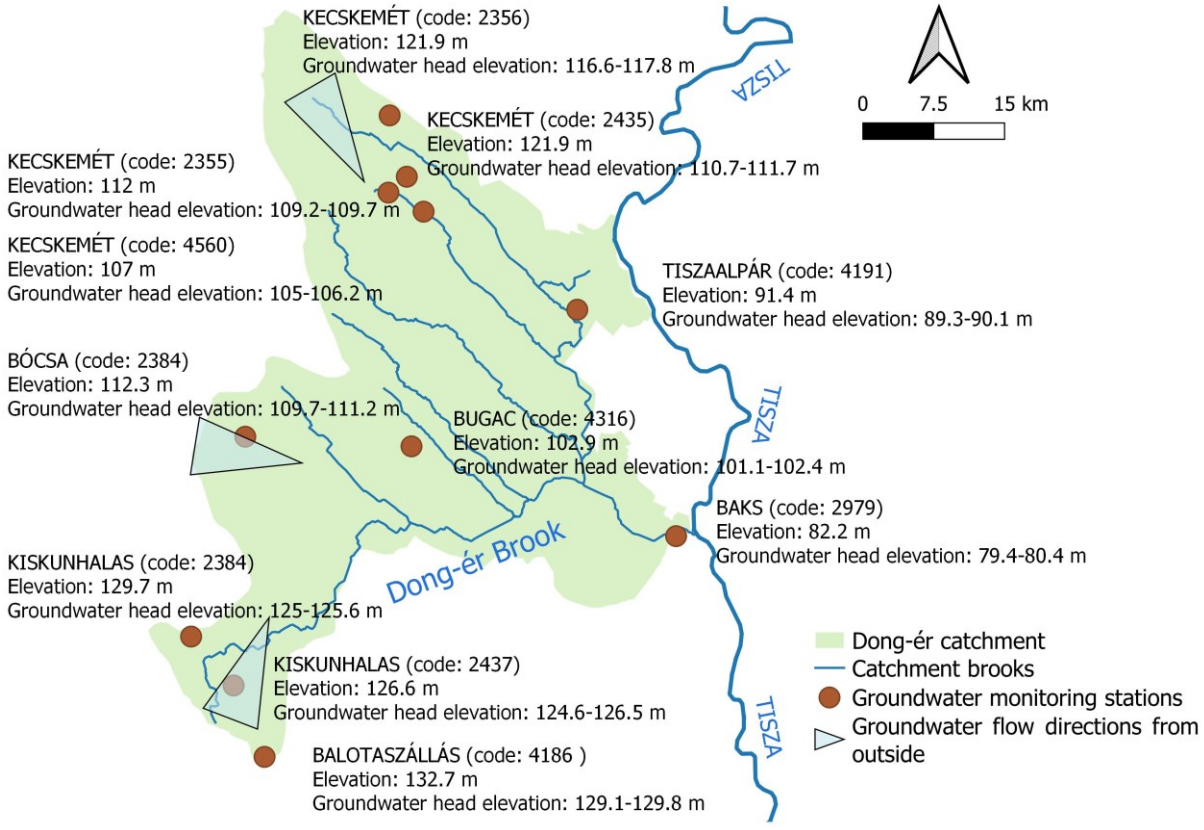

Fig. 6 The elevation of the groundwater measurement stations and the elevation of the terrain

rainy events. In high elevation areas, the height difference between the ground water level and the topography is not large, even considering the brooks bottom elevation, it is often lower than the groundwater level, so in the area near the settlements of Kecskemét, Kiskunhalas and Bócsa groundwater continuously replenishes the brooks and the deflation hollows. In low elevation areas such as Baks and Tiszaalpár settlements, where the groundwater level is also close to the terrain level, in the rainy season, when the groundwater level rises, the phenomenon of upwelling excess water inundation occurs and so on continuously adding water to the brooks. Only an amount of -96 mm to -105 mm of subsurface boundary outflow exits the catchment system to join the Tisza River flow (Fig. 5).

Subsurface water flowing from the outside into the Dong-ér catchment provides ~90% of the water for the brooks (overland outflows). It can be confirmed that for the entire water balance of the catchment, there is a close relationship between the subsurface inflows and overland outflow (surface water of brooks) components. In addition to the subsurface water inflow from the outside, the amount of rainwater that falls directly and infiltrates to replenish water into the brooks, and the source of wastewater from settlements, but according to actual observations, this amount is not significant.

A comparison of the water balance results of extreme precipitation events (2000 and 2014) shows that the sensitivity is in descending order of the following components: Infiltration include evapotranspiration (331.3%), overland flow to river (100%), subsurface storage change (-95.3%), evapotranspiration (75.4%) and overland storage change (58.3%) (Fig. 5). Water balance change from drought and rainy years are -497 mm and -84 mm, so in a rainy year the system can store 413 mm more, which is 877 million m^3 of water. Negative value of water balance change shows that the amount of loss is more than the amount that is in and flows into the system. Thus, the conclusion is that even in the year with a lot of precipitation, the water balance of Dong-ér catchment is still lacking water.

The next section is to analyse the sensitivity of the hydrological parameters shown in Figure 7 under the influence of temperature increase +1.5˚C and +2.2˚C. The actual evapotranspiration increased by 41% under the influence of +1.5˚C and increased by 67% when the daily temperature increased by +2.2˚C. The unsaturated zone deficit parameter also showed high sensitivity, namely an increase of 37% and 57%, respectively. A temperature increases of +1.5˚C causes actual transpiration to increase by 6% compared to soil evaporation. The largest inverse

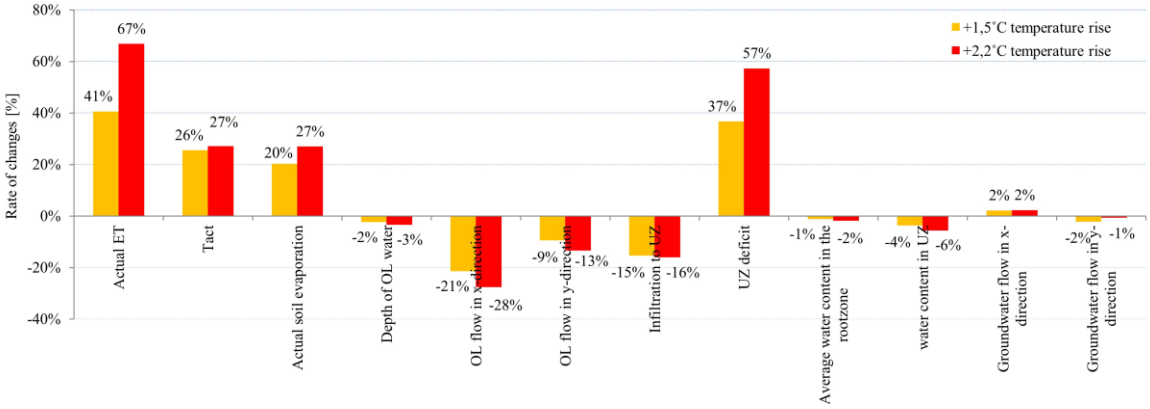

Fig. 7 Change in hydrological parameters due to temperature changes of +1.5 °C and +2.2 ° compared to the reference value on August 10, 2018 (Y = 0 horizontal axis)

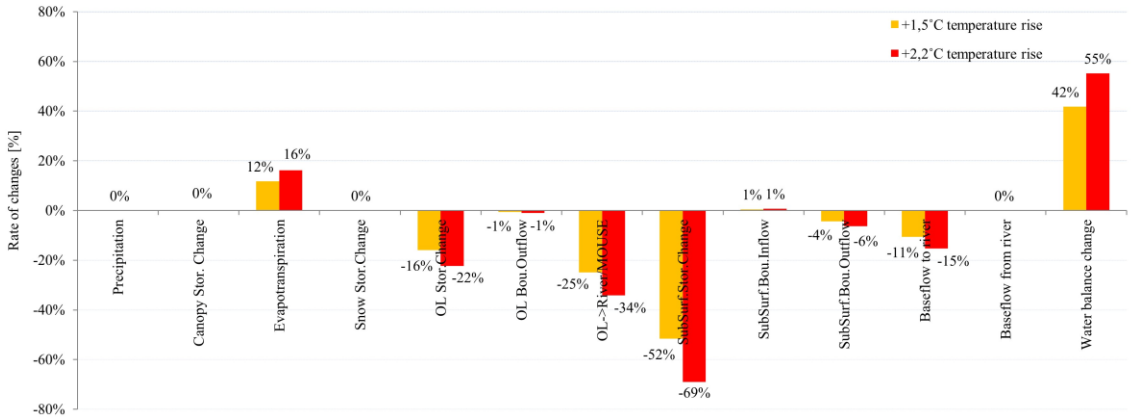

Fig. 8 Water balance values accumulated in the whole of 2018 due to temperature changes of +1.5 ˚C and +2.2 ˚C compared to the reference values (Y = 0 horizontal axis)

Table 3 Change in accumulated water balance in the whole of 2018 due to temperature changes of + 1.5 °C and + 2.2 °C and the differences compared to the reference value (DIFF1 and DIFF2)

Parameter	Reference	(+)1.5 ˚C	(+)2.2 ˚C	Change (%)	Change (%)
Precipitation	(+)589	(+)589	(+)589	0	%
Evapotranspiration	(-)795	(-)889	(-)924	12	16
OL boundary Inflow	0	0	0	0	0
OL boundary Outflow	(-)1042	(-)1036	(-)1032	-1	-1
Canopy Storage change	0	0	0	0	0
Snow Storage change	0	0	0	0	0
OL≥Brooks	(-)9	(-)7	(-)6	-22	-33
OL Storage change	14	12	11	-14	-21
UZ Storage change	-98	-153	-168	-56	-71
SZ Storage change	-39	-55	-63	-41	-62
Baseflow to brooks	(-)12	(-)11	(-)10	-8	-17
Baseflow from brooks	(+)4	(+)4	(+)4	0	0
Subsurface boundary inflow	(+)1132	(+)1137	(+)1140	0	1
Subsurface boundary outflow	(-)101	(-)97	(-)95	-4	-6
Infiltration include ET	(+)109	(+)64	(+)43	-41	-61
Exfiltration include ET	(-)1170	(-)1154	(-)1147	-1	-2
Water balance change	(-)357	(-)506	(-)554	42	55

Note: The sign in parentheses indicates the direction of the water flow. Not in parentheses is the value

proportionality change is the overland flow in x-direction parameter, even with a decrease of 21% for + 1.5˚C and 28% for a temperature rise of + 2.2˚C (Fig. 8). So, these hydrological parameters are the most sensitive to temperature rise.

Among the parameters in Figure 8, unsaturated deficit, actual evapotranspiration and infiltration to unsaturated emerged as the main factors, with higher values than other parameters. Temperature rise has the greatest effect on the value of the unsaturated deficit. In addition, increasing temperatures also increase actual evapotranspiration and naturally decrease the infiltration. The rest of the parameters have intraday values less than 1.0 mm. Meanwhile, the amount of precipitation on August 10, 2018 is zero. This again shows that the amount of water present and operating on this day is derived from the water that has been stored in the top layer from previous periods. Precipitation that reaches the ground surface, mostly infiltration into the deeper layers of the soil with delay and the rest will flow on the surface in the x direction (in the slope direction).

Based on the results in Table 3, the subsurface boundary inflow, overland boundary outflow and evapotranspiration components have a high weight on the studied water balance. The water balance of the Dong-ér catchment is highly dependent on the influence of subsurface boundary inflow from the external area. Evapotranspiration increases with increasing temperature greatly reduced subsurface (UZ and SZ) storage (from -48.5% to -66.5%). Overland storage change is reduced from -14% to -21%, so the baseflow to brooks and the sources to surface water are also reduced. Increasing temperature does not change the baseflow from minimum depths of brooks, where the water is always present, so the value does not change compared to 2018 (all equal to 4 mm). The conclusion is that increasing temperatures reduce the water retention of the brooks, especially in areas where its terrain level is higher than the groundwater level.

The overland boundary inflow in all three temperature conditions is zero, thus the surface watershed boundary has been correctly defined. Canopy and snow storage change in all three temperature conditions are zero, this is because the values are all very small, less than 0.03 mm so when rounding the number is zero.

The subsurface boundary inflow source is very stable and plays an important role in the water balance of the Dong-ér catchment. Subsurface boundary outflow parameters tend to decrease from -4% to -6%, partly due to additional seepage migration for groundwater and the rest being evaporated by vegetation. When considering the values of two parameters infiltration- and exfiltration including ET, it can be concluded that meanwhile temperature increases, infiltration decreases more strongly (-41% and -61%), while exfiltration decreases less.

The water balance change of 2018 show values around -357 mm, which practically more than

758 million m^3 of water is leaving the water system. The increase in temperature of +1.5˚C and +2.2˚C reduces the water balance of the Dong-ér catchment by 42% and 55%, i.e., more than 316 million m^3 and 418 million m^3 less water than in 2018. Increased temperatures directly and indirectly increase the amount of water lost through evapotranspiration and thus the water balance of the basin is significantly reduced. Based on these results, it can be concluded that subsurface storage change, infiltration include evapotranspiration, water balance change, overland flow into the brooks, overland storage components change to a greater extent than evapotranspiration changes, i.e., greater than 12% and 16%, so these parameters are sensitive to the increasing temperature of climate change.

CONCLUSION

The unsaturated zone deficit, infiltration to unsaturated zone, evapotranspiration and overland flows parameters seems to have a great weight in the daily hydrological circulation and have a highly sensitive to climate change conditions. The precipitation rapidly seeps the soil and temporarily stored in the upper soil layer and infiltrates into the deeper layers of the soil with delay and the rest will flow on the surface in the x direction (in the slope direction). During this time a large amount of water will leave the system through evapotranspiration.

Based on the relationship between manifestations of climate change and water balance components, probably the subsurface boundary inflow and evapotranspiration are the two main driving forces that constitute and regulate the water balance of the Dong-ér catchment. According to the models, the water balance in Dong-ér catchment is significantly determined by the subsurface boundary inflow since it continuously supplies about ~90% of the surface water. Subsurface boundary inflow does not show a close relationship with temperature change or extreme precipitation events. Meanwhile, evapotranspiration is highly dependent on the temperature. Due to the warming trend, the water retention of the Dong-ér Brook showed a decreasing trend, especially in areas where the groundwater level is deeper than the bed level of the brook. The components that play an important role in the water balance of the Dong-ér catchment in descending order are as follows: subsurface boundary inflow, overland boundary outflow, evapotranspiration and precipitation. However, among the components, subsurface storage change, infiltration include evapotranspiration, overland flow to brook, overland storage change and evapotranspiration components are the most sensitive to climate change.

Based on the water balance change of the model, the temperature increases of + 1.5˚C and +2.2˚C causes to lose more water than during the drought period in the Dong-ér catchment in 2000. Even such rainy years like 2014, the multi-annual water deficit can't be replenished from the system. Ultimately, this causes the water balance of catchment to be in a state of water shortage. In the light of climate change, water shortage is probably getting worse in the Dong-ér catchment.

The results of the study have also shown the effectiveness of the MIKE SHE model and the water balance calculation module as useful tools to analyse and evaluate the effects of the changing climatic conditions on the hydrological parameters. However, the MIKE SHE model also has disadvantages such as MIKE SHE only calculating the permeability in the vertical direction, the calculation of the permeability value wrong in the area with high slope. Besides, the need for a lot of data with good quality, the difficulty of monitoring data, and changing environmental conditions in the future are issues that need to be improved, so the values of the calculated parameters cannot be absolutely accurate but gives an approximate value and trend.

The results of this study can be a reference for managers, landowners and other stakeholders in the planning, management and effective use of water resources are in a state of decline in the context of increasingly complex climate change.

ACKNOWLEDGEMENT

I am grateful to DHI Hungary Ltd. for the MIKE SHE student license. Thanks to the director of ATIVIZIG, Dr. Péter Kozák and his colleagues for their professional advices and supports. I am grateful to Professor emeritus János Rakonczai for his encouraging supports for writing this article.

REFERENCES

Allen, R.G., Pereira, L.S., Raes, D., Smith, M. 1998. Crop evapotranspiration — guidelines for computing crop water requirements. *FAO Irrigation and drainage paper* 56. Food and Agriculture Organization, Rome. Online available at http://www.fao.org/3/x0490e/x0490e00.htm

Asadusjjaman, S., Farnaz, A. 2014. Investigation of Water Balance at Catchment Scale using MIKE-SHE. *International Journal of Engineering And Computer Science* 3(10), 8882–8887. Online available at https://www.ijecs.in/index.php/ijecs/article/download/1988/1838/

ATIVIZIG, 2016. River Basin Management Plan 2-20 Lower Tisza rightbank planning subunit (in Hungarian). Online available at http://www.vizugy.hu/vizstrategia/documents/C8F99A5D-2864-455E-85D6-7FB53AF0D179/VGT2__2_20_Also_Tisza_jobb_part_vegleges.pdf

Aune-Lundberg, L., Geir-Harald, S. 2020. The content and accuracy of the CORINE Land Cover dataset for Norway. *International Journal of Applied Earth Observation and Geoinformation* 96:102266. DOI: 10.1016/j.jag.2020.102266

Bahremnad, A., De Smedt, F. 2007. Distributed Hydrological Modeling and Sensitivity Analysis in Torysa Watershed, Slovakia. *Water Resources Management* 22, 393–408. DOI: 10.1007/s11269-007-9168-x

Benyhe, B., Právecz, T., Sipos, Gy. 2015. Assessment of different hydrological modelling software on a lowland minor catchment. In: Blanka, V., Ladányi, Zs. (eds.) Drought and Water Management in South Hungary and Vojvodina. University of Szeged, 320–323. (279–289.)

DHI, 2017. MIKE SHE Volume 1: User guide. Online available at https://manuals.mikepoweredbydhi.help/2017/Water_Resources/MIKE_SHE_Printed_V1.pdf

EEA. 2018. Corine Land Cover 2018. European Environmental Agency. Online available at https://www.eea.europa.eu/data-and-maps/data/external/corine-land-cover-2018

EU Water Framework Directive, 2004. DOI: 10.2779/75229. Online available at https://ec.europa.eu/environment/pubs/pdf/factsheets/wfd/en.pdf

Farsang, A. 2014. The potential pedological effects of aridification due to climate change (A klímaváltozás okozta szárazodás potenciális talajtani hatásai). In: Blanka, V., Ladányi, Zs. (eds.) Drought and Water Management in South Hungary and Vojvodina. University of Szeged. 137–141. (117–126.)

Fehér, Z.Zs. 2019. Large scale geostatistical modelling of the shallow groundwater time series on the Southern Great Hungarian Plain. Two approaches for spatiotemporal stochastic simulation of a non-complete monitoring dataset. *PhD dissertation*. University of Szeged. DOI: https://doi.org/10.14232/phd.10122

Feranec, J., Soukup, T., Hazeu, G., Jaffrain, G. 2016 (Eds.), European landscape dynamics. Corine land cover data, *CRC-Press*, Boca Raton, 9-14.

Fiala, K., Barta, K., Benyhe, B., Fehérváry, I., Lábdy, J., Sipos, Gy., Győrffy L. 2018. Operational drought and water scarcity monitoring system (Operatív aszály- és vízhiánykezelő monitoring rendszer) (In Hungarian). *Hidrológiai Közlöny, 98 (3)*. 14–24. *ISSN 0018-1323*. Online available at http://publicatio.bibl.u-szeged.hu/17598/1/Fiala_et_al2018 HidrologiaiKozlony.pdf

Graham, D.N., Butts, M. 2005. Flexible, integrated watershed modelling with MIKE SHE. In Singh, V.P., Frevert D.K. (eds.) Watershed Models, CRC Press, 245–272., ISBN: 0849336090

Hamby, D.M. 1994. A review of techniques for parameter sensitivity analysis of environmental models. *Environmental Monitoring and Assessment* 32, 135–154. DOI: 10.1007/BF00547132

Ibarra, S., Romero, R., Poulin, A., Glaus, M., Cervantes, E., Bravo, J., Pérez, R., Castillo, E. 2016. Sensitivity analysis in hydrological modelling for the Gulf of México. *Procedia Engineering 154*, 1152–1162. DOI: 10.1016/j.proeng.2016.07.531

IPCC 2018. Global Warming of 1.5˚C. Thematic Reports. Online available at https://www.ipcc.ch/sr15

K&K Mérnöki Iroda Kft. 2013. Harmonized activities related to extreme water management events – especially flood, inland inundation and drought (Extrém vízgazdálkodási eseményekkel kapcsolatos területi érzékenység felmérése – különösen árvíz, belvíz és aszály esetén) (in Hungarian), HUSRB/1203/121/145/01, Ref. No.: T-51/2013

Keilholz, P., Disse, M., Halik Ü. 2015. Effects of Land Use and Climate Change on Groundwater and Ecosystems at the Middle Reaches of the Tarim River Using the MIKE SHE Integrated Hydrological Model. *Water* 7(6), 3040–3056. DOI: 10.3390/w7063040

Kozák, P. 2020. Changes in surface runoff on the south-eastern slope of the Danube-Tisza Interfluve Sand Ridge in the context of climate change (in Hungarian). In: Farsang, A., Ladányi, Zs., Mucsi, L. (eds.) Climate change challenges – From global to local. *GeoLitera*, 109–115.

KÖTIVIZIG 2015. Tisza River Basin Management Plan by Middle Tisza District Water Directorate. (in Hungarian). Online available at https://www.vizugy.hu/vizstrategia/documents/1DF34F16-04AC-48B6-AD62-C62146FA5913/Tisza_RVGT_aprilis.pdf

Ladányi, Zs. 2010. Climate change impact in a sample area of Danube-Tisza Interfluve. In: Kiss, T. (ed.) Natural geographical processes and forms. Natural Geography Studies of the 9th National Conference of Geographical Doctoral Students (in Hungarian), 93–98. Online available at http://acta.bibl.u-szeged.hu/68110/1/2009_termeszetfoldrajzi_folyamatok_es_formak.pdf

Ladányi, Zs., Blanka, V., Armenski, T., Stankov, U., Sipos, Gy. 2014. Interviewing agricultural stakeholders and landowners. In: Blanka, V., Ladányi, Zs. (eds.) Drought and Water Management in South Hungary and Vojvodina. University of Szeged. 363–372. (339–359.)

Lu, J., Sun, G., McNulty, G. S., Comerford, B.N. 2006. Evaluation and application of the MIKE SHE model for a cypresspine flatwoods watershed in North Central Florida. *Second Interagency Conference on Research in the Watersheds*, 63–74.

Myneni, R., Knyazikhin, Y., Park, T. 2015. MCD15A2H MODIS/Terra+Aqua Leaf Area Index/FPAR 8-day L4 Global 500m SIN Grid V006. NASA EOSDIS Land Processes DAAC. DOI: 10.5067/MODIS/MCD15A2H.006

Nagy, Zs., Pálfi, G., Priváczkiné Hajdu, Zs., Benyhe, B. 2019. Operation of canal systems and multi-purpose water management – Dong-ér catchment (in Hungarian) In: Ladányi, Zs., Blanka, V. (eds.) Monitoring, risks and management of drought and inland excess water in South Hungary and Vojvodina: University of Szeged. 262–275. (83–96.)

OMSZ 2018a. Observed changes in Hungary. (in Hungarian) Online available at https://www.met.hu/eghajlat/eghajlatvaltozas/megfigyelt_valtozasok/Magyarorszag/

OMSZ 2018b. To the margin of the IPCC Thematic Report assessing a 1.5 degree global temperature rise. (in Hungarian) Online available at https://www.met.hu/ismeret-tar/erdekessegek tanulmanyok/index.php?id=2334&hir=Az_IPCC_1,5_fokos_globalis_homerseklet-emelkedest_ertekelo_Tematikus Jelentesenek_margojara

OVF 2016. Effects of climate change, hydrometeorological extremes. (in Hungarian) Online available at http://www.ovf.hu/hu/korabbi-hirek-2/a-klimavaltozas-hatasai-hidrometeorologiai-szelsosegek

Paparrizos, S., Maris, F. 2017. Hydrological simulation of Sperchios River basin in Central Greece using the MIKE SHE model and geographic information systems. *Applied Water Science* 7, 591–599. DOI: 10.1007/s13201-015-0271-5

Právetz, T., Sipos, G., Benyhe, B., Blanka, V. 2015. Modelling runoff on a small lowland catchment, Hungarian Great Plains. *Journal of Environmental Geography* 8 (1–2), 49–58. DOI: 10.1515/jengeo-2015-0006

Rakonczai, J., Farsang, A., Mezősi, G., Gál, N. 2011. Theoretical background of inland excess water formation (A belvízképződés elméleti háttere) (in Hungarian), *Hungarian Geographical Review* 135(4), 339–349.

Rakonczai, J., Fiala, K., Mesaros, M., Frank, A., Popov, S. 2014. Water management conflicts. In: Blanka, V., Ladányi, Zs. (eds.) Drought and Water Management in South Hungary and Vojvodina. University of Szeged, 78–80. (47–52.)

Singh, A. 2014. Conjunctive use of water resources for sustainable irrigated agriculture. *Journal of Hydrology*. 519, 1688–1697. DOI: 10.1016/j.jhydrol.2014.09.049

Sipos, Gy., Právecz T. 2014. Identification of water retention areas on the Dong-ér catchment using GIS. In: Blanka, V., Ladányi, Zs. (eds.) Drought and Water Management in South Hungary and Vojvodina. University of Szeged. 217–220. (157–167.)

Szatmári, J., van Leeuwen, B. (eds.) 2013. Inland Excess Water – Belvíz – Suvišne Unutrašnje Vode, Szeged: University of Szeged, Novi Sad: University of Novi Sad, 154 p.

Tóth, B., Weynants, M., Pásztor, L., Hengl, T. 2017. 3D Soil Hydraulic Database of Europe at 250 m resolution. *Hydrological Processes* 31(14), 2662–2666. DOI: 10.1002/hyp.11203. https://eusoilhydrogrids.rissac.hu/

van Leeuwen, B., Právetz, T., Liptay Z.Á., Tobak, Z. 2016. Physically based hydrological modelling of inland excess water. *Carpathian Journal of Earth and Environmental Sciences*, 11(2), 497–510

sciendo

Journal of Environmental Geography 14 (3–4), 14–25.

DOI: 10.2478/jengeo-2021-0008
ISSN 2060-467X

CONDITION ASSESSMENT OF SUBSURFACE DRAINED AREAS AND INVESTIGATION OF THEIR OPERATIONAL EFFICIENCY BY FIELD INSPECTION AND REMOTE SENSING METHODS

Norbert Túri[1*], János Rakonczai[2], Csaba Bozán[1]

[1]Research Center for Irrigation and Water Management (ÖVKI) Institute of Environmental Sciences (KÖTI)
Hungarian University of Agriculture and Life Sciences (MATE),
Anna-liget u. 35, 5540 Szarvas, Hungary
[2]Department of Geoinformatics, Physical and Environmental Geography, University of Szeged,
Egyetem u. 2-6, 6722 Szeged, Hungary
*Corresponding author, email: turi.norbert@uni-mate.hu

Research article, received 4 April 2021, accepted 12 October 2021

Abstract

The extreme weather events highlight the need to develop action concepts to maintain agricultural production security in the future. Hydrological extremes can occur within a year in the form of surplus water (i.e. inland excess water), water scarcity or even drought. These adverse effects are influenced, inhibited and also facilitated by human activity. Previously, complex amelioration interventions, including subsurface drainage, aimed to improve the productivity of agricultural areas with unfavourable water management properties. The current efficiency of the subsurface drain networks in the regulation of groundwater level or soil moisture content can be questioned from several aspects. After the end of the socialist era (after 1990s), lack of maintenance and operation tasks have become typical, and are still a problem today in Hungary. Unfortunately, there is no exact national cadastre on the tile drained areas, and data is only available to a limited extent in the original amelioration plan documentations. In the present study, we aimed to reveal the possibilities of delineating the subsurface drained areas, and to develop a new method of condition assessment. Three tile drained study sites were selected on the Great Hungarian Plain in Central Europe. Our field investigations revealed the typical problems of the drained areas: (1) excessive vegetation of the receiving channels; (2) inadequate condition of the receiving main channel bed; (3) soil compaction in multiple layers above the drainage network; and (4) poor condition of outlets of the drain pipes. The developed methodology enabled us to evaluate the soil and the surface/subsurface water of the tile drained areas, and the technical condition of the drains. The necessary action plans or treatments were also outlined to replace the unused drain networks into use. Based on the scientific literature, we also sketched the target conditions and technological solutions that are required for the installation of new drains. The organization of the derived data into a GIS database could serve as a basis for the development of a cadastre of the tile drained areas based on a regional approach.

Keywords: soil moisture regulation, tile drainage, condition assessment, GIS

INTRODUCTION

Human activity in agricultural areas fundamentally influences the structure, the conditions and the water management properties of soils. Typically, subsurface water management is carried out worldwide to improve soil conditions vulnerable to inland excess water or excess salt content. Inland excess water is a temporary inundation mainly on the agricultural fields which mostly arises due to snow melting, heavy rainfall, lack of runoff, upwelling of ground water, insufficient evaporation and low infiltration capacity of the soil (Barta et al., 2013; Van Leeuwen et al., 2013).

The problem of surplus water on agricultural fields could be solved by construction of subsurface drainage networks, which is common used all over the world. Tile drainage is a form of water management that removes excess water from the subsurface of the soil. In 1980, subsurface drained areas covered 1 million ha in Sweden, 2.5 million ha in Finland, 3.8 million ha in the UK, 4 million ha in France, and 6.8 million ha in Germany, 0.7 million ha in the Netherlands, and 0.04 million ha in Hungary (Szinay, 1983). The extent of tile drained areas has expanded greatly in the following decades. However, in Hungary only limited data is available on their extent. Hornyik (1984) stated that ca. 1.3 million ha arable land was in need of subsurface drainage. Babics (1989) referred that ca. 0.15 million ha had subsurface drained until 1989. As a comparison, in the mostly mountainous Slovenia, 72.000 ha of agricultural land have been drained (Maticic and Steinman, 2007), and in the hilly Czech Republic 1.1 million ha land had subsurface drains (Tlapáková et al., 2017). Thus, we can state that the amount of drains installed in Hungary lags far behind the European average.

Tile drainage is studied from two main point of views. The first group of researchers aimed to *identify the abandoned, non-functioning drainage networks*. Tlapláková et al. (2017) managed to detect drain tiles using an aerial thermal camera. The differences in surface

temperature caused by the difference in soil moisture described by Tlapákova et al. (2017). They found that the conditions for the identification of the drain networks by remote sensing methods depend on the type of current land cover. Tlapláková et al. (2015) distinguished three basic types of land cover for the best identification which are (a) permanent grasslands, (b) green arable lands, and (c) bare arable lands. The identification method was associated with various agrotechnical, plant developmental (phenophases) and precipitation parameters (Tlapáková et al., 2015). Koganti et al. (2020) applied ground penetrating radar (GPR) to detect subsurface tile drains in agricultural areas. According to their results, the detection of the drain tiles can be particularly successful and accurate using ground penetrating radar, but the results should be interpreted together with the available blueprints of the examined drainage networks. Djurović and Stričević (2004) studied a newly installed drainage system. They concluded that due to inadequate maintenance, the operational efficiency of the drains fell to a minimum level in short period of time.

The other group of researchers *investigated the operational efficiency of tile drainage networks*. They evaluated the role of the drains in crop yields (Bukovinszky et al., 1983; Jiang et al., 2019), examined the environmental effects of agrochemicals in natural watercourses, and the recirculation of effluent drainage waters (Shedekar et al., 2021), evaluated the efficiency of subsurface irrigation through drains (Tolomio and Borin, 2019), simulated and modelled the effects and the transport processes (Singh et al., 2006; Jiang et al., 2019; Luo et al., 2010). Brandyk et al. (1993) found that operation with a drainage-subirrigation system has numerous limits and disadvantages. According to their conclusions, the main problem is that it is not possible to raise the groundwater level above the drains in the summer season, especially in case of periods of drought. Sojka et al. (2020) performed DRAINMOD computer simulations to investigate the effect of climate change on controlled drain systems. Their simulations reflect that by applying controlled drainage and by blocking the outflow of drains in the beginning of the spring season, it is possible to retain water in the soil for later dry periods. A number of publications (Fehér, 1979; Mile, 1986; Bognár and Geredy, 1989; Forgóné, 1996) prove the beneficial effects of tile drainage with proper use and maintenance (groundwater level regulation, prevention of salinization processes, water reclamation etc.) on agricultural production (i.e. better yields, improved soil structure, better air-water-nutrient turnover in soil, reduced and less durable inland excess water cover on surface, increase in the number of days suitable for tillage). Tolomio and Borin (2019) investigated the effect of controlled drainage as well as free drains (non-controlled outflow) on groundwater levels at various crop fields. Their results showed that controlled drainage reduced the amount of effluent water by up to 69% compared to free drains. The practice of controlled drainage (which provides precise regulation of the groundwater level or soil moisture in the area with water level control structures at the outlet of the drainage pipes) is applied in the United States (https://transformingdrainage.org) and in several European countries, but it was not widespread in Hungary.

In addition to its beneficial effects on soil, subsurface drainage can also have a negative impact on the environment, primarily through the multiform agrochemicals that the drains could deliver to the recipient channels. Smith et al. (2015) reported the acceleration of mobility of phosphorus depletion from drained areas. In areas where 50-80% of agricultural land is drained, the excess introduction of agrochemicals taken into the water system can be critical. According to Shedekar et al. (2021), approximately 35% of the excess nitrogen entering U.S. water systems originated from drained areas. Karásek et al. (2015) mentioned that the location of drained areas is not completely known in many areas, and areas that were once drained may also function as grasslands that have now been declared nature reserves due to land use changes. They proposed to restore the drained areas to near-natural hydrological conditions to prevent the areas from drying out.

The first Hungarian studies were conducted to provide professional support for land amelioration interventions. The studies were mainly evaluating the effects of groundwater management on crop yields (Bognár and Geredy, 1989), the role of salt and nutrient movement (Bukovinszky et al., 1983; Lendvai, and Avas, 1983; Forgóné, 1996;), the possibilities of water replenishment by drainage or double-purpose operation of drains (Hornyik, 1984; Mile, 1986), or they analysed the overall effectiveness of the interventions (Bukovinszky, 1983; Fehér and Szalai, 1986). Bukovinszky (1983) emphasized that the comparative assessment of soil conditions before and after the interventions could be realized by continuous data collection and data provision in accordance with a full range of professional criteria. Several experiments were carried out on cultivated areas of state-owned farms and agricultural cooperatives, or on priority experimental sites of individual research institutes and universities. Some experiments were set up on a complex land amelioration model site, which made it possible to determine the rate of deepening of the leached soil layer and the yields that could be achieved in the long run (Nyiri and Fehér, 1977). Bukovinszky et al. (1983) studied the relationship between different plant species and drain scaling (15, 20, 25 m spacing, 0.0-0.1% fall). Their results showed that each plant species responded differently to drainage, thus they concluded that the application of different drainage pipe spacing according to the related tillage may be helpful to increase crop yields (Bukovinszky et al., 1983).

During the second half of the 20th century, researchers also dealt with the issue of dual operation of subsurface drains. The professional application of dual-purpose operation was only possible with a strictly and precisely planned drainage service (operation and maintenance), and only on suitable soils (Fehér and Szalai, 1986). Csaplár (1989) examined the technical conditions of the usability of the drain networks for water replenishment. Based on the applied measurements, the pressure loss of the water led into the drainage pipe from the open channel was significant. In the case of pipelines

longer than 100-120 m, the pressure drop was so significant that no substantial water replenishment was possible in the additional sections. Mile (1986) ran an interesting experiment of water replenishment through drains for 4 years. The results were encouraging, as despite of a drought the wheat and maize had reasonable yield on drained plots. Based on the results of their annually repeated spring and autumn soil tests, it was found that Na+ cations had accumulated to a harmful extent in the soil layer close to the surface, which may have been due to inadequate quality of restored irrigation water in the drains. Molnár (1987) formulated his statement, which is still valid today that water surplus and water shortage can occur within one year. In his experiments, water replenishment through the subsurface drain system was carried out on a 1200 ha large test area. Based on Molnár's results (1987) drought damage can be mitigated, if adequate deep tillage is applied (e.g. chisel-ploughing), the drain system (tiles and channels) is emptied in the non-growing season, and good quality irrigation water is used. It was also emphasized that, in practice, water replenishment through drains could only be applied for a short time, otherwise harmful salts could accumulate in the upper layers of the soil.

For almost 40 years, no comprehensive map, written archive or cadastre has been created about the exact location of tile drained areas in Hungary. However, for a future reinterpretation of subsurface drainage, it is required to know the location and condition of the areas that were once treated. The latest edition of the cadastre (Wittmann et al., 1981) contains the description of the tile drained areas of Hungary in tabular form. According to the cadastre, 40,000 ha of agricultural land was tile drained, and the total length of the installed drains was about 16,000 kilometres. The editors of the cadastre suggested regular expansion and further development of the cadastre in every five years, but this was not done. The tile drainage of lowland areas became more extensive in the 1980s and until 1989 the extent of the drained areas reached 150,000 ha (Babics, 1989).

The creation of a "modern" cadastre which contains tile drain lines and the required attribute data can now be solved by creating a GIS database. The database could include a base map, supplemented by point, line or polygon features containing attribute data (basic data from the design documentation and field survey results). A cadastral database containing such data could be suitable for carrying out spatial comparative studies, for example examining the correlations between inland excess water affected areas and subsurface drained areas, or changes in groundwater conditions at the tile drained areas.

The main goals of our research are to (1) explore the conditions of subsurface drains at the study areas, to determine their usability and formulate recommendations; (2) to find out if the tile drains are able to collect the excess water from the soil, and if the drains are able to drive the collected water into the recipient channel. It is also important to (3) evaluate the technical condition of the recipient channel and determine: (a) if the channel is capable to accept the effluent drain water, and (b) if the collector channel is capable to lead away the collected waters to the main channel system. Several field and laboratory tests were performed in tile drained pilot areas at different locations supplementing the traditional methods with more modern ones.

STUDY AREA

Most of Hungary (54.2%) is cultivated, as the large alluvial plains provide favourable topographical conditions and rich soils for crop cultivation. However, due to its low elevation, inland excess water can cause serious problems in wet years, therefore, the deepest areas were tile drained several decades ago. Three low-lying study sites were selected for our investigations on the eastern part of the Great Hungarian Plain.

The eastern part of the Great Hungarian Plain has diverse geomorphology, characterized by the former riverbeds of the Tisza River, the Körös River and its influents, which form depressions on the cultivated fields. These depressions toned to be drained because they are the most affected by the inland excess water inundations due to cohesive meadow and casting soils. The annual precipitation is 500–550 mm. In addition to the frequent droughts, the excess water can develop in the same year. The depth of groundwater varies with seasonal fluctuation. The land use is characterized by very high proportion of arable land, that is well above the national average. Main criteria for the selection of study sites were: (1) being strongly affected by amelioration interventions, (2) the availability of complete and detailed documentation (land amelioration plan), (3) the owner of the plot allowed and supported the field work, and (4) close distance to the home institution (Szarvas) enabling monitoring works. At one of the study site near Mezőtúr, a more complex survey was carried out. On the other two sites (near Zsadány and Csanytelek) less detailed studies were performed, only the general condition of drainage works and their environment were analysed (Fig. 1).

Land amelioration works in the Mezőtúr study site (182 ha) were completed in 1989, but the operating permit was only granted in 1994. Based on the soil database the Mezőtúr study site has hydromorphic meadow soil prone to salinization. During the implementation of the tile

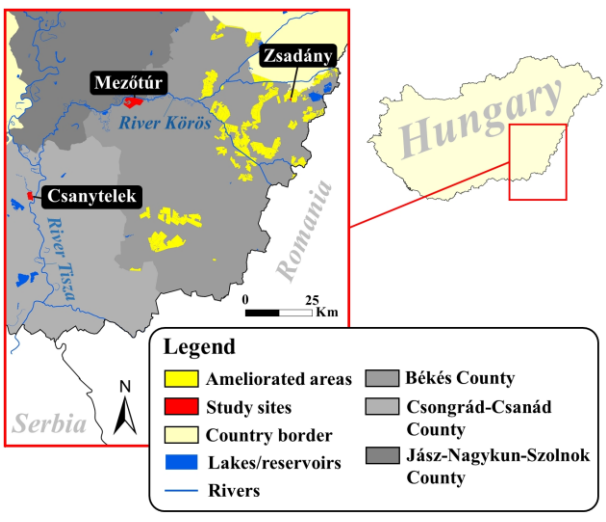

Fig. 1 The location of the pilot areas

drainage interventions, a parallel network of free drains was constructed on both sides of the field, while five targeted drains were established in the inner areas of the field (Fig. 2). In total 137 pipes, with a length of 33.2 km were installed in the area. At the west side of the study area, 46 drainage pipes were installed with uncontrolled outflows to the recipient channel. The installation spacing of the drains is 20 m and their installation depth varies between 85 and 120 cm. Despite these subsurface water management interventions, the area is still endangered by inland excess water inundations, as it is shown on the recent aerial photographs. Every autumn, the farmer of the plot creates ditches to allow inland excess water to run off the field in winter/spring period. Through these small ditches, several cubic meters of valuable topsoil eroded, causing sedimentation and blocked flow of accumulated water in the recipient channel. It is unfortunate, that the new owner, who acquired the land in the 1990s, does not show interest in the previous subsurface water management intervention. During the ordinary recipient channel maintenance (reaping and burning of reeds), the number of intact drainage pipes decreases and they become less usable.

Amelioration and subsurface drainage interventions also took place at the other two study sites before 1990. At Csanytelek pilot site (70 ha) subsurface drainage works were completed in 1987 with 28.8 km installed drains with 20 m of spacing; and Zsadány site (121 ha) has tile drained with 15 km installed drains with 20 m of spacing in 1989. These areas also became privately owned after being part of a large-scale farm, and similar conditions prevail over them. The most typical crops grown are cereals and corn.

METHODS

Considering that on tile drained areas, the agricultural activity is the most relevant, the field and laboratory tests focused on soil and water analyses. Our methodology consists of several related parts and are described below:

Data collection

Amelioration planning documentation for the study sites was obtained from the official archives (regional Water Management Authority). The documentation included permissions from design to operations, maps and blueprints of the subsurface drained areas, site plans, documentation of soil properties, cross sections of the drain recipient channels and roads, groundwater data, etc. After the data collection, paper maps of areas affected by land amelioration including tile drainage, were first identified on a base map and then georeferenced. In addition to the archive plan, documentation of the subsurface drainage interventions of the Mezőtúr study site we also collected remotely sensed data (orthophotos from 2000, 2005, and 2007, high resolution satellite imagery from Google Earth and UAV aerial imagery). In the case of the Mezőtúr study site, we used an updated digital version of the most detailed soil maps of Hungary made before 1945.

Remote sensing methods

UAV aerial photography was applied for identifying and mapping the drain network, as no precisely documented data exists on the location of the tile drain systems. To evaluate moisture conditions of the surface in case of bare soil or vegetation coverage altogether 9 UAV flight campaigns were executed at the Mezőtúr study site. Aerial imagery acquisitions were performed with a fix-winged Trimble UX5 HP, carrying a 36-megapixel (RGB + NIR (red, green, blue + near infrared)) Sony Alpha 7 camera, and a DJI Phantom 4 multicopter (for 12 megapixel RGB + NGB (red, green, blue + near infrared, green, blue) recordings). We studied the visible differences in soil moisture on the surface that could be used to identify the locations of properly functioning drainage pipes. Difference in surface reflectance was detected by 3-channel (RGB; NGB) cameras (Fig. 3). In the case of vegetation, multispectral or thermal images may provide more accurate results, than ours (Tlapáková et al., 2017).

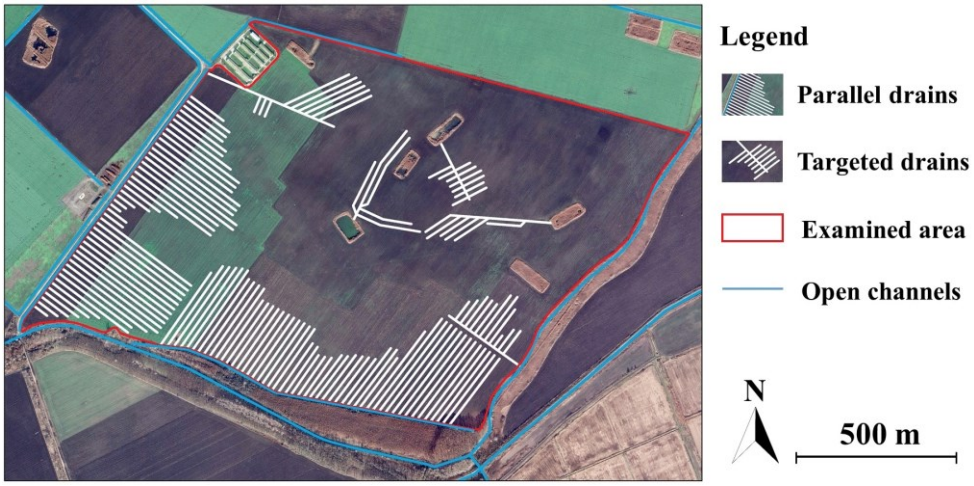

Fig. 2 The study site at Mezőtúr and its tile drain system.
Note, that the drains terminate in artificial canals or in artificial lakes

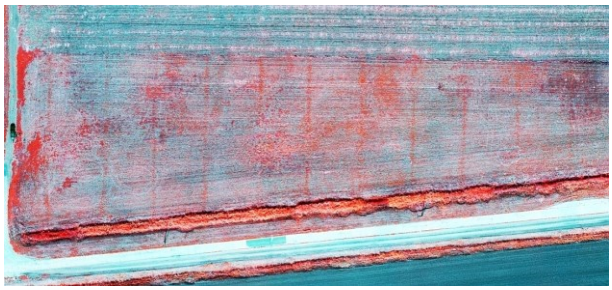

Fig. 3 False coloured composite image of drained alfalfa field made from NIR, green and blue spectral bands. The red colour indicates vegetation, blue colour indicates non-vegetation surfaces

Normalized Difference Vegetation Index (NDVI) and Green Normalized Difference Vegetation Index (GNDVI) maps were calculated, whereupon the differences become quantifiable. One of the campaigns was performed by the Department of Geoinformatics, Physical and Environmental Geography of the University of Szeged. They applied multispectral and thermal sensors (senseFly S.O.D.A / Parrot Sequoia+ / senseFly Deut T camera) on a fix winged eBee senseFly drone to investigate the operational efficiency of tile drain networks which appearance is based on spectral and temperature differences of the surface.

Soil sampling and analysis

During the Mezőtúr field campaign, we *opened soil profile* to describe the soil type of the tile drained area and characterize its mineral precipitations in each soil layer. *Undisturbed soil samples* were taken from the wall of the soil profile (0-130 cm) that we opened above a drainage pipe (2 sample replicates per 7 depths). Undisturbed soil samples were taken to determine the hydraulic conductivity of the soil, and to measure the permeability (k-factor) of the soil layers. A soil layer with a low k-factor can impede the infiltration and migration of water towards to the drains. The determination of the k-factor based on Darcy's law (Gray and Miller, 2004). This allows us to estimate the functionality of drainage in the area as well as to determine the required agrotechnical interventions. The k-factor can also be used to characterize whether the distance of the drainage pipes in the studied area is appropriate for the current soil conditions. The k-factor values of each layer of the studied soil profiles were so low, that their units were expressed in mm/day rather than cm/day.

Open-face Auger sampling was used to determine the soil texture, and the amount of water-soluble salts. Laboratory analysis of auger soil samples was performed to determine the texture of the soil and based on it, the water management properties were evaluated. Open-face Auger soil sampling was carried out above three drains, in-between these drains, and at three non-drained control points (from a depth of 0-100 cm, at every 10 cm) in order to determine the soil texture and salt content. As the auger soil sampling was performed in August 2019, during the evaluation of the data it had to be considered that summers are usually characterized by upward movement of soil moisture content via evaporation. The analysis of soil liquid limit, total dissolved salt content and the adsorbed Ca, K, Mg, Na ions on the surface of soil colloids were performed according to the relevant Hungarian laboratory examination standards (MSZ-08-0205:1978 Determination of physical and hydrophysical properties of soils; MSZ-08-0206-2:1978. Evaluation of some chemical properties of the soil (pH value, phenolphtaleine alkalinity expressed in soda, all water soluble salts, hydrolite and exchanging acidity)). We also followed the standard of MSZ-08-0214-2:1978 Quantitative and qualitative definition of the exchangeable soil cations was made using AAS Flame Photometry. The repetitive measurements on the proportion and ionic composition of salt content accumulated in deep soil layers or near the soil surface refers to the quantity and direction of the movement of salts, which was also monitored in tile drained areas.

Based on the performed *soil penetrometric measurements* the soil moisture conditions and as well as the soil compaction were determined with a custom designed soil penetrometer, to reveal the presumed moisture differences above or between the drain pipes. Soil resistance and moisture were three times sampled in 0-100 cm in 47 points (24 points over drains, 21 points in-between drains, 2 points in control area).

Water sampling and analysis

Water samplings were performed at the Mezőtúr study site from the effluent water of 5 drain outlets and from 3 sections of the recipient channel water. The comparison of the results refers to the discharge of nutrients and agrochemicals from the drains into the recipient water, which might pose risk to the environment.

Discharge measurement of effluent drainage water was also carried out, by measuring the filling time of the sampler with a given volume, thus the discharge data were expressed as liter/hour (l/h). By combining the discharge of the effluent water and its nutrient content, the input of harmful salts or pesticides into the recipient canal was calculated. However, it must be noted, that this calculation reflects the current state, and more repetitions are needed for more accurate estimations. The discharge of the drain water was highly fluctuating at the time of sampling, the highest measured discharge was 18-22 l/h, but there were also drain pipes with lower water discharge (6.5-7.5 l/h), being at the limit of measurability. For comparison, Lendvai and Avas (1983) sampled drains with a flow rate of 1800 l/h during their experiments.

Drain pipes operated just during the winter-spring period at the Mezőtúr study site, so water samples could be collected (and representative) just for this period to understand whether excess salt, nutrients, or suspended solids leave the soil during the winter, emphasising the leaching role of the drains. As the water of the canals usually is used for irrigation during the vegetation period, the water was categorized in terms of suitability as irrigation water (Filep, 1999). Water samples were analysed in the accredited laboratory of the Research Institute for Irrigation and Water Management (ÖVKI). The analysed parameters were pH value, EC (Soil electrical conductivity), bicarbonate, carbonate, ammonium ion, ammonium-nitrogen, nitrate ion, nitrate

nitrogen, nitrite, nitrite nitrogen, total nitrogen, orthophosphate ion, orthophosphate phosphorus, total phosphorus, total dry material, total solutes, total suspended solids, chloride, sulphate, calcium, magnesium, potassium and sodium.

Condition assessment of the drains

Technical condition assessment of the recipients, used for the determination of whether the recipient is suitable to (1) provide the operating conditions for the reception, (2) collect effluent drainage water. The actual condition of the drain pipes was surveyed applying an *endoscope camera*. On the photos, we looked for the presence of sediments in drainage pipes and perforations in the drainage pipes. Endoscope camera imagery was collected from the undamaged drain pipes to determine if any groundwater and soil moisture could infiltrate through the perforations of the pipes, or to see whether the drained water can flow through the pipe itself. Following Sojak and Ivarson (1980) observations, an important aspect was to observe the various sediments and mineral precipitates on the inner surface of the drain pipes (e.g. iron ochre or manganese oxide). Endoscope imagery was collected using a waterproof tube camera with adjustable brightness LED lighting, 5 m range, and 800x600 pixel resolution. To validate the filtration of the drainage pipes, a soil profile was also opened above one of the operating drains which we mentioned earlier.

RESULTS

Soil characteristics of Mezőtúr study site

The soil texture determined from the Open-face Auger soil samples (at 97 points) is 88% heavy clay and 12% clay. Soil infiltration rate (k-factor) was determined from undisturbed soil samples above the examined single drain pipe at Mezőtúr site. The soil layers with the highest infiltration rate (1.3-18.8 mm/day) were located directly 20 cm above and below the drain pipe (Table 1).

Several layers of the soil profile above the drain pipe can be considered impermeable for water, as the water did not get through the undisturbed soil samples during the 15-day laboratory test period at all. Based on the evaluation of the total soluble salinity in the soil samples, moderately saline and saline soil levels (total water soluble salinity 0.3-0.74 m/m%) appear both below and above the drains. It limits the growth of roots of most cultivated crops, and thus
has a yield-reducing effect (Soni et al., 2021). The results show that soil layers shallower than 50 cm do not contain harmful amounts of salts. The appearance of soil levels with higher salinity showed a large variance under 50 cm. There is no clearly detectable difference in the drained and non-drained fields, but the deep salinity is characteristic at the Mezőtúr study site. Soil resistance and moisture content values are related to each other; i.e. drier soils are more difficult to penetrate. Tests can therefore be performed on nearly saturated soils. In case of high replication rates, the results of soil resistance were used to determine the location of compacted layer (plough pan), which can prevent precipitation or excess water from the surface to infiltrate to deeper layers.

Table 1 The infiltration rates over a single examined drain pipe

Soil depth [cm]	k-factor [mm/day]
0	0.1565
15	0.8
25	0.035
50	1.134
80	0.518
100	1.3
120	18.8

Identification of drain systems

In general, after a precipitation event, the wet and drier parts of the study sites were easily separable in the case of bare soil surface. Contrary to our expectations we could not observe linear traces on UAV images suggesting the presence of drains at Mezőtúr study site. We observed drain lines only on the examined orthophotos (Institute of Geodesy, Cartography and Remote Sensing of Hungary) e.g. around Kunszentmárton, Hungary (Fig. 4).
The Mezőtúr study site was also surveyed during the vegetation period, when NDVI maps were created to entrust the detection of developmental differences in plant

Fig. 4 Appearance of tile drain lines near Kunszentmárton, Hungary. The drawn lines on the bare soil continue on the surface with vegetation too, where the lines still could be observed due to differences in vegetation growth or species composition (source: Institute of Geodesy, Cartography and Remote Sensing of Hungary)

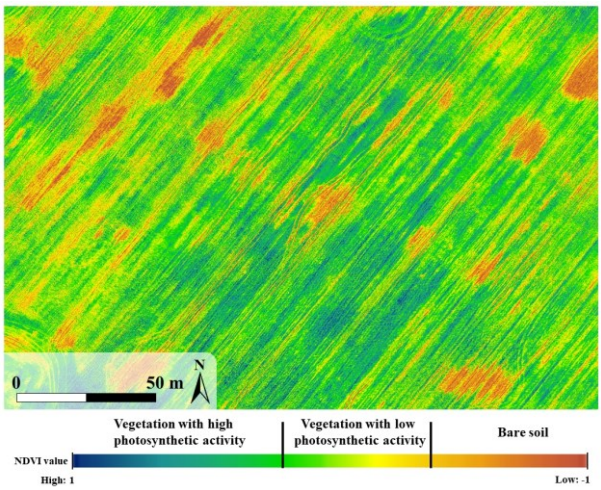

Fig. 5 Detail of the NDVI map of the Mezőtúr study site. The low NDVI values indicate the location of bare soil patches where the vegetation was destroyed by inland excess water

grown and phenophase. In April 2018, the soil moisture modifying effect of the drainage pipes on NDVI values could not be convincingly demonstrated. Due to the shallow roots of wheat grown in the area, the drainage pipes did not directly affect the moisture conditions to the near-surface root zone. At the same time, bare soil patches at the location of dried out inland excess water inundations or saturated soil conditions were very well observed (Fig. 5).

It should be noted that the appearance of inland excess water inundations fundamentally questions the efficiency of the operation of the drains, or the application of the correct agrotechnical treatments. In August 2018, an aerial photograph of a harvested alfalfa field right next to our pilot site was taken. Our experience suggests, that alfalfa had faster growth along the assumed soil drain pipes (Fig. 6). The original blueprint documentation reflects, that the pipes extend from the alfalfa field to the other plot with different land cover and land use, but there is no visible trace of them on that field. The reason for this phenomenon could be explained by the fact that alfalfa roots can penetrate into the deeper soil layers (as "bio-drains"), and thus they get better water supply along the drains. Similar phenomena can be experienced in stubble areas after crop harvest, where various weeds and volunteer crops indicate the location of drainage pipes. The UAV thermal imaging survey that was executed in March 2021 did not yield the expected results at Mezőtúr study site. The surface temperature showed no differences that suggesting the presence of drains.

Condition assessment of drains

During the first field survey (August, 2018) at the Mezőtúr test site, we found that only five drainpipe outlets were visible in the side slope of the channel. In situ inspection of the drain outlets was repeated three times. Finally, the number of identified drainage pipe outlets or their remains increased to 42 out of the 46 we found in the documentation of the area. In our experience, the documentation and the blueprints can only serve as an approximate reference for finding drain outlets. Contrary to the constant distance of 20 m stated in the plan documentation, various distances of 15-25 m between some pipes were found. In some cases, the PVC drain pipe outlets were melted, as the result of inappropriate maintenance of the channel: the farmer eliminated the excess vegetation by periodic burning (Fig. 7A). Despite of the critical injury of the pipelines, some pipes had outflowing drainage water. Other evidence of improper maintenance was a drain outlet (manufactured in 2012) that was found in the non-drained side slope of the channel, suggesting heavy disturbance (Fig. 7B).

Based on the results of the field inspections at Csanytelek and Zsadány sites, we concluded that the drain systems there are characterized by the same conditions and maintenance problems as at Mezőtúr plot. The Mezőtúr study site is unique, since here the outflow of drain pipes was visible, though their condition was unsatisfactory with a few exceptions. In the other two study sites, the drain outflows had already been destroyed and the pipe ends were buried in the side slope of the recipient channel. During the field survey at the Csanytelek site, no pipe outlets were found, but after the dredging of the drainage canal and removing the sludge,

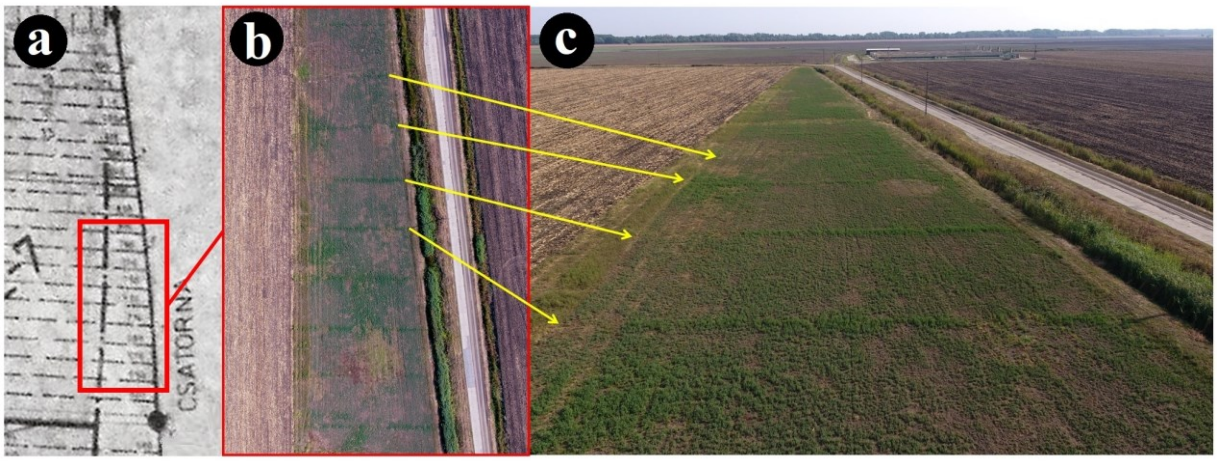

Fig. 6 Phenological differences in alfalfa plants over drains and the intermediate areas: (a) blueprint of the tile drains, (b) vertical aerial photo of the alfalfa field (UAV), (c) oblique aerial photo of the alfalfa field, where denser vegetation indicates the lines of the drain (UAV)

Fig. 7 Typical conditions of the drain pipes at the Mezőtúr study site: (a) melted PVC drain outlet in the channel side slope, (b) a few years old relocated drain pipe outlet, (c) open channel after sludge removal in Csanytelek, (d) ruptured drain pipe in spreaded sludge

some outlets were visible, as the excavator machine cut and teared the last sections of the pipes exposing them (Fig. 7C-D). In the case of the Zsadány study site, after the crop harvest the weeds in the field indicated the linear pattern of the drains. To verify their existence, the buried pipeline was excavated from the side slope of the recipient channel (Fig. 8).

In the Mezőtúr study site, endoscope camera inspections of five drain outlets gave good results. The condition of the inner tube was very good in the examined 4.5 m length (Fig. 9). Precipitates around the pipe perforations were visible, but these did not cause clogging. Most of the inspected drains were found free of dirt, but we also found a tube with sediment in the last 50 cm of the drain, at its outlet. The results suggest that drain pipes are permeable to water, and they can function. Along the recipient channel most of the drain outlets were damaged or buried, and they contained sediment. The causes of perforation clogging and precipitation on the drain pipes were also examined. We opened a soil section and performed a mechanical slope excavation, which proved that the perforations of the 30 years ago installed drain pipe are still permeable to water, i.e. they are free of blockages (Fig. 10).

Water quality of the drain and recipient waters

Compared to the recipient channel's water, nitrate, total nitrogen, total suspended solids, sulphate, calcium, magnesium and sodium appeared in excess in the drained water (Table 2). From the point of view of the Hungarian irrigation water classification (Filep, 1999), the collected inland excess water generated on the Mezőtúr study site had good quality, thus it diluted the water of the recipient channel. The results refer to wide range of parameters (Table 2). However, according to the analysis of the recipient water sample, its water quality was satisfactory

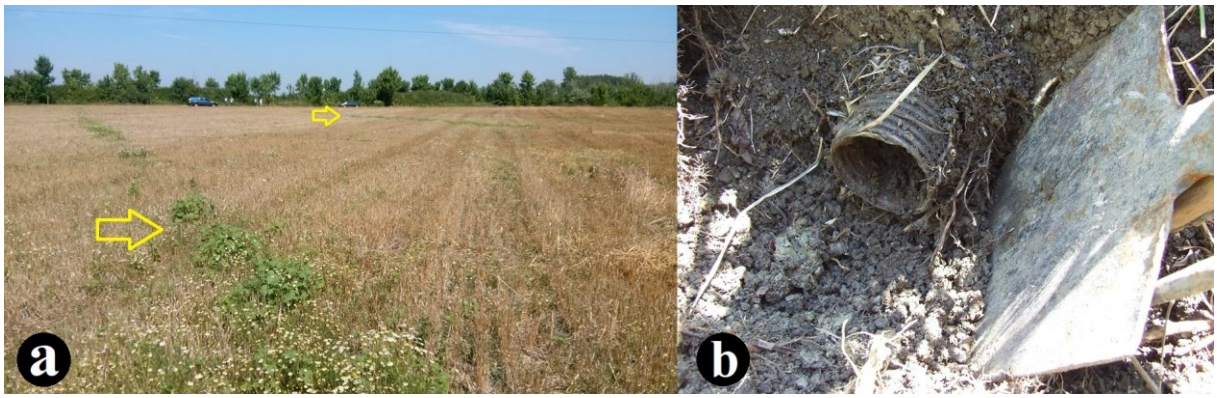

Fig. 8 Weeds indicate the location of the subsurface drain pipes (a) in Zsadány site. The same pipes were found buried in the recipient channel's side slope (b)

Fig. 9 The inspection of drain outlets and inner sections by endoscope camera

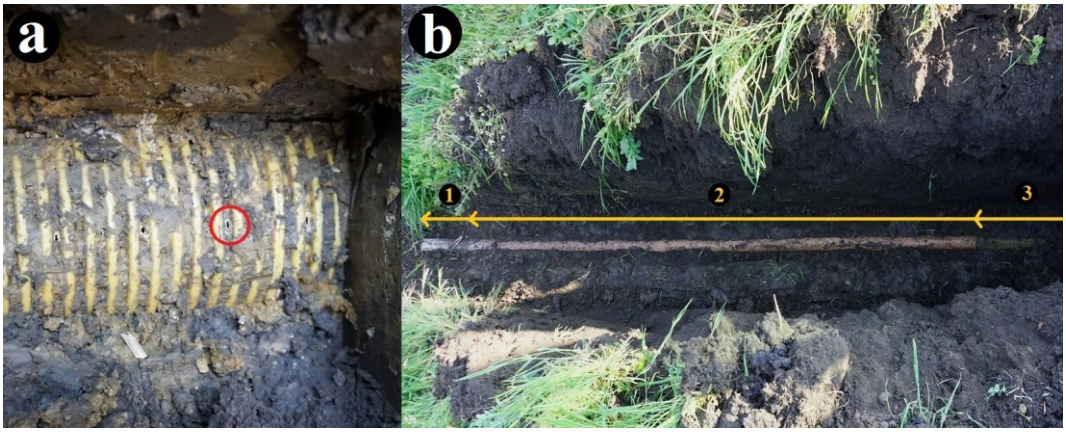

Fig. 10 Open perforations on drain tube (a), and the overview of one excavated pipe (b) with the following sections: (1) drain outlet, (2) intermediate pipe (not always applied), (3) perforated drain tube

to be used for irrigation quality improvement. This raises several environmental issues related to the protection of surface water, as mixed water from surface runoff and drainage effluent water has a direct and indirect impacts on the recipient. According to our results, in February 2018 the electrical conductivity (EC) of the drained water (mean: 2300 µS/cm) was almost three times higher than the values of the channel samples (mean: 780 µS/cm). In the samples from March 2018, in addition to the natural increases of the electrical conductivity values in both examined locations, the difference in mean values had only double (drained water: 3300 µS/cm; channel water: 1630 µS/cm). The increase in conductivity values from February to March can be related to the increase in ambient temperature or the duration of the high groundwater level. In terms of the electrical conductivity, the drainage water has 2-3 times higher values than the recipient water samples, which proves the role of drains in the loss of water-soluble plant nutrients from the soil (leaching)

DISCUSSION

On the selected study sites, various field and remote sensing methods were applied to assess the condition of the drained areas and to determine their future usability (Fig. 11). The evaluation was greatly facilitated by previous Hungarian research reports and results, mostly from the period 1981–1990, which were focused on the maintenance and proper operation of drain networks. Based on the results of our studies, we have drawn the following conclusions:

Babics's (1989) described ca. 150,000 ha of tile drained land in Hungary, however their extent did not change considerably in the last three decades. Tile drainage constructions were uncommon, but in some cases tile drainage was used as an accompanying element of linear irrigation plants. In our investigations, we reviewed a number of amelioration plan documentations and blueprints. However, among the documentations, we found only blueprints and descriptions of drain systems with free outflow (free drains). Unfortunately, the practice of controlled drainage, which is more widely used in other countries (Tolomio and Borin, 2019), has not developed in Hungary, except for at some experimental sites and farms. The favourable effect of tile drainage on crops which was reported by Bukovinszky et al. (1983) was not verifiable in our study sites. The vegetation modifying effect of tile drains was manifested only in the linear patterns experienced during UAV remote sensing data collection. Similar to the results of Tlapákova's (2015) research report, we found drainage trails on orthophotos which could be validated with the related blueprints. We also applied UAV thermal imagery, as described by Tlapákova (2017) but we did not get the expected results.

According to our results and experiences, we can state that intermittent outflow of inland excess water from the surface is not impeded by drainage pipes, but rather by soil with very poor water permeability. The soil is compacted in several layers, despite the fact that,

Table 2 Mean values of the analysed parameters of the water samples collected from the drains and from the recipient channel. (Only those parameters are indicated which showed large variations.)

		EC [µS/cm]	Nitrate [mg/l]	Total nitrogen content [mg/l]	Total suspended solids [mg/l]	Sulphate [mg/l]	Ca [mg/l]	Mg [mg/l]	Na [mg/l]
2018 February	drain	2300	130.5	34.5	14.25	1207	144	87.22	296.75
	channel	780	18.4	6.05	38	189	54.33	21.86	80
2018 March	drain	3300	46.1	12.35	88.6	2074	233.2	155.38	442
	channel	1630	6.7	2.85	37.25	569	133.5	52.72	178.5

according to the farmers, they apply chisel-plough in every 2–3 years. Based on these results, it is highly recommended to perform periodic deep cultivation or chisel-ploughing of the plot in order to improve the infiltration properties and the air-water balance of the soil. We agree with Fehér and Szalai's (1986) strict recommendations on the maintenance required for dual-operation of drains. However, we believe that following these recommendations is the basis of single operation drains.

It can be concluded, that nowadays the negligence of subsurface drainage works is common in Hungary, thus we assumed that the drain systems have lost their function in subsurface water management. Karásek et al. (2015) found that abandoned drained areas due to land use change may continue to function. Thus, for example, grasslands may dry out the soil more easily at a dry period. In our opinion, the impact and functionality of abandoned, non-maintained drainage systems is minimal. All these results prove that the subsurface water management interventions could work nowadays, while the beneficial effect of the complex melioration have been eliminated. The justification for the reactivation of drainage networks is unequivocal, but this cannot be generalized. It depends on the characteristics of the soils, actual weather conditions, and applied agro-technics. From the point of view of inland excess water management, the improvement of unfavourable soil infiltration conditions play key role in applying subsurface drainage. In this context, it becomes necessary to use suitable agrotechnical methods that facilitate the infiltration of excess water into the deeper soil layers, and to establish connection with the surface and subsurface drainage network. Another critical point is to ensure the longitudinal impermeability of the drains which typically results from the destruction and clogging of the outlets. Of course, maintenance work on open channel recipient systems cannot be omitted either. Taking these factors into account, the efficiency of the drains and the recipient channel of the studied Mezőtúr study site can be estimated as less than 50%, while the drainage network itself can be considered operational. The improvement of unfavourable infiltration conditions due to heavy textured soils requires a complex approach (agrotechnical interventions, chemical soil conditioning, appropriate surface water management and excess water control etc.). In the absence of these interventions, the regulation of groundwater and soil moisture cannot be realized even after the restoration of drainage systems and their recipient channels. Our water quality test results confirmed the findings of Shedekar et al. (2021) that drains are suitable for removing excess salts and agrochemicals from the tile drained plots, but we did not experience high discharge of drainage water at any of our study sites. The Mezőtúr study site is a typical example of cultivating an agricultural field without considering the possibilities and benefits of using the existing drainage network. We recommend two main treatment options and appropriate practices for using of drain networks in the future (Fig. 11).

The first way of possible application is further agricultural activity ignoring the existing drain network supplemented with the application of appropriate agrotechnics (e.g. chisel ploughing). Our other recommendation is further agricultural activity using the existing drain network, but it requires the following key steps for its success: restoration of drains and renovation of receiving channel; application of appropriate agrotechnics; prioritize proper maintenance of the drain network and channels; and training of farmers for proper operation of drain networks.

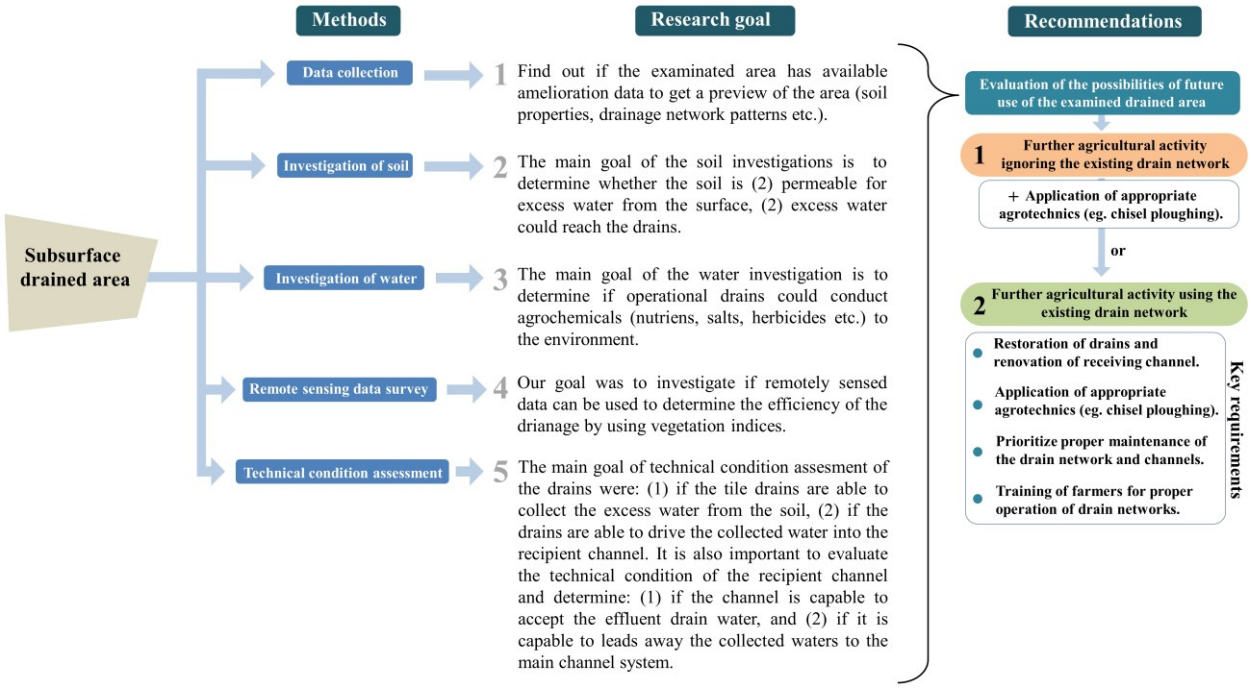

Fig. 11 Flow chart of the applied methods and their research goals to assess subsurface drain systems. The figure also includes our recommendations for the future use of drained areas

CONCLUSIONS

Our aims were to evaluate whether the location of the installed drainage networks can be delineated, whether their operational efficiency can be assessed, and whether they have a role in field-level drainage, water supply, or water retention. The combined methods applied in this survey are recommended to survey the condition of other tile drained areas and they could be adapted for their complex evaluation. Based on these results, interventions that are essential to make a drain system functional can be categorized into (1) reconstruction and (2) construction of new drainage systems of drained areas of any kind have a right to exist only with proper maintenance and operation. Given that 150,000 ha of subsurface drainage has been implemented in Hungary, with about 300,000 ha of buffer area, the reactivation of drained areas combined with the appropriate agro-technics would greatly contribute to maintaining production safety in agriculture.

ACKNOWLEDGEMENTS

This study was founded by Ministry of Agriculture (O14230 Development of agricultural water management – irrigation and excess water management, land use rationalization). Sampling instruments were provided by GINOP 2.3.3-15-2016-00042 project. Access to the original amelioration and drainage plan documentation was provided by Békés County Water Authority. We would like to thank to our colleagues at MATE KÖTI ÖVKI and Dr. Károly Barta, and Dr. Zalán Tobak for their technical support in the field and laboratory work.

REFERENCES

Babics, T. 1989. Jet-clean of tile drains. (Drének öblítéses tisztítása) *Melioráció – öntözés és tápanyaggazdálkodás* 8 (1) Agroinform, Budapest. ISSN 0238-8979, 15–17. (In Hungarian)

Barta, K., Bata, T., Benyhe, B., Brkic, M., Dogan, V., Dolinaj, D., Farsang, A., Norbert, G., Henits, L., Juhász, L., Kiss, T., Kovács, F., Mezosi, G., Mucsi, L., Mészáros, M., Obradovic, D., Pavic, D., Rakonczai, J., Savić, S., Zivanov, M. 2013. Inland Excess Water – Belvíz – Suvišne Unutrašnje Vode. 154 p., Szeged – Novi Sad, DOI:10.13140/2.1.5143.3920

Bognár, N., Geredy, E. 1989. Experimental observation of a double operation subsurface drain system on heavy texture soil. (Kettős működésű talajcsőrendszer kísérleti megfigyelése kötött talajon). *Agrokémia és talajtan*, 38 (1-2), 294–298. ISSN 0002-1873 (In Hungarian)

Brandyk, T., Skapski, K., Szatylowicz, J. 1993. Design and operation of drainage-subirrigation systems in Poland. *Irrigation and Drainage Systems* 7, 173–187. DOI:10.1007/BF00881278

Bukovinszky, L. 1983. Planning problems and possibilities of performance increase after amelioration. (A melioráció utáni teljesítménynövekedés tervezési problémái és lehetőségei) *Melioráció – öntözés és tápanyaggazdálkodás* 2 (3), Agroinform, Budapest. ISSN 0230-9203, 17–20. (In Hungarian)

Bukovinszky, L., Kun, A., Rekesztő, P. 1983. The effect of drainage and tillage on crop yields and soil salt balance in solonetz soils. (A drénezés és a talajművelés hatása a terméseredményekre és a talaj sóforgalmára szolonyeces réti talajon). *Melioráció – öntözés és tápanyaggazdálkodás* 2 (3), Agroinform, Budapest. ISSN 0230-9203, 13–17. (In Hungarian)

Csaplár, K. 1989. Investigation of the usability of subsurface drain systems for water retention and groundwater control. (Talajcsőrendszerek vízpótlásra való felhasználásának vizsgálata) *Melioráció – öntözés és* tápanyaggazdálkodás 8 (1), Agroinform, Budapest. ISSN 0238-8979, 40–46. (In Hungarian)

Djurović, N., Stričević, R. 2004. Actual state of drainage system on the experimental field "Radmilovac" and priority works to be done for the improvement of its working characteristics. *Journal of Agricultural Sciences (Belgrade)* 49, 169–177. DOI:10.2298/JAS0402169D

Fehér, F. 1979. Development of subsurface drainage works on cultivated lowland areas. (A síkvidéki, mezőgazdasági táblán belüli vízelvezető elemek fejlesztése) *Hidrológiai Közlöny* 59 (11), 519–523. (In Hungarian)

Fehér, F., Szalai, Gy. 1986. Actual tasks of land amelioration research, planning and practice development in agricultural fields. (A meliorációs kutatás, tervezés és gyakorlat fejlesztésének időszerű feladatai mezőgazdasági területeke) *Hidrológiai Közlöny* 66 (3), 128–132. (In Hungarian)

Filep, Gy. 1999. Quality and qualification of irrigation waters. (Az öntözővizek minősége és minősítése) *Agrokémia és Talajtan*. 48 (1-2). 49-63. ISSN 0002-1873 (In Hungarian)

Forgóné, N. M. 1996. Impact of land amelioration interventions on the water management and salt balance of soils. (A meliorációs beavatkozások hatása a talajok vízgazdálkodására és sóforgalmára) *Hidrológiai Közlöny* 76 (2), 84–88. (In Hungarian)

Gray, W., Miller, C. 2004. Examination of Darcy's Law for Flow in Porous Media with Variable Porosity. *Environmental Science & Technology* 38, 5895–5901. DOI:10.1021/es049728w

Hornyik, B. 1984. Multipurpose application of subsurface drainage at the Tiszántúl area. (Többcélú talajcsövezés a Tiszántúlon) *Melioráció – öntözés és tápanyaggazdálkodás* 3 (1), Agroinform, Budapest. ISSN 0231-410 X, 8–13. (In Hungarian)

Jiang, Q., Qi, Z., Xue, L., Bukovsky, M., Madramootoo, C., Smith, W. 2019. Assessing climate change impacts on greenhouse gas emissions, N losses in drainage and crop production in a subsurface drained field. *Science of The Total Environment* 705, 135969. DOI:10.1016/j.scitotenv.2019.135969

Karásek, P., Tlapáková, L., Podhrázská, J. 2015. The location and extent of systematic drainage in relation to land use in the past and at present and in relation to soil vulnerability to accelerate infiltration in the protected landscape area Železné hory. *Acta Universitatis Agriculturae Et Silviculturae Mendelianae Brunensis* 63 (4), 1121–1131 DOI:10.11118/actaun201563041121

Koganti, T., Van De Vijver, E., Allred, B., Greve, M., Ringgaard, J., Iversen, B. 2020. Mapping of Agricultural Subsurface Drainage Systems Using a Frequency-Domain Ground Penetrating Radar and Evaluating Its Performance Using a Single-Frequency Multi-Receiver Electromagnetic Induction Instrument. *Sensors* 20, 3922. DOI:10.3390/s20143922

Lendvai, Z., Avas, K. 1983. Investigation of nutrient leaching in tile drained areas. (Tápanyagkilúgzás vizsgálata talajcsövezett területeken) *Melioráció – öntözés és tápanyaggazdálkodás* 2 (2), Agroinform, Budapest. ISBN 963502-253-0, 48–52. (In Hungarian)

Luo, W., Sands, G., Youssef, M., Strock, J.S., Song, I., Canelon, D. 2010. Modeling the impact of alternative drainage practices in the northern Corn-belt with DRAINMOD-NII. *Agricultural Water Management*. 97. 389–398. DOI:10.1016/j.agwat.2009.10.009

Maticic, B., Steinman, F. 2007. Assessment of land drainage in Slovenia. *Irrigation and Drainage* 56. S127–S139. DOI:10.1002/ird.338

Mile, S. 1986. Recent experiences of water recharge of soil through the tile drains in Békés County. (A drénen keresztül történő vízvisszapótlás újabb tapasztalatai Békés megyében) *Melioráció – öntözés és tápanyaggazdálkodás* 5 (3), Agroinform, Budapest. ISSN 0231-410 X, 43–50. (In Hungarian)

Molnár, E. 1987. The main directions of soil moisture regulation researches at the XIII. International Congress of Soil Science Society. (A talajnedvesség szabályozási kutatások főbb irányai a nemzetközi talajtani társaság XIII. Kongresszusa tükrében) - A talajnedvesség szabályozásának lehetőségei drénezéssel a Magyar Alföldön. *Melioráció – öntözés és tápanyaggazdálkodás* 6 (1), Agroinform, Budapest. ISSN 0231-410 X, 35–38. (In Hungarian)

Nyiri, L., Fehér, F. 1977. Information about the researches at the complex amelioration pilot site in Karcagpuszta, Hungary. (Tájékoztató a Karcagpusztai komplex meliorációs

modelltelepen folyó kutatómunkáról) Kézirat. DATE KI, Karcag. (In Hungarian)

Shedekar, V.S., King, K.W., Fausey, N.R., Islam, K.R., Soboyejo, A.B.O., Kalcic, M.M., Brown, L.C. 2021. Exploring the effectiveness of drainage water management on water budgets and nitrate loss using three evaluation approaches. *Agricultural Water Management* 243, 106501 DOI: 10.1016/j.agwat.2020.106501

Singh, R; Helmers, M., Qi, Z. 2006. Calibration and Validation of DRAINMOD to Design Subsurface Drainage Systems for Iowa's Tile Landscapes. *Agricultural Water Management*, 221–232. DOI:10.1016/j.agwat.2006.05.013

Smith, D.R., King, K.W., Johnson, L., Francesconi, W., Richards, P., Baker, D., Sharpley, A.N. 2015. Surface Runoff and Tile Drainage Transport of Phosphorus in the Midwestern United States. *Journal of Environmental Quality* 44 (2), 495–502 DOI:10.2134/jeq2014.04.0176

Sojak, M., Ivarson, K.C. 1980. Iron and Manganese Oxide problems in tiledrains. Factsheet (Ontario. Ministry of Agriculture and Food) pp. 3.

Sojka, M., Kozłowski, M., Kęsicka, B., Wróżyński, R., Stasik, R., Napierała, M., Jaskuła, J., Liberacki, D. 2020. The Effect of Climate Change on Controlled Drainage Effectiveness in the Context of Groundwater Dynamics, Surface, and Drainage Outflows. Central-Western Poland Case Study. *Agronomy* 10, 625. DOI:10.3390/agronomy10050625

Soni, S., Kumar, A., Sehrawat, N., Kumar, A., Kumar, N., Sharma, C., Mann, A. 2021. Effect of saline irrigation on plant water traits, photosynthesis and ionic balance in durum wheat genotypes. *Saudi Journal of Biological Sciences* 28, DOI:10.1016/j.sjbs.2021.01.052

Szinay M. 1983. Data of tile drained areas from some European countries, and Hungary. (Néhány európai ország talajcsövezési adatai és a hazai értékelés). *Hidrológiai Tájékoztató* 23 (2), 16–17. (In Hungarian)

Tlapáková, L., Žaloudík, J., Kolejka, J. 2017. Thematic survey of subsurface drainage systems in the Czech Republic. *Journal of Maps* 13 (2), 55–65. DOI:10.1080/17445647.2016.1259129

Tlapáková, L., Žaloudík, J., Kulhavý, Z., Pelíšek, I. 2015. Use of Remote Sensing for Identification and Description of Subsurface Drainage System Condition. *Acta Universitatis Agriculturae et Silviculturae Mendelianae Brunensis* 63, 1587–1599. DOI:10.11118/actaun201563051587

Tolomio, M., Borin, M. 2019. Controlled drainage and crop production in a long-term experiment in North-Eastern Italy. *Agricultural Water Management* 222 (2019) 21–29. DOI:10.1016/j.agwat.2019.05.040

Transforming Drainage Project. Online available at: https://transformingdrainage.org

Van Leeuwen, B., Henits, L., Mészáros, M., Tobak, Z., Szatmári, J., Pavic, D., Savić, S., Dolinaj, D. 2013. Classification Methods for Inland Excess Water Modeling. *Journal of Environmental Geography* 6 (1-2), 1–8. DOI:10.2478/v10326-012-0001-5

Wittmann, M., Szalai, S., Regős, F., Rupert, T., Szalóki, L., Primás, A., Gróf, M., Ughy, Gy. 1981. Cadastre of subsurface drained areas of Hungary. (Magyarország talajcsövezett területeinek katasztere) Vízgazdálkodási Intézet IV. Szakágazati Iroda, Vízrendezési és Mezőgazdasági Vízellátási Osztály. Budapest. 1–159. (In Hungarian)

sciendo

Journal of Environmental Geography 14 (3–4), 26–38.

DOI: 10.2478/jengeo-2021-0009
ISSN 2060-467X

SELF-HEATING COAL WASTE FIRE MONITORING AND RELATED ENVIRONMENTAL PROBLEMS: CASE STUDIES FROM POLAND AND UKRAINE

Ádám Nádudvari[1*], Anna Abramowicz[1], Justyna Ciesielczuk[1], Jerzy Cabała[1], Magdalena Misz-Kennan[1], Monika Fabiańska[1]

[1]University of Silesia, Faculty of Natural Sciences, 60 Będzińska Street, 41-200 Sosnowiec, Poland
*Corresponding author, email: adam.nadudvari@us.edu.pl

Research article, received 5 September 2021, accepted 11 October 2021

Abstract

The self-heating of coal waste dumps is considered as a serious environmental issue, wherever active or inactive coal mining has been present. This issue is introduced from two active coal mining regions from Poland (Upper Silesian Coal Basin) and Ukraine (Donetsk Coal Basin) based on mineralogy, organic petrography and geochemistry, and remote sensing techniques. Thermally affected coal wastes reveal changes recorded by organic and mineral matter. Irregular cracks and fissures appear within and at the edges of organic matter particles, which are oxidised, devolatilised and plasticised. Mineral phases underwent oxidation, dehydration, structure rebuilding and recrystallisation. Highest temperatures generated during the fire cause melting and paralava formation. During self-heating, some chalcophile elements like Hg (mostly present as HgS), Pb, Zn can be enriched and released, or different organic pollutants like phenols (originated from vitrinite particles), different PAHs with alkyl substitutes, chlorinated PAHs, or sulphur heterocycles are formed. The introduced remote sensing techniques helped to localise and monitor hot spots with different temperature ranges. Applying SWIR bands of Landsat hot spots from extremely burning dumps in Ukraine were successfully localised, however, only night-time scenes with SWIR can be used. The sun's disturbing effects should be considered as an influential factor for both thermal imaging camera or satellite images. Thermal cameras can reveal the most detailed signs of low to high temperature anomalies with different cracks and line shapes.

Keywords: coal waste dumps, self-heating, remote sensing, organic – inorganic pollutants

INTRODUCTION

Coal wastes are produced during coal mining and coal processing. Usually, such wastes contain 5–30% organic matter and ca 70–95% of minerals, mainly sulphides (e.g., pyrite or sphalerite), alumino-silicates, carbonates, and other minerals rich in heavy metals (Skarżyńska, 1995; Finkelman, 2004; Huang, 2004; Sütő et al., 2007; Zhao et al., 2008a, 2008b; Kang et al., 2011; Xiao et al., 2015). After deposition in dumps located in close vicinity of coal mines, the waste starts to weathering what might lead to the exothermic oxidation of the organic mater known as self-heating, which may lead to self-ignition (Zhang and Kuenzer, 2007; Carras et al., 2009; Masalehdani et al., 2009; Misz-Kennan and Fabiańska, 2011). Susceptibility to self-heating is increased by air temperature, wind, organic-matter rank, ash content, surface area exposed to air, particle size, moisture and oxygen content, shape, layering and compaction of the dumped pile (Skarżyńska, 1995; Lohrer et al., 2005; Pone et al., 2007). In the case of bituminous or sub-bituminous coals and coal wastes, the temperature increases slowly until a threshold temperature of 60–80°C, and then the temperature rises fast, followed by self-ignition and burning of the waste. The temperature inside a coal waste dump is typically highly variable ranging from ambient to ~ 500°C, however, at the end stages of heating in the subsurface, the self-combustion temperatures can reach up to 1000–1300°C (Carras et al., 1994, 1999; Skarżyńska 1995; Heffern and Coates 2004; Sütő et al., 2007; Querol et al., 2008; Ribeiro et al., 2010; Jendruś 2016).

Coal-waste dumps, are typically occupying large areas and are located nearby urban areas, thus they have potential health and environmental impacts (Querol et al., 2008; Zhang, 2008; Zhao et al., 2008b; Li, 2010; Liu and Liu, 2010; Li et al., 2011; Zhou et al., 2014; Nádudvari et al., 2020a, 2021b). Toxic elements in coals are associated with organic matter and minerals, e.g., clays and sulphides (Vassilev et al., 2001; Ciesielczuk et al., 2014). Such waste dumps emit enormous quantities of greenhouse gases: CO_2, CH_4, and such harmful compounds as NO_x, NH_3, SO_x, H_2S, HCl, CH_2O, benzenes, phenols, PAHs, heavy metals (Kruszewski et al., 2018, 2020; Nádudvari et al., 2021b). In the dumps elevated Hg (~100–1078 mg/kg) and Pb concentrations (~600–2000 mg/kg) can be reached, reflecting evaporation of these metals from deeper parts of the dumps. The acidic pH levels (3.0–4.5) may help to mobilise these elements (Nádudvari et al., 2021b).

The aim of the paper is to describe and understand the complex processes occurring within coal waste dumps based on organic petrography, mineralogy, and organic geochemistry and combine remote sensing techniques. On the selected Polish dumps the ongoing self-heating was well documented e.g. Misz-Kennan and Fabiańska (2011), Nádudvari (2014), Fabiańska et al. (2019),

Kruszewski et al. (2018) and Nádudvari et al. (2018, 2021, 2021b) therefore these researches were provided good insight about the state of self-heating, pollution levels – especially heavy metals e.g. Hg, Pb or organic pollutants: benzene, phenols, PAHs. In Poland and Ukraine many of those coal waste dumps are surrounded by urban areas (Fig. 1), so their self-heating pose a serious threat to the local community through, among others, environmental pollutions, odorous smells and surface collapsing. Therefore the application of remote sensing techniques and thermal imaging cameras are crucial to protect society - prevent self-heating, conduct its proper monitoring and warn about the hazard.

STUDY AREA

The self-heating phenomenon of coal waste dumps most often occurs in coal basins, where the large number of dumps are created near the coal mines. In this paper, we focus on some of the largest coal basins in Europe: Upper Silesian Coal Basin (USCB; southern Poland) and Donetsk Coal Basin (DCB; eastern Ukraine) (Fig. 1). In both basins, large-scale coal mining began in the 19th century. Since then, many dumps have been created there, which have subsequently undergone numerous processes. As the waste in both cases came from coal mines, their composition was relatively similar. The coals of the DCB and USCB are from bituminous coal to anthracite and have high ash yields and high sulfur contents (Panov et al., 1999; Kędzior, 2019). The dumps in USCB are characterised by enormous diversity in the area, volume, and shape. These objects often fit well into the highly urbanised landscape (especially in the Katowice district). In the DCB case, dumps have large-area with a typically conical structure (for this reason such dumps are often called as Donetsk type – Fig. 1D). These dumps stand out above the landscape, towering over the surrounding settlements. Regardless of the differences and similarities between the two basins, the self-heating phenomenon was detected in both regions, and its impact on the natural environment and society was determined (Panov et al., 1999; Fabiańska et al., 2019; Nádudvari et al., 2018, 2020a, 2021b; Abramowicz et al., 2021).

METHODS

Approx. 500–1000 g were taken from the dumps up to 10 cm-s depth and collected/stored in alumina foil to prevent other organic matter contamination. Samples were manually cleaned from roots, wood tissues and dried at room temperature (ca 22°C) for ca. 5 days. After they were uniformed and about 200 g milled and powdered in a rotary mill very fine grain size. These samples were used for GC-MS analysis.

For petrographic analyses the samples were air dried, crushed to < 1mm, embedded in epoxy resin and polished blocks were prepared. Sometimes also oriented fragments of coal wastes were embedded in epoxy resin, and polished blocks were prepared. Samples were examined in reflected white fluorescent light. That allows to identify various macerals and forms of alteration of organic matter. The identification was carried out at 500 points in each sample according to ISO 7404-3 (2009). At the same time, minerals and mineral phases were identified. The aim of petrographic investigations was to establish the maceral composition of the wastes and their degree of alteration. Reflectance measurements were carried out at 50–100 points on each sample depending on

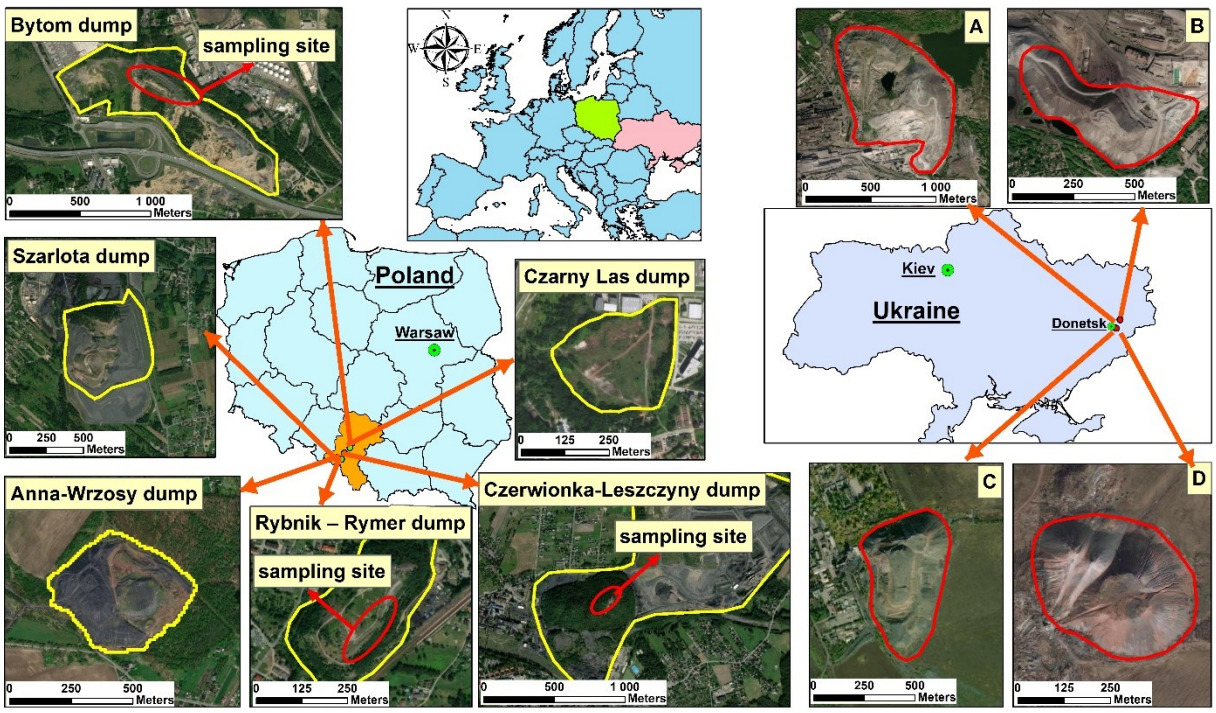

Fig. 1 Location of the studied coal wastes dumps from Poland and Ukraine. Background map: GoogleEarth – 2021

the number of available particles and according to ISO 7404-5 (2009). The vitrnite reflectance was aimed to determine the rank of original organic matter and their thermal alteration. It was done using Axioplan II optical microscope equipped with immersion objective and applied magnification of 500X.

Gas chromatography-mass spectrometry (GC–MS) samples were powdered (ca 18–20 g) and extracted using dichloromethane (DCM) and methanol (1:1) with an ultrasonic bath at 30–40°C for 15–20 min. The extracts were pooled, filtered, and the solvents evaporated at room temperature. The dry residue was dissolved in 0.5 ml of DCM and analysed by GC-MS an Agilent Technologies 7890A gas chromatograph and Agilent 5975C Network mass spectrometer with a Triple-Axis detector (MSD) at the Institute of Earth Sciences, Faculty of Natural Sciences, University of Silesia. Helium (grade 6.0) was used as a carrier gas at a constant flow of 2.6 ml/min. Separation was obtained on fused silica capillary column, DB-5 (60 m × 0.25 mm i.d.; film thickness 0.25 μm) coated with a chemically bonded phase (5% phenyl, 95% methylsiloxane), for which the GC oven temperature was programmed from 45 (1 min) to 100°C at 20 °C/min, then to 300°C (held for 60 min) at 3°C/min, with a solvent delay of 10 min. The GC column outlet was connected directly to the ion source of the MSD. The GC–MS interface was set at 280°C, while the ion source and the quadrupole analyser were set at 230 and 150°C, respectively. Mass spectra were recorded from 45 to 550 da (0–40 min) and 50 to 700 da (> 40 min). The MS was operated in the electron impact mode, with an ionisation energy of 70 eV. The results were obtained in full scan mode and processed with the Hewlett-Packard Chemstation software. The studied compounds were identified according to their mass spectra (using peak areas acquired in the manual integration mode), by comparison of peak retention times with those of standard compounds, by interpretation of MS fragmentation patterns, and from mass spectral databases GEOPETRO, NIST17 (National Institute of Standards and Technology) and Wiley (W10N11) (Philp, 1985; McLafferty and Stauffer, 1989).

Mineral phase identification was established using X-ray diffraction and scanning microscopy. Powdered samples were determined using a fully automated X-ray Philips PW 3710 diffractometer operated at 45 kV and 30 mA, CuKα radiation, and equipped with a graphite monochromator. Mineral morphologies and spatial relationships between components were examined in thin sections and samples fragments using a Philips XL 30 ESEM/TMP scanning electron microscope in environmental mode, coupled with an energy-dispersive spectrometer (EDS; EDAX type Sapphire). Analytical conditions of the SEM included: accelerating voltage of 15 kV; a working distance of ca 10 mm; counting time of 40 s. All these researches were carried out at the Faculty of Natural Sciences, University of Silesia, Sosnowiec, Poland.

The remote sensing and thermal camera monitoring possibilities of self-heating coal waste was applied by Landsat satellite and thermal camera images. Application of remote sensing for such hot spots must be taken into account solar influences (e.g., different albedo, slope, aspect or vegetation cover) can significantly influence thermal anomalies (Zhang and Kuenzer, 2007). However, extended observation permits persistent heat sources due to self-heating to be recognised, as well as their migration, intensification, and disappearance, when they are hot enough for detection with satellite sensors (Nádudvari, 2014). Using the Thermal Infrared Sensors (TIRS) of satellite images, i.e., Landsat series, ASTER is the cost-effective and time-saving technique for monitoring coal waste fires and detecting their thermal anomalies. Several authors have successfully applied Landsat, ASTER night-time and winter-time images for localising such coal- or coal-seam fires worldwide (e.g., Voigt et al., 2004; Gangopadhyay et al., 2005; Chatterjee, 2006; Zhang and Kuenzer, 2007; Prakash et al., 2011; Guha and Kumar, 2012). Therefore, to monitoring such coal waste fires, only night-time and/or daylight snow-covered images should be used (Nádudvari et al., 2021a). The most effective sensor for hot spot detection is Landsat 7 ETM+ as the TIRS band has 60 m resolution compared with Landsat 4-5 TM (120 m) or Landsat 8 OLI (100 m) because ETM+ can detect properly smaller hot spots which Landsat 8 OLI, or TM cannot. However, adding the SWIR (short wavelength infrared) bands (30 m) can precise the TIRS temperatures (Nádudvari et al., 2020b). Lower temperature phenomena, such as small ground thermal anomalies, must be studied in the thermal infrared (TIR) window (8–14 μm) (Bonneville et al., 1985; Bonneville and Kerr 1987). Self-heating can also be classified using the self-heating intensity index (SHII) introduced by Nádudvari et al. (2021a). It can be calculated from the highest (pixel max), and lowest (pixel min) values based on the area of a coal waste dump taken from Landsat, ASTER (TIRS) bands. This index can help to classify the fires of ongoing self-heating where snow-covered or night-time Landsat, ASTER images are available (Nádudvari et al., 2021a). However, in the case of daylight cold, snow-covered images, the albedo, solar radiation, slope and aspect can significantly impact the thermal anomalies. That can indicate low thermal activity, which is usually visible on Landsat thermal map with a 2–3°C difference between pixel max (hot spot)—pixel min (cold, snow-covered surface with no thermal activity). Hot spots with lower thermal activity or their extensions smaller than the TIRS satellite sensor capabilities making difficult to detect such hot surfaces (Nádudvari and Ciesielczuk, 2018; Nádudvari et al., 2021a).

Pictures from the camera mounted on the drone can reach a resolution of several centimetres, therefore such measurements provide the best option to monitor self-heating dumps. It is mainly due to the distance of the measuring device from the measured surface and the specification of used devices. Pictures from the drone can be planned depending on weather and terrain conditions. On the other hand, generally available satellite images are taken at specific times and under a fixed lens setting, regardless of weather and terrain conditions. It introduces additional uncertainty to the results presented by the satellite images and necessitates appropriate corrections (e.g., radiometric calibration, atmospheric correction, etc.).

RESULTS AND DISCUSSION

Coal petrography

All components present in coal wastes were divided into mineral and organic particles. Mineral particles are composed of minerals and various mineral phases and quantitatively usually dominate in coal wastes. Organic particles are composed of organic matter that was altered to various degrees (Misz-Kennan et al., 2020). With regard to various levels of alteration organic matter is further divided into three groups: unaltered (1), altered (2) and newly formed (3).

The first group in coal wastes is representing the original organic matter i.e. huminite/vitrinite, liptinite and inertinite maceral groups (Fig. 2A) showing the same optical features (colour in reflected light, reflectance, fluorescence, morphology) as unaltered macerals. For their further division the terminology described in, ICCP (1998, 2001), Sýkorová et al. (2005) and Pickel et al. (2017) was used.

In second group (altered particles), the particles showing such signs of the alteration as paler colour, paler/darker colour oxidation rims, cracks and fissures, plasticised edges and higher vitrinite reflectance

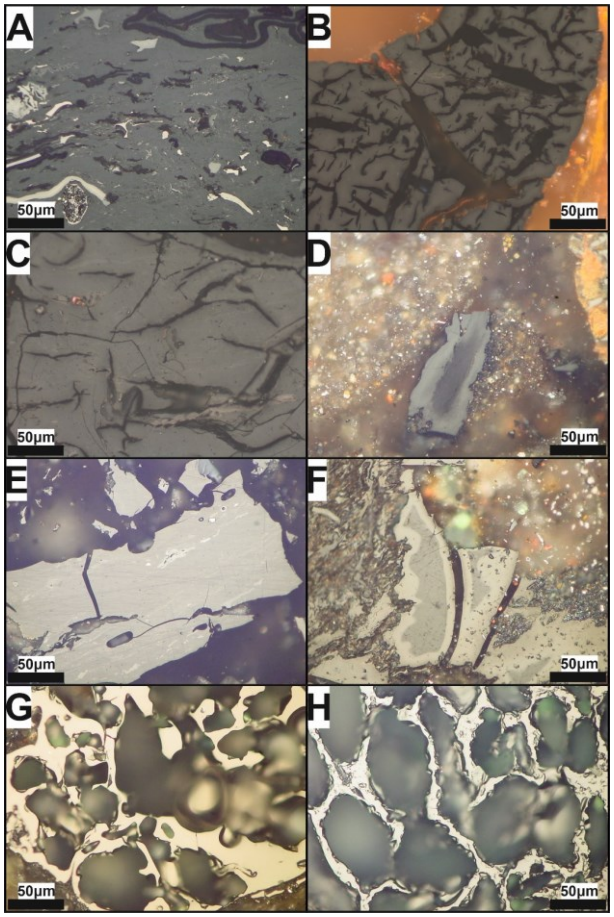

Fig. 2 Characteristic forms of self-heated coal wastes from Upper Silesian Coal Basin. A: well-preserved trimacerite particle; B – C: irregular crack with oxidation rims; D – F: thermally altered particles with paler oxidation rims; E: particle with devolatilisation and plasticised edges in paler colour caused by temperature; G – H: chars containing randomly distributed pores.

(Misz et al., 2007; Misz-Kennan, 2010; Misz-Kennan and Fabiańska, 2010, 2011; Ribeiro et al., 2016; Misz-Kennan et al., 2020). Cracks and fissures occur within the particles, and their size varies from a few to a few tens of µm (Fig. 2B, C and F). Cracks can also occur perpendicular to the edges of particles (Fig. 2C). Oxidation rims that are paler with higher reflectance or darker with lower reflectance comparing to the central part of the particles occur around the edges and/or around the cracks and fissures (Fig. 2F). With prolonged oxidation, gradually, the whole particle becomes paler in colour (Fig. 2E). Some particles have rounded edges caused by the plasticity of organic matter that was a consequence of a higher heating rate. Oxidation rims can also occur around such plasticised edges (Kus and Misz-Kennan, 2017). Another form of alteration are pores caused by devolatilisation that are usually round or oval, and their size varies from a few to a few tens of µm. Their presence causes the classification of the particle as porous, while the absence of pores makes the particle massive (Misz-Kennan, 2010; Misz-Kennan et al., 2020).

The third group contains particles representing products of low-temperature oxidation, self-heating or self-combustion. The following forms are included in this group: pyrolytic carbon forming from condensation of organic compunds previusly released from decomposition of organic matter (Kwiecińska and Pusz, 2016); bitumen being a product of expulsion of hydrocarbons from organic matter, mostly liptinite and vitrinite, during self heating, occurring as small droplets and /or thread like structures (Misz et al., 2007; Misz-Kennan, 2010; Misz-Kennan and Fabiańska, 2010, 2011) or can fill cracks and various empty spaces (Gentzis and Goodarzi, 1989; Alpern et al., 1992; Jacob, 1993; Sýkorová et al., 2018) and appearing in fluorescent with yellow – oragne to light green colour (Nádudvari and Fabiańska, 2016). Chars derived largely from vitrinite and inertinite as product of self-heating or spontaneous combustion and containing randomly distributed pores (Kwiecińska and Petersen, 2004; Lester et al., 2010). Graphite mostly formed from precipitation of carbon-saturated C–O–H fluids as product of self-heating or spontaneous combustion (Kwiecińska and Petersen, 2004). Coke formed from organic matter heated in the strongly limited access of air and hardened into coke as a product of self-heating or spontaneous combustion (Kwiecińska and Petersen, 2004; Suárez-Ruiz and Crelling, 2008).

The presence of individual forms of organic matter gives an indication of the heating history of the dumps (Fig. 2). The presence of unaltered organic matter suggests that the wastes were recently deposited or were not influenced by oxidation/weathering (Fig. 2A). The paler the colour of the forms and higher reflectance indicates thermal alteration (Fig. 2D and F). Massive forms suggest that the heating rate was low, while the presence of porosity caused by devolatilisation and plasticised edges suggests a higher rate of temperature increase within the dump (Fig. 2E). Moderately altered organic matter in the wastes has irregular cracks and fissures, cracks perpendicular to the edges of particles, paler/darker in colour oxidation rims forming around the edges and/or cracks (Fig. 2B and C), and chars formed by

high temperatures during self-heating – combustion (Fig. 2G and H).

Mineralogy

The mineral composition of coal wastes deposited in dumps in the Upper Silesian Coal Basin reflects the primary composition of gangue rocks and mineral matter associated with coal seams. They are quartz, clay minerals as illite, montmorillonite or kaolinite, chlorite, micas, mainly muscovite with associated dispersed organic matter. Subordinately occur Na- and K-feldspars, carbonates such as calcite, dolomite, siderite or siderite-magnesite, framboidal pyrite, and accessory zircon, monazite and xenotime. Self-heating and self-ignition processes that led to short or long-termed coal-waste fire with or without oxygen access can modify the primary mineral composition. Structures of mineral phases which are not stable at higher temperatures can be destroyed, and amorphous and metastable phases formed. Highest temperatures can lead to melting and paralava formation (Ciesielczuk et al., 2014, 2015; Pierwoła et al., 2018). Overburned parts of the dumps dominate in combusted phases as cristobalite-tridymite, celsian, anorthite, cordierite, indialite, mullite, olivine, augite, spinel group, hematite, and glass. Minerals as anatase, lead, zinc, iron sulphides and chalcopyrite occur in traces. Exhalating phases with sal ammoniac, native sulphur and K-, Mg-, Fe-, NH_4-, Al-sulphates, and chlorides are blooming around vents. Additionally, gypsum, bassanite and goethite can form due to weathering (Fig. 3-4).

Heavy metals in coal wastes are associated with silicates (especially clays), carbonates, sulphides, oxides, and phosphates (Swaine, 1994). Chalcophile elements, i.e. As, Se, Cd, Cu, Pb, Zn, Hg, are associated with sulphide minerals as chalcopyrite ($CuFeS_2$), galena (PbS), and sphalerite (ZnS) or as organically-bound species (Taylor et al., 1981; Raask, 1985; Finkelman, 1995; Monterroso and Macias, 1998). Pyrometamorphic and weathering processes influence the chemical composition of the wastes. During combustion, As, Hg, Se, and Cd can be released from sulphide minerals as these elements are highly volatile (Zhou and Ren, 1992; Querol et al., 1995; Luo et al., 2002; Głodek and Pacyna, 2009; Pirrone et al., 2010; Langner et al., 2013). According to Nádudvari et al. (2021b) the concentration of Pb, Cd, Zn, Hg, As in thermally-altered coal waste and samples rich in pyrolytic bitumen is enriched. Important to note is that clinkers, the burnt-out product of coal waste fire considered for reusage, may also contain higher concentrations of them.

Mercury in bituminous coals is mainly related to pyrite or other Fe-sulphides, whereas, in lower rank coals, it tends to be organic-bound (Kolker et al., 2006; Hower et al., 2008). Hg concentration in coals from USCB ranges from 0.1 to 0.4 mg/kg. During combustion, Hg starts to be released at 100–150°C, and ~90% of it in coal is emitted into the atmosphere (Liu et al., 2000; Guo et al., 2003; Wagner and Hlatshwayo, 2005). Therefore in self-heated coal wastes at low temperatures, Hg enrichment is not significant and ranges from 0.2 to 0.5 mg/kg (Hlawiczka et al., 2003; Abramowicz et al., 2021), whereas at high

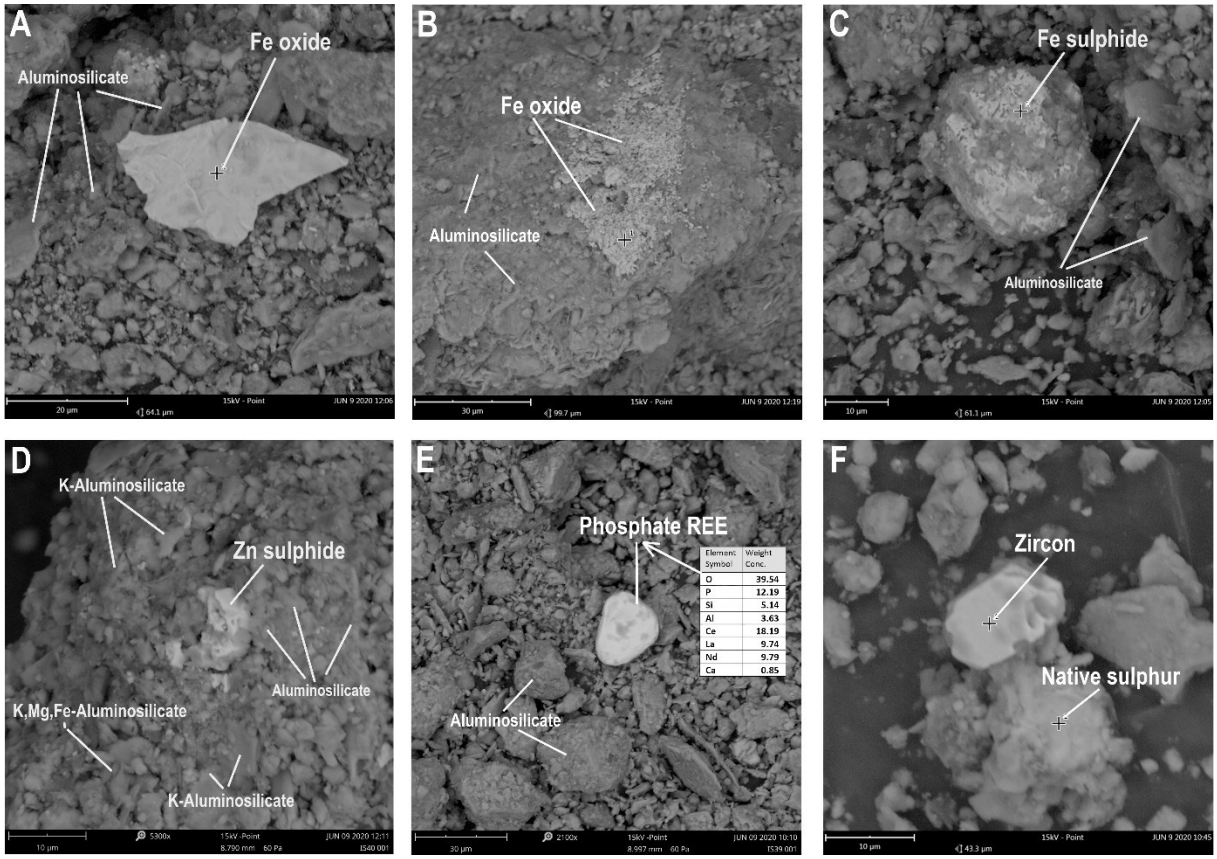

Fig. 3 SEM-BSE images of mineral phases from the thermally affected part of the Bytom dump (coordinates: 50.377516N, 18.900200E)

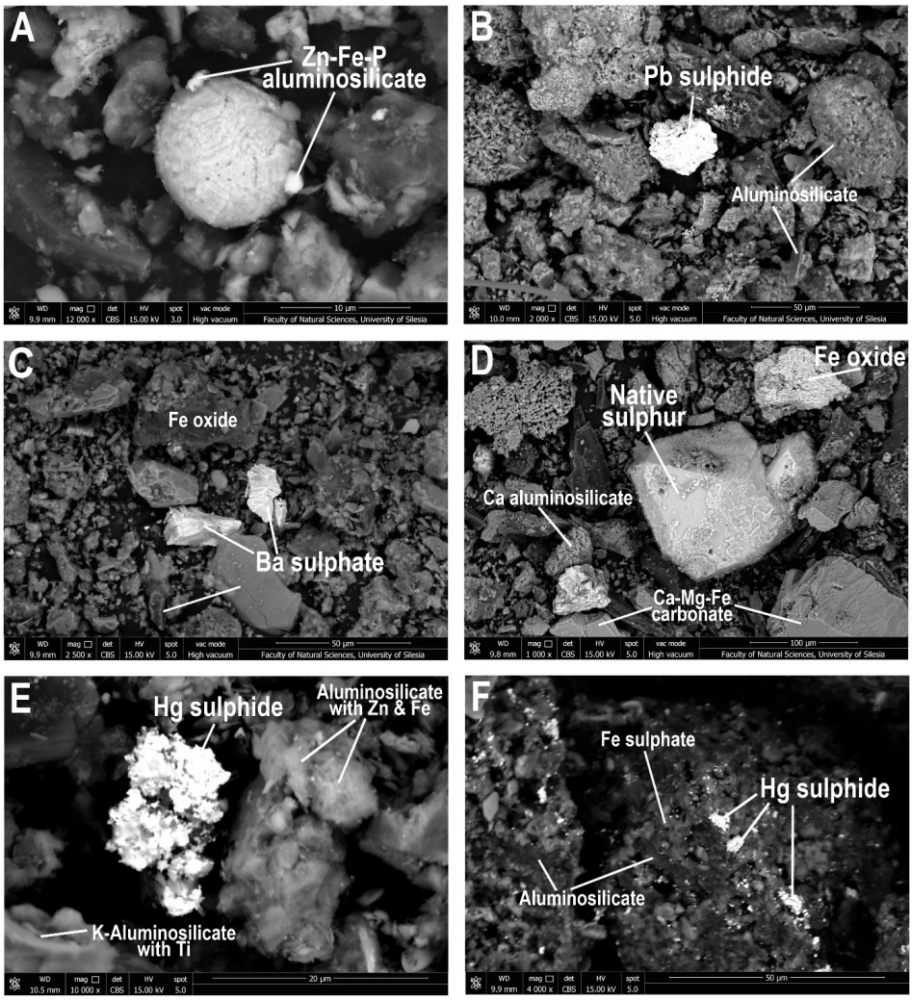

Fig. 4 SEM-BSE images of mineral phases affected by self-heating of coal wastes at the Bytom (A-E) and Czerwionka-Leszczyny (F) dumps (coordinates: 50.159672N, 18.679375E)

temperatures reaches the value of 1078 mg/kg (Nádudvari et al., 2021). In Poland, it is estimated that 24% of Hg emissions come from coal which is burnt in power plants and individual homes (Hlawiczka et al., 2003; Głodek and Pacyna, 2009).

Organic geochemistry of coal wastes

Phenols (phenol C1 - methylphenols and C2 - dimethyphenol, and ethylphenols) are typical products of self-heating dumps and are usually commonly identified in coal waste samples (Fig. 5). That reflects the thermal destruction of vitrinite via coking conditions they may represent the relatively early stages of self-heating (Skręt et al., 2010; Misz-Kennan and Fabiańska, 2011; Nádudvari et al., 2015). Especially high concentrations occur in samples containing pyrolytic bitumen or thermally affected wastes, whereas burned out coal wastes (clinker) usually contains no or small concentrations since phenols are easily evaporable by higher temperatures or leached by water (Nádudvari et al., 2015, 2016). Therefore, the identification of these toxic compounds is important around those dumps, especially in Ukraine, where a large number of burning coal waste dumps pose a serious environmental-pollution threat (Nádudvari et al., 2021a). Phenols easily dissolve in water and are prone to leaching. Potential environmental hazards of phenols are related to their toxicity; they irritate skin and cause necrosis, damage of kidneys, liver, muscle, eyes, and are carcinogenic (Clayton and Clayton, 1994; EPA, 2000).

PAHs are another significant pollutants formed by self-heating (incomplete combustion) see (Fig. 5). Usually, 2- and 3-ring PAHs dominate in these wastes (Nádudvari et al., 2021b). The majority of PAHs are carcinogenic, mutagenic, generally stable and tend to accumulate in the environment (Wagoner, 1976; Grimmer et al., 1983; Achten and Hofmann, 2009; Prus et al., 2015). In the study of Nádudvari et al. (2021b) phenanthrene, anthracene, chrysene, benzo[*a*]anthracene, benzo[*a*]pyrene, benzo[*b*]fluoranthene, and benzo[*k*]fluoranthene in many samples several times surpassed the acceptable values of Polish limits for post-industrial areas (Dz.U., 2016). Lifetime cancer risks in the vicinity of the dump are high due to the heavy metal and PAH pollution, especially when there are elevated Hg concentrations (~100–1078 mg/kg), Pb (~600–2000 mg/kg) considered. Additionally, the low pH levels (3.0–4.5) may help to mobilise these elements (Nádudvari et al., 2021b). Such coal wastes are also a source of other toxic compounds such as pyridines, quinolines, light sulphur compounds like thiophenol, benzo[*b*]thiophene or

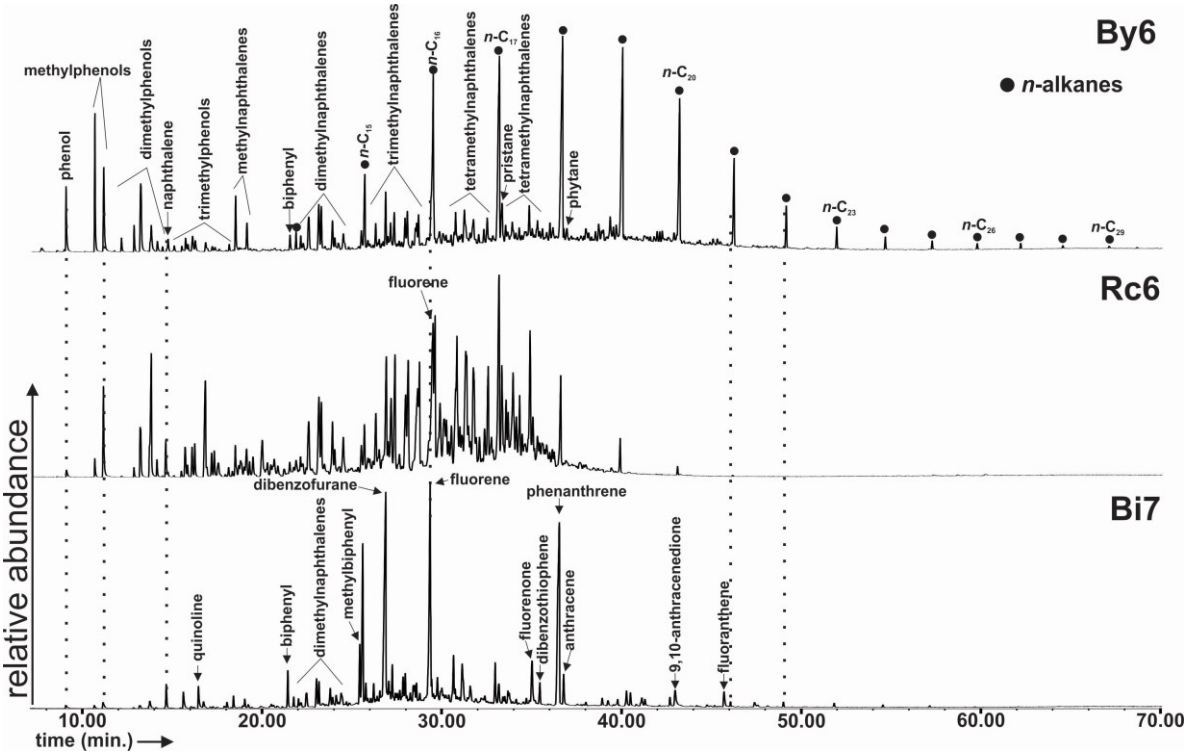

Fig. 5 Representative TIC - Total Ion Chromatograms of self-heated coal wastes in Poland. By6 (Bytom dump): thermally altered, Rc6 (Rybnik – Rymer dump): precipitated (pyrogenic) bitumen crust, Bi7 (Bytom dump): thermally altered coal waste.

more harmful chlorinated PAHs present in the bitumen (Fabiańska et al., 2014; Nádudvari et al., 2018), and also identified in emitted gases (Kruszewski et al., 2018). Chlorinated compounds formed during self-heating, e.g. dichloropropane, dichloromethane, chloroethene, chlorobenzene, dichlorobenzenes, and trichlorobenzene were previously reported by Kruszewski et al. (2018) or Nádudvari et al. (2018, 2021b). These compounds are considered persistent organic pollutants (POPs) (Nádudvari et al., 2018). These compounds, e.g. phenols, quinolines, pyridines, chlorinated PAHs are commonly identified in waste water from coking plants (Sun et al., 2018; Gao et al., 2019). Abundant naphthalene together with alkyl derivatives is characteristic for the expelled pyrogenic bitumen (Fig. 5) that lacks heavier PAHs and nitrogen heterocycles because of their higher boiling temperatures (Nádudvari et al., 2018). Also, oxidation products of PAHs can be recognised (Fig. 5) e.g. transformation fluorene to fluorenone, or anthracene to anthracenedione.

Typical characteristical feature of organic matter caused by pyrolysis during self-heating is the monomodal Gaussian distribution of short to middle chain n-alkanes (Fig. 5 - By6) and the high contents of alkylbenzenes and alkylmethylbenzenes (Nádudvari et al., 2020a). According to Radke and Willsch (1993), large quantities of n-alkanes (n-C_{15}–C_{26}), long-chain alkylbenzenes, alkyltoluenes, and benzo[b]thiophenes are produced between 170 and 360°C through the primary cracking of the coal matrix. Also, self-heating hot spots are characterised by high concentrations of emitted gases like H_2, CO_2, CH_4, C_2H, C_3H_8, C_2H_4 and with two, three times less O_2 content (Fabiańska et al., 2019; Nádudvari et al., 2020a).

Remote sensing and thermal camera monitoring possibilities

Self-heating hot spots on coal waste dumps usually appear as high-temperature surface anomalies (Figures 6 and 7). According to the self-heating intensity index (SHII), burning dumps in Figure 6 (SHII: A: 21; B: 14.5, C: 11, D: 7.5) and Figure 7 (SHII: 9) can be classified as extreme self-heating with extended high surface temperatures. The index is also suitable to describe a long-term self-heating evolution (see Nádudvari et al., 2021a). The highest surface temperatures were detected in Ukrainian dumps (Figure 6B and D) reaching 327 – 376°C. It may indicates opened fires or strong smouldering on the surface. Such surface temperature anomalies can be visible on day-time–night-time Landsat SWIR bands in case of cooling lava flows (Rothery et al., 1988; Pieri et al., 1990; Oppenheimer 1991; Nádudvari et al., 2020b) or burning coal seam fires (Chatterjee, 2006; Huo et al., 2014). The SWIR bands (Fig. 6) were counted according to Nádudvari et al. (2020b), who applied e.g. SWIR and NIR, red, green, blue, panchromatic bands for lava flow surface temperature detections. However, applying SWIR or TIR bands of night-time Landsat images for burning coal wastes similarly to lava flow temperature estimations seems to be the best way to avoid sun disturbance. The NDSI vs TIRS is also a good option for self-heating hot spot determinations (Fig. 7). Therefore the availability of night-time or snow-covered Landsat scenes always limits the application of such satellite images.

Remote sensing measurements using a thermal imaging camera are one of the possibilities of thermal monitoring of coal-waste dumps. This kind of camera

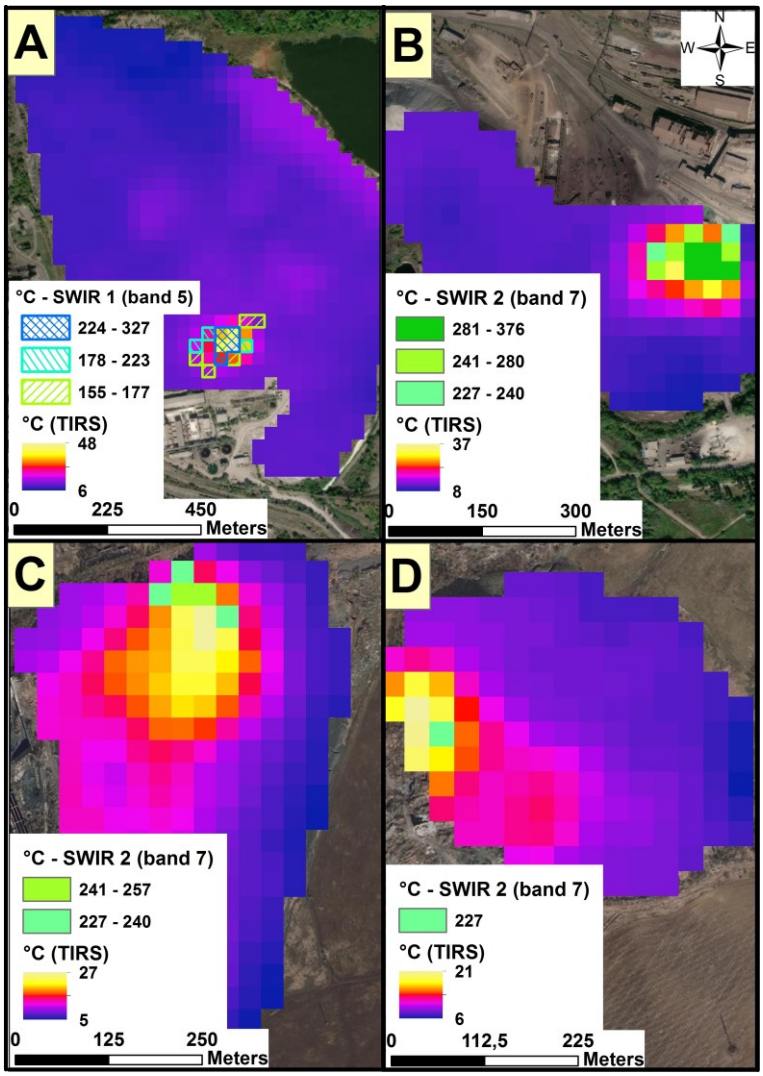

Fig. 6 Ukranian coal waste dumps from the Donetsk Coal Basin. Location of the dumps:
A: 48,225887N, 38,243042E; B: 48.213413N, 38.244355E; C: 47.999718N, 37.947060E; D: 47.985495N, 37.986345E.
The Landsat 7 ETM+, night-time satellite image acquired: 13.05.2002 – scene center time: 18:52:12.
Background map: GoogleEarth – 2021.

operates based on infrared radiation in the wavelength range from 780 nm to 1 mm. These devices provide data in the form of a raster image in which all pixels have assigned thermal values. The accuracy of measurements varies depending on the class and type of equipment and how it is used. Thermal imaging cameras can be collected in fieldwork directly from the ground or placed on an unmanned aerial vehicle (Abramowicz and Chybiorz, 2020). However, to obtain reliable results, photos should be taken in appropriate conditions - in the absence of wind, fog, rain, air pollution, and with stable air temperature and total cloud cover (alternatively before sunrise or after sunset). In the case of very diverse objects, such as dumps, using the camera should be adapted to the shape and land cover of the measured object. Using a handheld camera from the ground makes it possible to reach surfaces that are difficult to get from the air, e.g., areas covered by dense vegetation or with difficult relief. However, taking such photos is more labour-intensive and time-consuming compared to aerial photos. Photos from the air are a good way, especially in massive objects, the surface of which cannot be accessed in any other way.

Infrared images (satellite, aerial and terrestrial) enable only mapping the surface temperature of coal-waste dumps. Invasive methods should be used to measure the actual temperatures at the epicentre of a subsurface fire, including a pyrometer with a probe (Abramowicz and Chybiorz, 2019). Unfortunately, unlike camera images, measurements with a pyrometer provide only point data that require subsequent interpolation. Interfering with the body of the dump by making holes to measure the subsurface temperatures carries additional risks because such interference adds air to the interior of the dump. If higher targets do not require it, it is worth staying with the surface temperature analyses based on infrared images. On their basis, it is possible, inter alia, to the determination of the impact of a fire on the vegetation cover (Abramowicz et al., 2021b) or land development (Abramowicz et al., 2021a). Subsurface fires not only affect the place of their location but also interfere with the

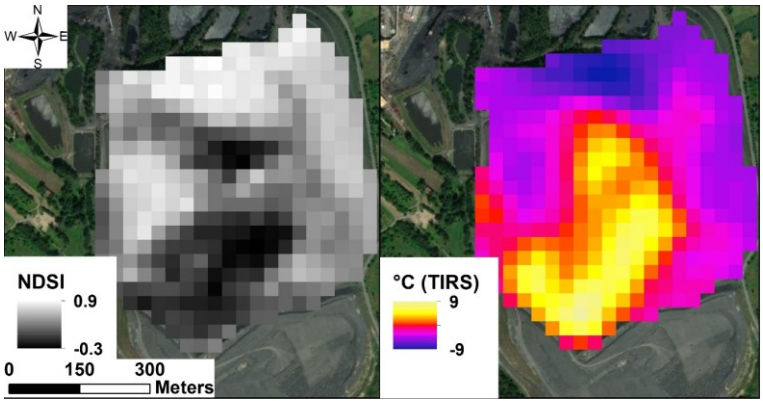

Fig. 7 An example of a self-heating dump (Szarlota) from Poland, Upper Silesian Coal Basin (coordinates: 50.062546N, 18.441930E; satellite image: Landsat 7 ETM+, data acquired: 26.02.2001 – daylight snow-covered image).NDSI - Normalised Difference Snow Index. Southern part of the dump is constructed after the image acquisition. High NDSI values indicate abundant snow cover and below 0.4 melted snow which correlating with the TIRS image. Background map: GoogleEarth – 2021.

elements of the environment directly below, above, or next to the thermally active zones, including soil, water, air, and vegetation (Homoki et al., 2000; Abramowicz et al., 2021b; Lewińska-Preis et al., 2021; Nádudvari et al., 2021a).

In Figure 8 the burning Anna dump (Poland) is presented, and the image was taken by a drone. The dump was flattened, and currently, the fire was extinguishing as the surface temperatures indicate it (<30°C). However, this dump underwent a strong self-heating on the eastern and southern part in 2010 or 2018 as detected by archive satellite images (Nádudvari, 2014, Nádudvari et al., 2021b). The drone image reveals more details, e.g. erosion gullies could promote self-heating, as it is seen on the southern part or initial stages of self-heating on the west side of the dump (Fig. 8 and 9B). Also, such fires usually are visible as cracks, line shapes (Fig. 8 and 9A-B) or extended spots (Fig. 9C) in such detailed thermal images. After burning out, blocks can erode or slide down (Fig. 9B), which may intensify the fire by more oxygen access to the deeper hot spots.

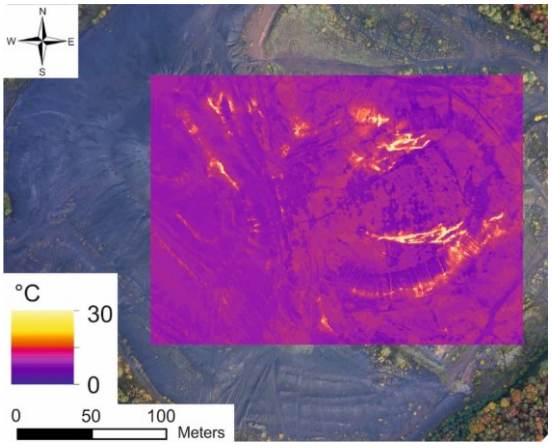

Fig. 8 Thermal image of Anna-Wrzosy dump (Poland) taken with the IR camera on a drone - resolution 20 cm (background: orthophotomap with resolution 3.5 cm). The drone operations were carried out before sunrise on 05.11.2020 in windless and rainless weather and with an air temperature of 5°C. (coordinates: 50.045445N, 18.421978E)

CONCLUSIONS

Self-heating and self-ignition processes affect poorly constructed coal waste dumps all over the world. They are uncontrolled, hard to extinguish and difficult to predict. Examples from the Upper Silesian (Poland) and Donetsk Coal Basins (Ukraine) were studied in detail to help to understand the phenomena.

Thermal alteration of coal particles causes their devolatilisation and plasticisation. Moderate heating causes the formation of irregular cracks and fissures perpendicular to the edges of particles, paler/darker in colour oxidation rims forming around the edges and cracks. Additionally, expelled pyrogenic bitumen is also a common form around self-heated particles. Oxidation rims are usually paler than the central part of the particles. With prolonged oxidation, gradually, the whole particle becomes paler in colour up to whitish.

The primary mineral matter of coal wastes is composed of quartz, clay minerals as illite, montmorillonite or kaolinite, chlorite, micas, mainly muscovite with subordinate feldspars, carbonates, pyrite, chalcopyrite and accessory zircon, monazite, apatite and xenotime. Unstable minerals under higher temperature phases rebuild their structures, releasing hazardous elements like Pb, Cd, Zn, Hg, As. These elements migrate from the hot spots and enrich in the cooler surface in e.g. sulphide minerals as HgS.

Different organic pollutants like phenols (originated from vitrinite particles), different PAHs with alkyl substitutes or oxidised PAHs, chlorinated PAHs, or sulphur heterocycles are formed. Therefore the high concentrations of PAHs and heavy metals making these coal waste dumps are potential risk for humans as they might contribute to cancer.

The introduced different remote sensing techniques helped to localise and monitor hot spots with different temperature ranges despite disadvantages of these methods. The application of SWIR bands of Landsat contribute to the successfull localisation of hot spots of extremely burning dumps in Ukraine. However, only night-time scenes with SWIR can be used, but these night-time data are rarely available and usually cloudy. The snow-covered images can be used to localise the hot spots;

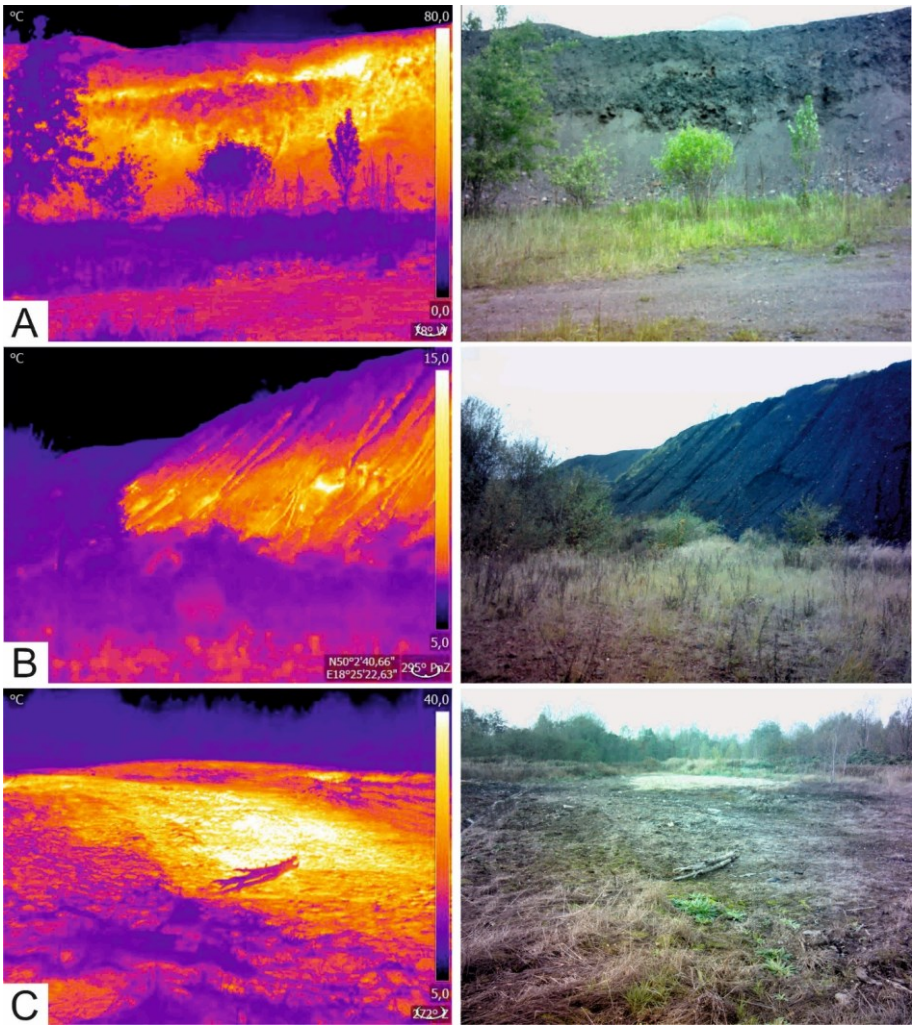

Fig. 9 Infrared photos of selected coal-waste dumps in the Upper Silesian Coal Basin (Poland): A: Bytom dump (27.05.2021, air temperature: 17°C), coordinates: 50.377516N, 18.900200E; B: Anna-Wrzosy dump in Pszów (01.11.2020, air temperature: 6°C); C: Czarny Las dump in Ruda Śląska (02.11.2019, air temperature: 10°C), coordinates: 50.280664N, 18.850826E

however, better TIRS band resolution of Landsat 7 ETM+ is more advantageous. The sun's disturbing effects should be considered as an influential factor for both thermal imaging camera or satellite images. Thermal cameras can reveal the most detailed signs of low to high temperature anomalies with different cracks and line shapes. Our research indicates the only by combining the different investigation techniques, such as applied here, the understanding of complex processes occuring within coal waste dumps can be achieved.

REFERENCES

Abramowicz, A., Chybiorz, R. 2019: Fire detection based on a series of thermal images and point measurements: the case study of coal-waste dumps. *International Archives of the Photogrammetry, Remote Sensing and Spatial Information Sciences* XLII-1/W2, 9–12. DOI: 10.5194/isprs-archives-XLII-1-W2-9-2019

Abramowicz, A., Chybiorz, R. 2020. Identification of fire changes using thermal IR images: the case of coal-waste dumps. *Proceedings of the 15th Quantitative InfraRed Thermography Conference*. Porto, Portugal, 21-30 September 2020. DOI: 10.21611/qirt.2020.114

Abramowicz, A., Rahmonov, O., Chybiorz, R. 2021a. Environmental management and landscape transformation on self-heating coal-waste dumps in the Upper Silesian Coal Basin. *Land* 10(1), 23. DOI: 10.3390/land10010023

Abramowicz, A., Rahmonov, O., Chybiorz, R., Ciesielczuk, J. 2021b. Vegetation as an indicator of underground smoldering fire on coal-waste dumps. *Fire Safety Journal* 121, 103287. DOI: 10.1016/j.firesaf.2021.103287

Abramowicz, A., Rahmonov, O., Fabiańska, M.J., Nádudvari, Á., Chybiorz, R., Michalak, M. 2021c. Changes in soil chemical composition caused by self-heating of coal-waste dump. *Land Degradation and Development* 32(15) 4340–4349. DOI: 10.1002/ldr.4040

Achten, C., Hofmann, T. 2009. Native polycyclic aromatic hydrocarbons (PAH) in coals – a hardly recognized source of environmental contamination. *Science of Total Environment* 407, 2461–2473. DOI: 10.1016/j.scitotenv.2008.12.008

Alpern, B., Lemos de Sousa, M.J., Pinheiro, H.J., Zhu, X. 1992. Optical Morphology of Hydrocarbons and Oil Progenitors in Sedimentary Rocks – Relations with Geochemical Parameters. Publicações do Museu e Laboratório Mineralógico e Geológico da Faculdade de Ciências do Porto. pp. 61.

Bonneville, A., Kerr, Y.A. 1987. A thermal forerunner of the 28th March 1983 Mount Etna eruption from satellite thermal infrared data. *Journal of Geodynamics* 7, 1–31. DOI: 10.1016/0264-3707(87)90061-5

Bonneville, A., Vasseur, G., Kerr, Y. 1985. Satellite thermal infrared observations of Mount Etna after the 17th March 1981 eruption. *Journal of Volcanology and Geothermal Research* 36, 209–232. DOI: 10.1016/0377-0273(85)90074-5

Carras, J.N., Bainbridge, N.W., Saghafi, A., Szemes, F., Roberts, O.C., Haneman, D. 1994. The Self-heating of Spoil Piles from Open

Cut Coal Mines, Vol. 1 Characterisation, Field Measurements and Modelling. NERRDC 1609 Final Report. Australian Coal Association, Brisbane, p. 128.

Carras, J.N., Bus, J., Roberts, O.C., Szemes, F. 1999. Monitoring of Temperature and Oxygen Profiles in Selfheating Spoil Piles. ACARP Project C6003 Final Report. Australian Coal Association, Brisbane, p. 19.

Carras, J.N., Day, S.J., Saghafi, A., Williams, D.J. 2009. Greenhouse gas emissions from low-temperature oxidation and spontaneous combustion at open-cut coal mines in Australia. *International Journal Coal Geololgy* 78(2), 161–168. DOI: 10.1016/j.coal.2008.12.001

Chatterjee, R.S. 2006. Coal fire mapping from satellite thermal IR data—A case example in Jharia Coalfield, Jharkhand, India. *ISPRS Journal of Photogrammetry and Remote Sensing* 60(2), 113–128. DOI: 10.1016/j.isprsjprs.2005.12.002

Ciesielczuk, J., Misz-Kennan, M., Hower, J.C., Fabiańska, M.J. 2014. Mineralogy and geochemistry of coal wastes from the Starzykowiec coal-waste dump (Upper Silesia, Poland). *International Journal Coal Geololgy* 127, 42–55. DOI: 10.1016/j.coal.2014.02.007

Ciesielczuk J., Kruszewski Ł., Majka J. 2015. Comparative mineralogical study of thermally-altered coal-dump waste, natural rocks and the products of laboratory heating experiments. *International Journal of Coal Geology* 139, 114–141. DOI: 10.1016/J.COAL.2014.08.013

Clayton, G.D., Clayton, F.E. 1994. Patty's Industrial Hygiene and Toxicology (4th ed.). John Wiley & Sons Inc. New York, Vol. 2A, 132 p.

Dz. U. pos. 1395 (Journal of Laws) 2016. Regulation of the Minister of Environment of September 1, 2016 on the method of assessing the pollution of the earth's surface.

EPA, 2000 - United States Environmental Protection Agency Phenol, Online available at: https://www.epa.gov/sites/default/files/2016-09/documents/phenol.pdf

Fabiańska, M., Ciesielczuk, J., Nádudvari, Á., Misz-Kennan, M., Kowalski, A., Kruszewski, Ł. 2019. Environmental influence of gaseous emissions from self-heating coal waste dumps in Silesia, Poland. *Environmental Geochemistry and Health* 41(2), 575–601. DOI: 10.1007/s10653-018-0153-5

Fabiańska, M.J., Ciesielczuk, J., Misz-Kennan, M., Kruszewski, Ł., Nádudvari, Á. 2014. Organic compounds in water collected in burning coal-mining waste dumps in Lower Silesia, Poland. Mineralogia - Special Papers 42, 50–51.

Finkelman, R.B. 1995. Modes of occurrence of environmentally-sensitive trace elements in coal. In: Swaine, D.J., Goodarzi, F. (eds.) Environmental Aspects of Trace Elements in Coal. Springer, Dordrecht, 27–50.

Finkelman, R.B. 2004. Potential health impacts of burning coal beds and waste banks. *International Journal Coal Geololgy* 59, 19–24. DOI: 10.1016/J.COAL.2003.11.002

Gangopadhyay, P.K., Malthuis, B., van Dink, P. 2005. ASTER derived emissivity and coal-fire related surface temperature anomaly a case study in Wuda, North China. *International Journal of Remote Sensing* 26(24), 5555–5571. DOI: 10.1080/01431160500291959

Gao, G., Wang, L., Li, Z., Xie, Y., He, Q., Wang, Y. 2019. Adsorptive removal of pyridine in simulation wastewater using coke powder. *Processes* 7(7), 459–478. DOI: 10.3390/pr7070459

Gentzis, T., Goodarzi, F. 1989. Organic petrology of a self-burning coal wastepile from Coleman, Alberta, Canada. *International Journal Coal Geololgy* 11(3-4), 257–271. DOI: 10.1016/0166-5162(89)90118-3

Głodek, A., Pacyna, J.M. 2009. Mercury emission from coal-fired power plants in Poland. *Atmospheric Environment* 43(35), 5668–5673. DOI: 10.1016/j.atmosenv.2009.07.041

Grimmer, G., Brune, H., Deutsch-Wenzel, R., Naujack, K.-W., Misfeld, J., Timm, J. 1983. On the contribution of polycyclic aromatic hydrocarbons to the carcinogenic impact of automobile exhaust condensate evaluated by local application onto mouse skin. *Cancer Letters* 21(1), 105–113. DOI: 10.1016/0304-3835(83)90089-7

Guha, A., Kumar, K.V. 2012. Structural controls on coal fire distributions - remote sensing based investigation in the Raniganj Coalfield, West Bengal. *Journal of the Geological Society of India* 79(5), 467–475. DOI: 10.1007/s12594-012-0071-6

Heffern, E.L., Coates, D.A. 2004. Geology of natural coal bed fires, Powder River Basin, USA. *International Journal Coal Geololgy* 59(1-2), 25–47. DOI: 10.1016/j.coal.2003.07.002

Hlawiczka, S., Kubica, K., Zielonka, U. 2003. Partitioning factor of mercury during coal combustion in low capacity domestic heating units. *Science of Total Environment* 312 (1-3), 261–265. DOI: 10.1016/S0048-9697(03)00252-3

Homoki, E., Juhász, Cs., Baros, Z., Sütő, L. 2000. Antropogenic geomorphological research on waste heaps in the East-Borsod coal basin (NE Hungary). Z Badań nad wpływen antropopresji na środowisko. Sosnowiec, Studenckie Koło Naukowe Geografów Uniwersytetu Śląskiego, 24-31.

Hower, J.C., Campbell, J.L., Teesdale, W.J., Nejedly, Z., Robertson, J.D. 2008. Scanning proton microprobe analysis of mercury and other trace elements in Fe-sufides from a Kentucky coal. *International Journal Coal Geololgy* 75, 88–92. DOI: 10.1016/j.coal.2008.03.001

Huang, W. 2004. Study on spontaneous combustion mechanism and prevention technology of coal gangue (Doctoral thesis). Chongqing University, Chongqing, p. 2004.

Huo, H., Jiang, X., Song, X., Li, Z.L., Ni, Z., Gao, C. 2014. Detection of coal fire dynamics and propagation direction from multi-temporal nighttime Landsat SWIR and TIR data: A case study on the Rujigou Coalfield, Northwest (NW) China. *Remote Sensing* 6(2), 1234–1259. DOI: 10.3390/rs6021234

International Committee for Coal and Organic Petrology, (ICCP). 1998. New vitrinite classification (ICCP system 1994). *Fuel* 77(5), 349–358. DOI: 10.1016/S0016-2361(98)80024-0

International Committee for Coal and Organic Petrology, (ICCP) 2001. The new inertinite classification (ICCP System 1994). *Fuel* 80(4), 459–471. DOI: 10.1016/S0016-2361(00)00102-2

ISO 7404-3 2009. Methods for the petrographic analysis of coals—part 3: method of determining maceral group composition. International Organization for Standardization, Geneva, Switzerland (4 p.).

ISO 7404-5 2009. Methods for the petrographic analysis of coals—part 5: method of determining microscopically the reflectance of vitrinite. International Organization for Standardization, Geneva, Switzerland (11 p).

Jacob, H. 1993. Nomenclature, classification, characterization and genezis of natural solid bitumen (migrabitumen). In: Parnel, J., Kucha, H., Landais, P. (eds.) Bitumens in Ore Deposits. Special Publication of No.9 the Society for Geology Applied to Mineral Geology. Springer – Verlag, Berlin, Heidelberg, pp. 11–27.

Jendruś, R. 2016. Chemical and physical aspects of fires on coal waste dumps. Zeszyty Naukowe Wyższej Szkoły Technicznej w Katowicach 8, 131–149

Kang, Y., Liu, G., Chou, C.L., Wong, M., Zheng, L., Ding, R. 2011. Arsenic in Chinese coals: distribution, modes of occurrence, and environmental effects. *Science of Total Environment* 412–413, 1–13. DOI: 10.1016/j.scitotenv.2011.10.026

Kędzior, S. 2019. Distribution of methane contents and coal rank in the profiles of deep boreholes in the Upper Silesian Coal Basin, Poland. *International Journal of Coal Geology* 202, 190-208. DOI: 10.1016/j.coal.2018.12.010

Kolker, A., Senior, C.L., Quick, J.C. 2006. Mercury in coal and the impact of coal quality on mercury emissions from combustion systems. *Applied Geochemistry* 21(11), 1821–1836. DOI: 10.1016/j.apgeochem.2006.08.001

Kruszewski, Ł, Fabiańska, M.J., Segit, T., Kusy, D., Motyliński, R., Ciesielczuk, C., Deput, E. 2020. Carbon nitrogen compounds, alcohols, mercaptans, monoterpenes, acetates, aldehydes, ketones, SF6, PH3, and other fire gases in coal-mining waste heaps of Upper Silesian Coal Basin (Poland) – a re-investigation by means of in situ FTIR external database approach. *Science of Total Environment* 698, 134274. DOI: 10.1016/j.scitotenv.2019.134274

Kruszewski, Ł., Fabiańska, M., Ciesielczuk, J., Segit, T., Orłowski, R., Motyliński, R., Kusy, D., Moszumańska, I. 2018. First multi-tool exploration of a gas-condensate-pyrolysate system from the environment of burning coal mine heaps: an in situ FTIR and laboratory GC and PXRD study based on Upper Silesian materials. *Science of Total Environment* 640–641, 1044–1071. DOI: 10.1016/j.scitotenv.2018.05.319

Kus, J., Misz-Kennan, M., ICCP 2017. Coal weathering and laboratory (artificial) coal oxidation. *International Journal of Coal Geology* 171, 12–36. DOI: 10.1016/j.coal.2016.11.016

Kwiecińska, B., Pusz, S. 2016. Pyrolytic carbon – definition, classification and occurrence. *International Journal of Coal Geology* 163, 1–7. DOI: 10.1016/j.coal.2016.06.014

Kwiecińska, B., Petersen, H.I. 2004. Graphite, semi-graphite, natural coke, and natural char classification-ICCP system. *International Journal of Coal Geology* 57(2), 99–116. DOI: 10.1016/j.coal.2003.09.003

Langner, P., Mikutta, C., Suess, E., Marcus, M.A., Kretzschmar, R. 2013. Spatial distribution and speciation of arsenic in peat studied with microfocused X-ray fluorescence spectrometry and X-ray absorption spectroscopy. *Environmental Science and Technology* 47(17), 9706–9714. DOI: 10.1021/es401315e

Lester, E., Alvarez, D., Borrego, A.G., Valentim, B., Flores, D., Clift, D.A., Rosenberg, P., Kwiecińska, B., Barranco, R., Petersen, H.I., Mastalerz, M., Milenkova, K.S., Panaitescu, C., Marques, M.M., Thompson, A., Watts, D., Hanson, S., Predeanu, G., Misz, M., Wu, T. 2010. The procedure used to develop a coal char classificationCommission III Combustion Working Group of the International Committee for Coal and Organic Petrology. *International Journal of Coal Geology* 81(4), 333–342. DOI: 10.1016/j.coal.2009.10.015

Lewińska-Preis, L., Szram, E., Fabiańska, M.J., Nádudvari, Á., Misz-Kennan, M., Abramowicz, A., Kruszewski, Ł., Kita, A. 2021. Selected ions and major and trace elements as contaminants in coal-waste dump water from the Lower and Upper Silesian Coal Basins (Poland). *International Journal of Coal Science and Technology*. DOI: 0.1007/s40789-021-00421-9

Li, H.J. 2010. Comprehensive Utilization of Coal Gangue. Chemical Industry Press, Beijing.

Li, W., Chen, L., Zhou, T., Tang, Q., Zhang, T. 2011. Impact of coal gangue on the level of main trace elements in the shallow groundwater of a mine reclamation area. *Mining Science and Technology* 21(5), 715–719. DOI: 10.1016/j.mstc.2011.03.004

Liu, G., Yang, P., Zhang, W., Wang, G., Feng, Q. 2000. Research on separation of minor elements from coal during combustion. *Journal of China University of Mining and Technology* 10, 62–65.

Liu, H.B., Liu, Z.L. 2010. Recycling utilization patterns of coal mining waste in China. *Resources, Conservation and Recycling*. 54(12), 1331–1340. DOI: 10.1016/j.resconrec.2010.05.005

Lohrer, C., Schmidt, M., Krause, U. 2005. A study on the influence of liquid water and water vapour on the self-ignition of lignite coal-experiments and numerical simulations. *Journal of Loss Prevention in the Process Industries* 18(3), 167–177. DOI: 10.1016/j.jlp.2005.03.006

Luo, K., Xu, L., Li, R., Xiang, L. 2002. Fluorine emission from combustion of steam coal of north China plate and northwest China. *Chinese Science Bulletin* 47, 1346–1350. DOI: 10.1360/02tb9298

Misz, M., Fabiańska, M., Ćmiel, S. 2007. Organic components in thermally altered coal waste: preliminary petrographic and geochemical investigations. *International Journal of Coal Geology* 71(4), 405–424. DOI: 10.1016/j.coal.2006.08.009

Misz-Kennan, M. 2010. Thermal alterations of organic matter in coal wastes from Upper Silesia, Poland. *Mineralogia* 41(3-4), 105–237. DOI: 10.2478/v10002-010-0001-4

Misz-Kennan, M., Fabiańska, M. 2010. Thermal transformation of organic matter in coal waste from Rymer Cones (Upper Silesian Coal Basin, Poland). *International Journal of Coal Geology* 81(4), 343–358. DOI: 10.1016/j.coal.2009.08.009

Misz-Kennan, M., Fabiańska, M.J. 2011. Application of organic petrology and geochemistry to coal waste studies. *International Journal of Coal Geology* 88(1), 1–23. DOI: 10.1016/j.coal.2011.07.001

Misz-Kennan, M., Kus, J., Flores, D., Avila, C., Büçkün, Z., Choudhury, N., Christanis, K., Joubert, J,P., Kalaitzidis, S., Karayigit, A.I., Malecha, M., Marques, M., Martizzi, P., O'Keefe, J.M.K., Pickel, W., Predeanu, G., Pusz, S., Ribeiro, J., Rodrigues, S., Singh, A.K., Suárez-Ruiz, I., Sýkorová, I., Wagner, N.J., Životić, D., ICCP 2020. Development of a petrographic classification system for organic particles affected by self-heating in coal waste. (An ICCP Classification System, Self-heating Working Group – Commission III). *International Journal of Coal Geology* 220, 103411 DOI: 10.1016/j.coal.2020.103411

Masalehdani, N.N., Mees, F., Dubois, M., Coquinot, Y., Jean-Luc, Potdevin, Fialin, M., Blanc-Valleron, Marie-Madelein E. 2009. Condensate minerals from a burning coal-waste heap in Avion, Northern France. *The Canadian Mineralogist* 47 (3), 573–591. DOI: 10.3749/canmin.47.3.573

McLafferty, F.W., Stauffer, D.B. (eds.) 1989. The Wiley/NBS Registry of Mass Spectral Data, 7 Volume Set. John Wiley and Sons, New York. ISBN: 978-0-471-62886-6.

Monterroso, C., Macias, F. 1998. Drainage waters affected by pyrite oxidation in a coal mine in Galicia (NW Spain): composition and mineral stability. *Science of Total Environment* 216(1-2), 121–132.

Nádudvari, Á., Fabiańska, M.J., Misz-Kennan, M. 2015. Distribution of phenols related to self-heating and water washing on coal-waste dumps and in coaly material from the Bierawka river (Poland). *Mineralogia* 46(1-2), 29–40. DOI: 10.1515/mipo-2016-0005

Nádudvari, Á, Fabiańska, M.J., Marynowski, L., Kozielska, B., Konieczyński, J., Smołka Danielowska, D., Ćmiel, S. 2018a. Distribution of coal and coal combustion related organic pollutants in the environment of the Upper Silesian Industrial Region. *Science of Total Environment* 628–629, 1462–1488. DOI: 10.1016/j.scitotenv.2018.02.092

Nádudvari, Á., Abramowicz, A., Fabiańska, M., Misz-Kennan, M., Ciesielczuk, J. 2021a. Classification of fires in coal waste dumps based on Landsat, Aster thermal bands and thermal camera in Polish and Ukrainian mining regions. *International Journal of Coal Science and Technology* 8, 441–456. DOI: 10.1007/s40789-020-00375-4

Nádudvari, Á., Kozielska, B., Abramowicz, A., Fabiańska, M., Ciesielczuk, J., Cabała, J., Krzykawski, T. 2021b. Heavy metal- and organic-matter pollution due to self-heating coal-waste dumps in the Upper Silesian Coal Basin (Poland). *Journal of Hazardous Materials* 412, 125244. DOI: 10.1016/j.jhazmat.2021.125244

Nádudvari, Á., Abramowicz, A., Maniscalco, R., Viccaro, M. 2020b. The Estimation of Lava Flow Temperatures Using Landsat Night-Time Images: Case Studies from Eruptions of Mt. Etna and Stromboli (Sicily, Italy), Kīlauea (Hawaii Island), and Eyjafjallajökull and Holuhraun (Iceland). *Remote Sensing* 12(16), 2537. DOI: 10.3390/rs12162537

Nádudvari, Á., Ciesielczuk J. 2018. Remote sensing techniques for detecting self-heated hot spots on coal waste dumps in Upper Silesia, Poland, chapter 18. In: Stracher G.B. (ed.) Coal and peat fires: a global perspective: vol 5: case studies—advances in field and laboratory research, 1st edn. Elsevier, Amsterdam, pp 387–406.

Nádudvari, Á., Fabiańska, M.J. 2016. Use of geochemical analysis and vitrinite reflectance to assess different self-heating processes in coal-waste dumps (Upper Silesia, Poland). *Fuel* 181, 102–119. DOI: 10.1016/j.fuel.2016.04.129

Nádudvari, Á., Fabiańska, M.J., Misz-Kennan, M., Ciesielczuk, J., Kowalski, A. 2020a. Investigation of organic material self-heating in oxygen-depleted condition within a coal-waste dump in Upper Silesia Coal Basin, Poland. *Environmental Science and Pollution Research* 27(8), 8285–8307. DOI: 10.1007/s11356-019-07336-8

Oppenheimer, C. 1991. Lava Flow Cooling Estimated from Landsat Thematic Mapper Infrared Data: The Lonquimay Eruption (Chile, 1989). *Journal of Geophysical Research* 96(B13), 21865–21878. DOI: 10.1029/91JB01902

Panov, B.S., Dudik, A.M., Shevchenko, O.A, Matlak, A.S. 1999. On pollution of the biosphere in industrial areas: the example of the Donets coal Basin. *International Journal of Coal Geology* 40(2-3), 199-210. DOI: 10.1016/S0166-5162(98)00069-X

Philp, R.P. 1985. Fossil Fuel Biomarkers: Application and Spectra. Elsevier, Amsterdam. ISBN-10: 0444424717.

Pickel, W., Kus, J., Flores, D., Kalaitzidis, S., Christanis, K., Cardott, B.J., Misz-Kennan, M., Rodrigues, S., Hentschel, A., Hamor-Vido, M., Crosdale, P., Wagner, N., ICCP 2017. Classification of liptinite – ICCP System 1994. *International Journal of Coal Geology* 169, 40–61. DOI: 10.1016/j.coal.2016.11.004.

Pieri, D.C., Glaze, L.S., Abrams, M.J. 1990. Thermal radiance observations of an active lava flow during the June 1984 eruption of Mount Etna. *Geology* 18(10), 1018–1022. DOI: 10.1130/0091-7613(1990)018<1018:TROOAA>2.3.CO;2

Pierwoła, J., Ciesielczuk, J., Misz-Kennan, M., Fabiańska, M.J., Bielińska, A., Kruszewski, Ł. 2018. Structure and thermal history of the Wełnowiec dump, Poland: A municipal dump rehabilitated with coal waste. *International Journal Coal Geololgy* 197, 1–19. DOI: 10.1016/j.coal.2018.08.001

Pirrone, N., Cinnirella, S., Feng, X., Finkelman, R.B., Friedli, H.R., Leaner, J., Mason, R., Mukherjee, A.B., Stracher, G.B., Streets, D.G., Telmer, K. 2010. Global mercury emissions to the atmosphere from anthropogenic and natural sources. *Atmospheric Chemistry and Physics* 10(13), 5951–5964. DOI: 10.5194/acp-10-5951-2010

Pone, J.D.N., Hein, K.A.A., Stracher, G.B., Annegarn, H.J., Finkleman, R.B., Blake, D.R., McCormack, J.K., Schroeder, P. 2007. The spontaneous combustion of coal and its by-products in the Witbank and Sasolburg coalfields of South Africa. *International Journal Coal Geololgy* 72(2), 124–140. DOI: 10.1016/J.COAL.2007.01.001

Prakash, A., Schaefer, K., Witte, W.K., Collins, K., Gens, R., Goyette, M.P. 2011. A remote sensing and GIS based investigation of a boreal forest coal fire. *International Journal Coal Geololgy* 86(1), 79–86. DOI: 10.1016/j.coal.2010.12.001

Prus, W., Fabiańska, M.J., Łabno, R. 2015. Geochemical markers of soil anthropogenic contaminants in polar scientific stations nearby (Antarctica, King George Island). *Science of Total Environment* 518–519, 266–279. DOI: 10.1016/j.scitotenv.2015.02.096

Querol, X., Izquierdo, M., Monfort, E., Alvarez, E., Font, O., Moreno, T., Alastuey, A., Zhuang, X., Lu, W., Wang, Y. 2008. Environmental characterization of burnt coal gangue banks at Yangquan, Shanxi Province, China. *International Journal Coal Geololgy* 75(2), 93–104. DOI: 10.1016/j.coal.2008.04.003

Querol, X., Fernandez-Turiel, J.L., Lopez-Soler, A. 1995. Trace elements in coal and their behaviour during combustion in a large power station. *Fuel* 74(3), 331–343. DOI: 10.1016/0016-2361(95)93464-O

Raask, E. 1985. The mode of occurrence and concentration of trace elements in coal. *Progress in Energy and Combustion Science* 11(2), 97–118. DOI: 10.1016/0360-1285(85)90001-2

Radke, M., Willsch, H. 1993. Generation of alkylbenzenes and benzo[b]thiophenes by artificial thermal maturation of sulfur-rich coal. *Fuel* 72(8), 1103–1108. DOI: 10.1016/0016-2361(93)90316-t

Ribeiro, J., da Silva E.F., Flores, D. 2010. Burning of coal waste piles from Douro Coalfield (Portugal): petrological, geochemical and mineralogical characterization. *International Journal Coal Geololgy* 81(4), 359–372. DOI: 10.1016/j.coal.2009.10.005

Ribeiro, J., Suárez-Ruiz, I., Ward, C., Flores, D. 2016. Petrography and mineralogy of self-burning coal wastes from anthracite mining in the El Bierzo Coalfield (NW Spain). *Journal Coal Geololgy* 154–155, 92–106. DOI: 10.1016/j.coal.2015.12.011

Rothery, D.A., Francis, P.W., Wood, C.A. 1988. Volcano monitoring using short wavelength infrared data from satellites. *Journal of Geophysical Research: Solid Earth* 93(B7), 7993–8008. DOI: 10.1029/JB093iB07p07993

Skarżyńska, K.M. 1995. Reuse of coal mining wastes in civil engineering – Part 1: properties of minestone. *Waste Management* 13(1), 3–42. DOI: 10.1016/0956-053X(95)00004-J

Skręt, U., Fabiańska, M.J., Misz-Kennan, M. 2010. Simulated water-washing of organic compounds from selfheated coal wastes of the Rymer Cones Dump (Upper Silesia Coal Region, Poland). *Organic Geochemistry* 41(9), 1009-1012. DOI: 10.1016/j.orggeochem.2010.04.010

Suárez-Ruiz, I., Crelling, J. (eds.) 2008. Applied Coal Petrology. The Role of Petrology in Coal Utilization. Elsevier, Amsterdam. 388 pp.

Sun, X., Xu, H., Wang, J., Ning, N., Huang, G., Yu, Y., Ma, L. 2018. Kinetic research of quinoline, pyridine and phenol adsorption on modified coking coal. *Physicochemical Problems of Mineral Processing* 54(3), 965–974. DOI: 10.5277/ppmp1898

Sütő, L., Kozák, M., McIntosh, R.W., Püspöki, Z., Beszeda, I. 2007. Secondary mineralisation processes in coal pit heaps and its impact on the environment in NE Hungary. *Acta Ggm Debrecina* 2, 41–45.

Sýkorová, I., Pickel, W., Christianis, K., Wolf, M., Taylor, T.G., Flores, D. 2005. Classification of huminite - ICCP System 1994. *International Journal Coal Geololgy* 62(1-2), 85–106. DOI: 10.1016/j.coal.2004.06.006

Sýkorová, I., Kříbek, B., Havelcová, M., Machovič, V., Laufek, F., Veselovský, F., Špaldoňová, A., Lapčák, L., Knésl, I., Matysová, P., Majer, V. 2018. Hydrocarbon condensates and argillites in the Eliška Mine burnt coal waste heap of the Žacléř coal district (Czech Republic): products of high- and low-temperature stage of self-ignition. *International Journal Coal Geololgy* 190, 146–165. DOI: 10.1016/j.coal.2017.11.003

Swaine, D.J. 1994. Trace-elements in coal and their dispersal during combustion. *Fuel Processing Technology* 39(1-3), 121–137. DOI: 10.1016/0378-3820(94)90176-7

Taylor, L.T., Hausler, D.W., Squires, A.M. 1981. Organically bound metals in a solvent refined coal: metallograms for a Wyoming subbituminous coal. *Science* 7(4508), 644–646. DOI: 10.1126/science.213.4508.644

Vassilev, S.V., Eskenazy, G.M., Vassileva, C.G. 2001. Behaviour of elements and minerals during preparation and combustion of the Pernik coal, Bulgaria. *Fuel Processing Technology* 72(2), 103–129. DOI:10.1016/S0378-3820(01)00186-2

Voigt, S., Tetzlaff, A., Zhang, J., Künzer, C., Zhukov, B., Strunz, G., Oertel, D., Roth, A., van Dijk, P., Mehl, H. 2004. Integrating satellite remote sensing techniques for detection and analysis of uncontrolled coal seam fires in North China. *International Journal Coal Geololgy* 59(1-2), 121–136. DOI: 10.1016/j.coal.2003.12.013

Wagner, N.J., Hlatshwayo, B. 2005. The occurrence of potentially hazardous trace elements in five Highveld coals, South Africa. *International Journal Coal Geololgy* 63(3-4), 228–246. DOI: 10.1016/j.coal.2005.02.014

Wagoner, D. 1976. Compilation of Ambient Trace Substances. Draft of Report Prepared by Research Triangle Institute under Contract No. 68-02-1325. US Environmental Protection Agency (EPA),

Xiao, J., Li, F., Zhong, Q., Bao, H., Wang, B., Huang, J., Zhang, Y. 2015. Separation of aluminum and silica from coal gangue by elevated temperature acid leaching for the preparation of alumina and SiC. *Hydrometallurgy* 155, 118–124. DOI: 10.1016/j.hydromet.2015.04.018

Zhang, C.S. 2008. New Approaches in Gangue Resource Comprehensive Utilization. Chemical Industry Press, Beijing, p. 2008.

Zhang, J., Kuenzer, C. 2007. Thermal surface characteristics of coal fires 1: results of in-situ measurements. *Journal of Applied Geophysics* 63, 117–134. DOI: 10.1016/j.jappgeo.2007.08.002

Zhao, Y., Zhang, J.Y., Huang, W.C., Li, Y., Song, D.Y., Zhao, F.H., Zheng, C. 2008a. Arsenic emission during combustion of high-arsenic coals from Southwestern Guizhou. China. *Energy Conversion and Management* 49(4), 615–624. DOI: 10.1016/j.enconman.2007.07.044

Zhao, Y., Zhang, J., Chou, C.-L., Li, Y., Wang, Z., Ge, Y., Zheng, C. 2008b. Trace element emissions from spontaneous combustion of gob piles in coal mines, Shanxi, China. *International Journal Coal Geololgy* 73(1), 52–62. DOI: 10.1016/j.coal.2007.07.007

Zhou, C., Liu, G., Wu, D., Fang, T., Wang, R., Fan, X. 2014. Mobility behavior and environmental implications of trace elements associated with coal gangue: a case study at the Huainan Coalfield in China. *Chemosphere* 95, 193–199. DOI: 10.1016/j.chemosphere.2013.08.065

Zhou, Y., Ren, Y. 1992. Distribution of arsenic in coals of Yunnan province, China, and its controlling factors. *International Journal Coal Geololgy* 20(1-2), 85–98. DOI: 10.1016/0166-5162(92)90005-H

sciendo

Journal of Environmental Geography 14 (3–4), 39–46.

DOI: 10.2478/jengeo-2021-0010
ISSN 2060-467X

TEMPORAL RELATIONSHIP OF INCREASED PALAEODISCHARGES AND LATE GLACIAL DEGLACIATION PHASES ON THE CATCHMENT OF RIVER MAROS/MUREŞ, CENTRAL EUROPE

Tamás Bartyik[1]*, György Sipos[1], Dávid Filyó[1], Tímea Kiss[1], Petru Urdea[2], Fabian Timofte[2]

[1]Geomorphological and Geochronological Research Group, Department of Geoinformatics, Physical and Environmental Geography, University of Szeged, H-6722 Szeged, Egyetem u. 2-6, Hungary
[2]Department of Geography, West University of Timişoara, B-dul. Vasile. Parvan Nr. 4, 300223, Timişoara, Romania
*Corresponding author, email: bartyikt@geo.u-szeged.hu

Research article, received 5 October 2021, accepted 19 October 2021

Abstract

River Maros/Mureş has one of the largest alluvial fans in the Carpathian Basin. On the surface of the fan several very wide, braided channels can be identified, resembling increased discharges during the Late Glacial. In our study we investigated the activity period of the largest channel of them, formed under a bankfull discharge three times higher than present day values. Previous investigations dated the formation of the palaeochannel to the very end of the Pleistocene by dating a point bar series upstream of the selected site. Our aim was to obtain further data on the activity period of the channel and to investigate temporal relationships between maximum palaeodischarges, deglaciation phases on the upland catchment and climatic amelioration during the Late Pleistocene.
The age of sediment samples was determined by optically stimulated luminescence (OSL). The investigation of the luminescence properties of the quartz extracts also enabled the assessment of sediment delivery dynamics in comparison to other palaeochannels on the alluvial fan.
OSL age results suggest that the activity of the channel is roughly coincident with, but slightly older than the previously determined ages, meaning that the main channel forming period started at 13.50±0.94 ka and must have ended by 8.64±0.82 ka. This period cannot directly be related to the major phases of glacier retreat on the upland catchments, and in terms of other high discharge channels only the activity of one overlaps with a major deglaciation phase at ~17-18 ka. Based on these, high palaeodischarges can be rather related to increased Late Glacial runoff, resulted by increasing precipitation and scarce vegetation cover on the catchment. Meanwhile, the quartz luminescence sensitivity of the investigated channel refers to fast sediment delivery from upland subcatchments. Therefore, the retreat of glaciers could affect alluvial processes on the lowland by increasing sediment availability, which contributed to the development of large braided palaeochannels.

Keywords: OSL dating, River Maros/Mureş, deglaciation, luminescence sensitivity, sediment delivery

INTRODUCTION

According to Starkel (2002, 2007) and Vandenberghe (2008), in Eastern and Northern Europe the periods of the most intensive fluvial activity can be related to the beginning of interstadials, partly as a consequence of the accelerated retreat of ice sheets and mountain glaciers. This hypothesis however needs to be attested at different catchments at different latitudes (Antoniazza and Lane, 2021). The key to this question is to find relationships between archives located on upland catchments and on alluvial fans.

Alluvial fans are major elements of the central part of the Carpathian Basin, and as such research related to these geomorphological units has a well-established literature in Hungary (e.g. Gábris, 1995; Gábris and Nádor, 2007; Mezősi, 2011; Kiss et al., 2015). Among these sedimentary bodies the Maros/Mureş Alluvial Fan is one of the largest ones, and special in several respects: fluvial activity has been the dominant process up till the river regulation works and this is recorded by a complex set of palaeochannels; parts of the river's upland catchment were affected by glaciation during the Last Glacial Maximum and the Late Glacial. Consequently, the alluvial fan is an excellent candidate for investigating upland–lowland interactions under the changing environment of the Late Pleistocene and the Holocene.

The evolution of the Maros/Mureş Alluvial Fan, the discharge and age of its palaeochannels have been extensively studied by previous authors (Katona et al., 2012; Sipos, 2012; Sümeghy et al., 2013; Kiss et al., 2013, 2014, 2015; Sümeghy, 2014). A great number of paleodrainage directions were identified, being active from the Late Glacial to the Early Holocene (Kiss et al., 2013, 2015; Sümeghy, 2014). Based on the reconstruction of the channels, the discharge and sediment transport capacity of the river increased significantly during this period. Bankfull discharge calculations suggest that by the end of the Pleistocene, the river was several times larger than today, and its dimensions steadily decreased during the Holocene (Kiss et al., 2014).

According to Kiss et al. (2014) and Sümeghy (2014), the highest bankfull discharge palaeochannels were occupying the northern half of the alluvial fan and were active between 15.2±2.0 ka and 9.6±1.3 ka (Fig. 1B). These channels had mostly a braided pattern, and the largest of them, located near Orosháza (palaeochannel "D" on Fig. 1B) could have a bankfull discharge of ~2600 m3/s (Katona et al., 2012). During the transition from the Late Glacial to the Holocene, only slight variations can be detected in bankfull discharge values (Kiss et al., 2015; Sümeghy, 2014).

Previous research has shown that climate change played a major role in affecting water and sediment yields, and thus determining fluvial aggradation and erosion processes (Vandenberghe, 2008; Gábris, 2013). For example, the climatic fluctuations of the Pleistocene and parallel variations of runoff and vegetation cover resulted a cyclic change in the activity of Eastern European sub-basins, which could lead to the formation of sediment pulses (e.g. Starkel et al., 2007, Antoniazza and Lane, 2021). Furthermore, changing runoff and sediment conditions could also affect the number of sediment cycles observed along rivers. Similar processes were hypothesised for River Maros/Mureş (Sipos, 2012), draining the waters of several mountain ranges of the Eastren and Southern Carpathians, which were heavily glaciated during the Pleistocene (Urdea, 2004). The repeated retreat of glaciers could alter both the water and sediment discharge of the river (Sipos, 2012).

Recent surface exposure dating (SED) results in the northern and southern valleys of the Retezat Mts. (Southern Carpathians), being the highest mountain range on River Maros/Mureş catchment, suggest that the maximum extent of glaciers and the onset of deglaciation occurred at ~20-21 ka, the same as in the rest of Europe. Deglaciation in the area was uneven, and several separate stages can be identified on the basis of the age of moraines at different altitudes (Ruszkiczay-Rüdiger et al., 2016, 2017, 2021). However, due to rapid glacier retreat, these phases partially overlap (Ruszkiczay-Rüdiger et al., 2021). Based on the measurements of Ruszkiczay-Rüdiger et al. (2016), the youngest moraines in the northern valleys of the Retezat Mts. are related to a minor glacial advance at ~14.5 ka during the GI-1 interstadial (Bølling/Allerød). There is no direct evidence for later glaciation cycles in the area, i.e the last moraines in the area have been stable for nearly 13.5 ka (Ruszkiczay-Rüdiger et al., 2016).

Based on the above, the major aim of the present study was to investigate the possible temporal linkages between Late Glacial deglaciation processes on the upland catchment and lowland fluvial processes related to River Maros/Mureş, with special emphasis on the largest palaeochannel identifiable on the alluvial fan of the river. Besides, by using a novel approach we attempted to assess the dynamics of sediment delivery from upland sediment sources.

STUDY AREA AND SAMPLING

River Maros/Mureş is the fourth largest river of the Carpathian Basin, and it is the largest tributary of the Tisza River (Fig. 1A). The area of its catchment is ~30,000 km^2, it drains the waters of the Transylvanian Basin, and it is bordered by the Apuseni Mountains and the Eastern and Southern Carpathians. The highest range on the catchment, affected greatly by Pleistocene glaciation is the Retezat Mts., with a maximum height of 2509 m (Fig. 1A). The northern, western and major southern exposure valleys of the mountain range are all drained to River Strei, a tributary of the Maros/Mureş. The actual mean discharge of the river at its lowland section is 160 m^3/s, while its bankfull discharge can reach 850 m^3/s (Fiala et al., 2007).

Samples for OSL dating were collected from sediments related to the largest palaeochannel generation (palaeochannel "D"), located north of the axis of the alluvial fan, along the Kétegyháza – Orosháza – Hódmezővásárhely line. This channel was also investigated by Kiss et al. (2014) and Sümeghy (2014) at Orosháza (Fig. 1B). Based on their data, the channel was active between 12.4±2.1 and 9.6±1.3 ka (Sümeghy, 2014). The channel is characterised by a change from a braided to a meandering channel pattern near Orosháza and a braided pattern again on its lower reaches. The width of the channel can reach up to 1000 m, its average bankfull depth was estimated to be 2.8 m on the basis of topographical and shallow geophysical surveys (Katona et al., 2012). The bankfull discharge of the palaeochannel was estimated to be ~2600 m^3/s (Katona et al., 2012; Sümeghy, 2014).

Sediment samples were collected 30 km downstream of the Orosháza site (Kiss et al., 2014) near the former confluence with the palaeo-Tisza River (Fig. 1B). A total of four samples were collected from two sampling sites in a recently opened sand quarry, located in the area of the former village of Csomorkány, north-east of the town of Hódmezővásárhely (Fig. 1B).

The first sampling point (CSOM1) represents the point bar on the left bank of the former palaeochannel, while at the second sampling point (CSOM2) an aeolian sand sheet with parabolic dune forms was sampled (Fig. 1C). Based on the topography and the dominant wind direction (N-NW), the aeolian sediments investigated were blown out from the abandoned channel, and can indicate the minimum age of fluvial activity.

At the first CSOM1 profile, coarse grain cross-bedded deposits were observed, interbedded with thin silty layers, referring to a cyclic deposition during channel development (Fig. 2). The first sample (OSZ1468) was collected at 81.5 m asl., from a cross-bedded, coarse-grained fluvial deposit, while the second sample (OSZ1467) was taken from a sand layer between two silty deposits (Fig. 2). The third sample (OSZ1466) was collected at 82.5 m asl., from, above the topmost silt layer.

At the second sampling point (CSOM2), one sample was collected (OSZ1469) at a depth of 70 cm compared

to the ground surface level (~85.2 m asl), from a medium to coarse-grained, homogeneous, unstratified sand deposit. Based on its stratigraphic features the deposit was interpreted as an aeolian sand sheet; its material was presumably blown out of the already abandoned channel (Fig. 2).

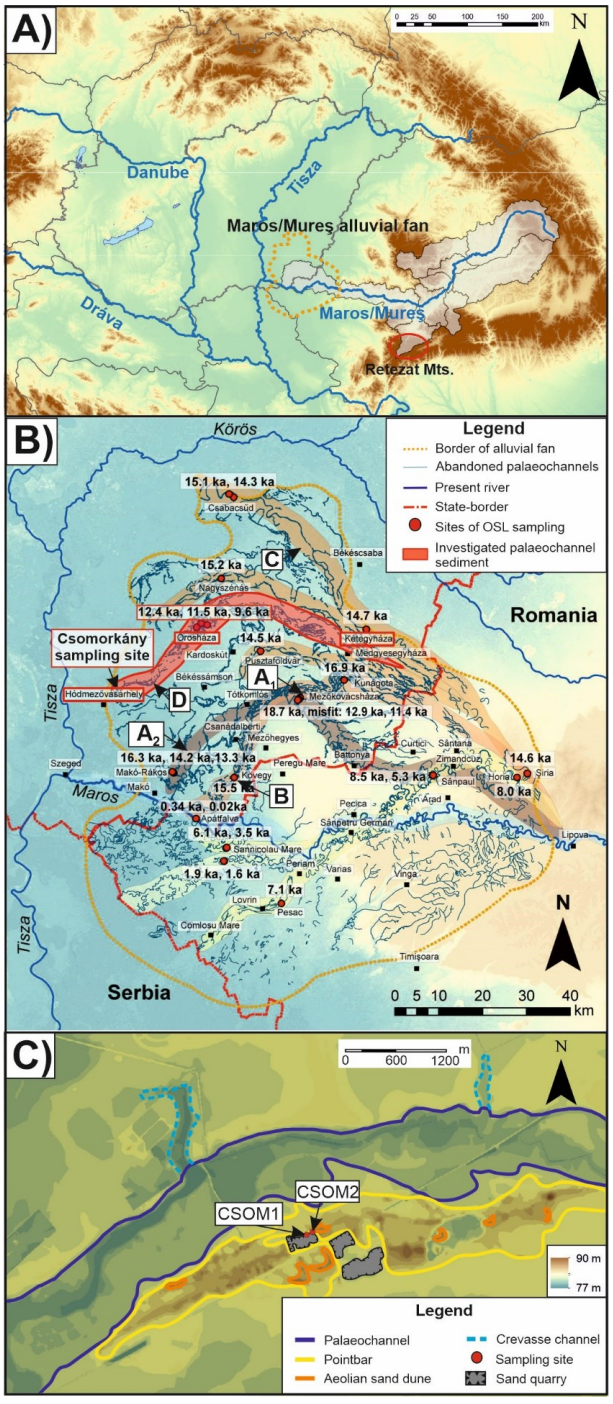

Fig. 1 A) Location of the Maros/Mureş Alluvial Fan and the Retezat Mts. in the Carpathian Basin;
B) Position of palaeochannels on the alluvial fan (after Sipos, 2012), those being active during the Late Glacial are marked by capital letters (following the system of Kiss et al., 2015), and the location of the Csomorkány sampling site;
C) DEM and most important geomorphological features of the Csomorkány sampling site.

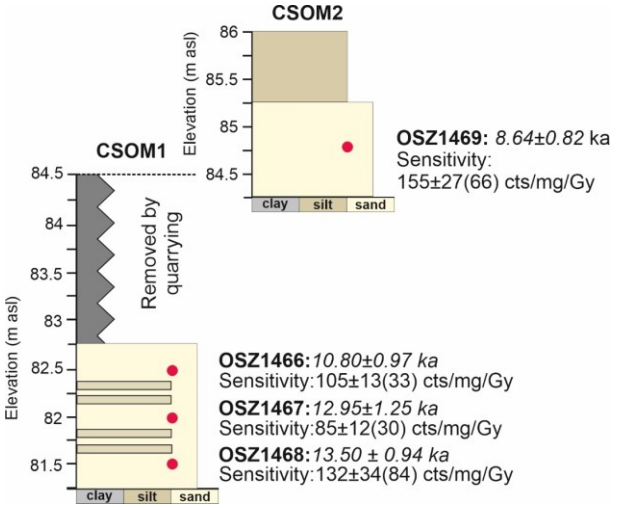

Fig. 2 The vertical position of sampling profiles and sampling points with the obtained OSL ages and quartz sensitivity values.

METHODS

The geomorphology of the study area was studied on the basis of a topographic map (scale of 1:10000). Geomorphological features were mapped using ESRI ArcGIS 10.4.1 (Fig. 1C).

At both sites, OSL samples were taken from an open profile of the sand quarry using an Eijkelkamp undisturbed sampler with light tight steel cylinders. An additional ~500 g of sediment was taken from around the OSL samples to determine the environmental dose rate necessary for age calculation. As most of the surface sediments have been removed by quarrying, the original altitude of the terrain could only be estimated using topographical maps (scale: 1:10000) made well before the opening of the quarry. The exact elevation of sampling points (m asl) was measured using an RTK GPS.

Optically Stimulated Luminescence (OSL) is a method to investigate the age of the last deposition of sediments, and thus it is suitable to date fluvial activity periods, for example the formation of palaeochannels and point bars (Rittenour, 2008). Although, the method is primarily used for dating, there is a number of additional information provided by luminescence measurements that can help to refine geomorphological reconstruction. One of these is measuring the OSL response to unit radioactive dose, by which the so called luminescence sensitivity, a parameter largely dependent on the petrological background and the sedimentation history of grains (Sawakuchi et al., 2018, Bartyik et al., 2021a), of the investigated mineral extract (this time quartz) can be assessed (Gray et al., 2019).

The preparation of the collected OSL samples has followed usual laboratory techniques (Mauz et al., 2002; Sipos et al., 2016). First a 1 cm thick layer was removed from each end of the sampling cylinders. The samples were then dried to constant weight to determine *in situ* water content. The coarse-grained sand was separated using sieves of 150-200 µm and 220-300 µm. The most abundant fraction was then subjected to acid treatment, using 10% HCl to remove the carbonate content and 10%

H_2O_2 to remove the organic matter content of the sample. The quartz fraction, essential for OSL measurements, was separated using an adjustable density heavy liquid (LST-Fastfloat). The separated quartz minerals were subjected to a 40% hydrogen fluoride (HF) treatment for further purification and accurate calculation of the dose rate. The clean quartz grains were spread on a 1 cm diameter stainless steel disc using a 2 mm mask. For luminescence sensitivity measurements, grains were placed in 1 cm diameter stainless steel cups. The weight of the samples in the sample carrier was recorded using an analytical balance for the mass normalisation of results later.

Equivalent dose (D_e) and sensitivity measurements were both carried out using a RISØ TL/OSL-DA-20 luminescence reader. Irradiation was made using a calibrated $^{90}Sr/^{90}Y$ beta source. Luminescence intensities were detected through a Hoya U-340 filter placed between the sample and the photomultiplier.

The Single Aliquot Regeneration (SAR) protocol, developed by Wintle and Murray (2006), was used to determine the De of quartz samples. Prior to De measurements a combined preheat and dose recovery test was performed on two samples (OSZ1466, OSZ1469) in order to determine optimal heating parameters. Based on the dispersion, skewness and kurtosis of single aliquot results, the minimum age model (MAM) was used to calculate sample equivalent dose values (Galbraith et al., 1999; Arnold et al., 2007).

The luminescence sensitivity of samples was assessed using both OSL and TL (thermoluminescence) responses for the same dose. Measurements and evaluation followed the steps of Nian et al. (2019) and Bartyik et al. (2021a). The previously bleached samples were irradiated with a uniform dose of 24 Gy. OSL sensitivity was determined using the first 0.5 s of the continuous wave OSL (CW-OSL) luminescence decay curves. For calculating TL sensitivity, the signal obtained in the 80-120°C range (TL 110°C peak) of the growth curve was integrated. These data were then normalised by sample mass, dose and background. The error of sensitivity results is expressed both using standard error (SE) and standard deviation (SD), the later one is put in parentheses hereinafter.

Environmental dose rate (D*), which is also essential for the calculation of the OSL age, was determined by measuring the specific activity of sediment samples using a Canberra XtRa extended range gamma spectrometer equipped with a Coaxial type Germanium detector. The cosmic dose rate was calculated using the empirical formula of Prescott and Hutton (1994).

RESULTS AND DISCUSSION

Luminescence properties

The preheat and dose recovery tests on sample OSZ1466 and OSZ1467 resulted very high recuperation values, close to the 5% threshold at all temperature ranges investigated (Fig. 3). In such cases, as suggested by Murray and Wintle (2003), an additional high temperature stimulation (280°C) (Hot Bleach) was added to the SAR protocol at the end of each measurement cycle.

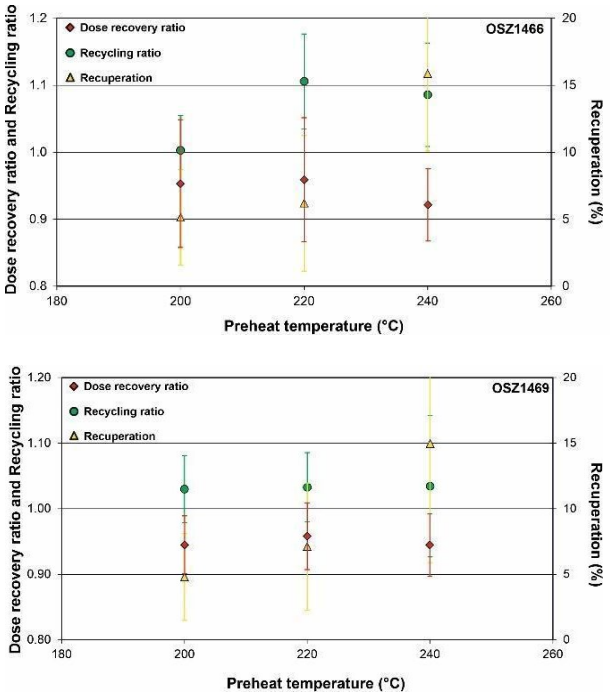

Fig. 3 Preheat and dose recovery test results for samples OSZ1466 and OSZ1469.

Consequently, the error caused by high recuperation values could be significantly reduced. Based on the combined preheat and dose recovery tests, a 200°C preheat temperature was chosen for subsequent measurements, as samples passed other SAR criteria (Wintle and Murray, 2006) also at this temperature (Fig. 3).

During sensitivity measurements, each sample produced an adequate amount of luminescence signal. The lowest sample in the CSOM1 section, OSZ1468, had a sensitivity of 132±34(84) cts/mg/Gy, while the two samples above (OSZ1467, OSZ1466) had slightly lower values: 85±12(30) cts/mg/Gy and 105±13(33) cts/mg/Gy (Table 1). Sample OSZ1469 with an aeolian origin had the highest CW-OSL sensitivity, being 155±27(66) cts/mg/Gy.

In terms of the TL 110°C peak sensitivity values, no significant differences could be identified at the CSOM1 profile (Table 1). OSZ1466 yielded 1517±148(419) cts/mg/Gy, OSZ1467 1447±106(300) cts/mg/Gy and the lowest sample OSZ1468 1530±211(597) cts/mg/Gy. However, the OSZ1469 sample from CSOM2 had a TL sensitivity of 2160±290(821) cts/mg/Gy, which is significantly higher than in the case of the previous samples (Table 1).

After plotting the two sensitivity parameters against each other it became possible to compare quartz sensitivities to previous data obtained from other sediments related either to the Maros/Mureş, Tisza or Danube Rivers (Fig. 4) investigated by Bartyik et al. (2021a). The detailed comparison of the CW-OSL and TL 110°C peak sensitivities of the Csomorkány quartz with the results of the Carpathian Basin fluvial samples (Bartyik et al., 2021a), reflects that the CSOM1 section samples represent a transitional sensitivity level (Fig. 4).

Table 1 Dose rate, equivalent dose and sensitivity data of the investigated samples.

Lab ID	OSZ1466	OSZ1467	OSZ1468	OSZ1469
Altitude of the sample [m asl]	82.5	82	81.5	84.8
Water content [%]	10±2	10±2	10±2	10±2
U [ppm]	1.35±0.02	1.47±0.02	1.21±0.02	1.51±0.02
Th [ppm]	4.81±0.11	5.11±0.12	4.33±0.11	5.27±0.12
K [ppm]	1.34±0.04	1.26±0.04	1.14±0.03	1.21±0.04
D* [Gy/ka]	1.85±0.04	1.65±0.04	1.60±0.04	1.84±0.04
D_e [Gy]	19.97±1.73	21.38±1.94	21.66±1.44	15.93±1.46
Age [ka]	10.80±0.97	12.95±1.25	13.50±0.94	8.64±0.82
CW-OSL sensitivity mean±SE(SD) [cts/mg/Gy]	105±13(33)	85±12(29)	132±34(84)	155±27(66)
TL 110°C peak sensitivity mean±SE(SD) [cts/mg/Gy]	1517±148(419)	1447±106(300)	1530±211(597)	2156±290(821)

It is also clear that the CSOM1 samples have considerably lower CW-OSL values compared to the mean of all other Maros/Mureş sediments (175±10(67) cts/mg/Gy) from other palaeochannels on the alluvial fan (Bartyik et al., 2021a; Fig. 4). This average value is only approached by the aeolian sample in the CSOM2 profile (OSZ1469). The same trend can be identified concerning the TL 110°C peak sensitivity. In this case the average value of CSOM1 samples, being 1476±86(437) cts/mg/Gy is also significantly lower than the average TL sensitivity of other samples from the alluvial fan, being 2193±146(506) cts/mg/Gy. From among the samples studied by Bartyik et al. (2021a) one represented the same palaeochannel, but was collected at the Orosháza site investigated by Sümeghy (2014). This sample plots very close to CSOM1 samples and just like these it can clearly be differentiated from other Maros/Mureş Alluvial Fan samples (Fig. 4). Consequently, the low sensitivity of samples is not site specific, but can be characteristic for the entire palaeochannel.

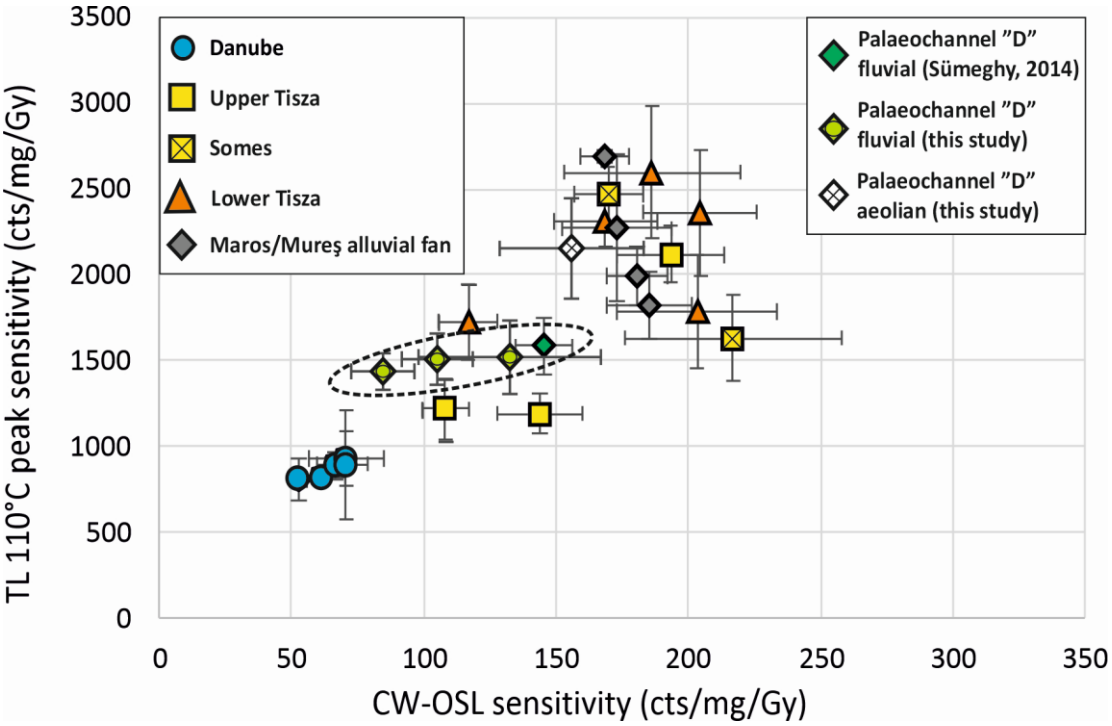

Fig. 4 CW-OSL and TL 110°C peak sensitivity results compared to the sensitivity results of Bartyik et al. (2021a). Values measured for the fluvial samples at the Csomorkány site and at the upstream Orosháza site are circled with a dashed line.

Low sensitivity values experienced in case of palaeochannel "D" can be explained by two factors. Firstly by the increased contribution of catchments rich in low sensitivity quartz to the sediment mixture of the palaeochannel. For example, it was demonstrated by Bartyik et al. (2021b) that the quartz sensitivity in a major tributary of the Maros/Mureş (River Strei), collecting the sediments of the Northern and Southern slopes of the Retezat Mts., is lower than the sensitivity of quartz from other catchments. Consequently, after the deglaciation this catchment could provide a considerable input to the main river. Secondly, as the number of sedimentary cycles can increase significantly the sensitivity of quartz grains (see e.g. Preusser et al., 2006; Fitzsimmons, 2011), the fast transfer of sediments from the upper catchments to the alluvial fan can also explain the low sensitivity of fluvial sediments related to palaeochannel "D". Taking into consideration that the redeposited aeolian sample at the investigated site (OSZ1469) has higher sensitivity than fluvial ones, it seems probable that the second factor, i.e. limited sediment recycling due to fast sediment transfer can be the main reason behind low sensitivity values of palaeochannel "D".

OSL quartz ages

The lowermost sample (OSZ1468) from the CSOM1 profile gave an age of 13.50±0.94 ka. A very similar result was obtained for the sample above (OSZ1467), giving an OSL age of 12.95±1.25 ka, meaning practically that the two layers can be related to the same fluvial cycle. These ages refer to channel sediment deposition during the GI-1 interstadial. The topmost sample at the CSOM1 profile is significantly younger and refers to another depositional event, in the Early Holocene at 10.80±0.97 ka. These data, by considering the uncertainty of OSL ages refer to a channel forming fluvial activity between ~14.5 and 9.8 ka ago (Table 1., Fig. 5).

The results of the samples from the CSOM1 profile are mostly in agreement with the OSL ages measured by Kiss et al. (2015) and Sümeghy (2014) on the upstream part of the same palaeochannel, determining an activity period between 12.4±2.1 and 9.6±1.3 ka. However, the present results slightly push back the start of major channel development along the investigated channel generation.

Sample OSZ1469, collected from the CSOM2 profile gave an OSL age of 8.64±0.82 ka, which is considerably younger than the fluvial records of the Csomorkány sampling site. During this period, the Maros/Mureş already shifted to the southern part of its alluvial fan (Kiss et al., 2015). The stratigraphy and the geomorphological setting suggest that aeolian activity started in the area after the avulsion, as the channel became dry. The higher luminescence sensitivity sample (OSZ1469) also refers to aeolian redeposition which can significantly increase sensitivity values as demonstrated by Fitzsimmon (2011) or Sawakuchi et al. (2011).

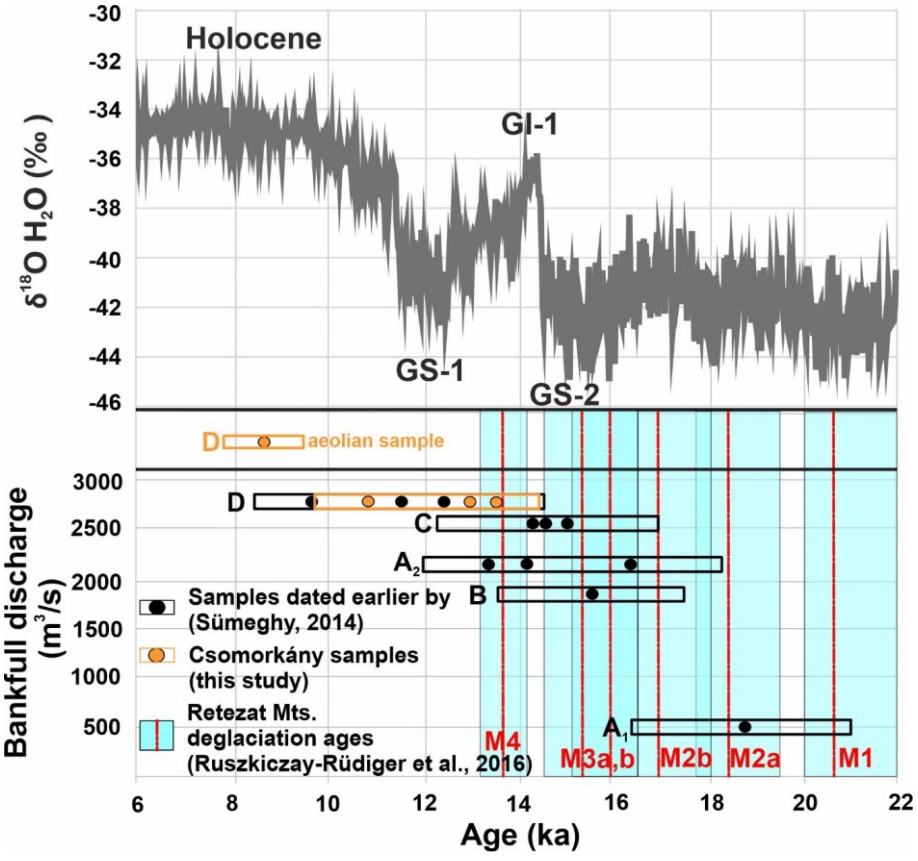

Fig. 5 Deglaciation phases in the northern valleys of the Retezat Mts. (Ruszkiczay-Rüdiger et al., 2016, 2021). B: palaeochannel activity periods on the Maros/Mureş Alluvial Fan (this study and Sümeghy, 2014) and the bankfull discharges of channels (Katona et al., 2012; Kiss et al., 2014), fitted to benthic $\delta^{18}O$ records (Lisiecki and Raymo, 2005).

Relationship of fluvial activity and deglaciation history

If the activity periods of palaeochannels along with their attributed discharge values determined by Kiss et al. (2015) and Katona et al., (2012) are compared to the deglaciation phases of the Retezat Mts., one can see that the lowest bankfull discharge palaeochannel "A1" coincides with the M1 (~22-20 ka) and M2 (~17-18 ka) deglaciation periods of the Late Glacial (Fig. 5). The elevation of M1 and M2 terminal moraines on the northern and southern slopes is 1080-1130 m asl. and 1220-1610 m asl (Ruszkiczay-Rüdiger et al., 2021), respectively, equalling to equilibrium line altitudes (ELA) of 1830-1900 m and 1960-1970 m (Ruszkiczay-Rüdiger et al., 2016). This means that the most intensive retreat of glaciers did not have a significant effect on the discharge of River Maros/Mureş on the alluvial fan.

The activity of channels with significantly higher discharges (palaeochannels: A2, B, C and D) can rather be related to deglaciation phases M3 and M4, occurring after minor glacier advance, leaving behind moraines at 1700-1880 m and 2050-2010 m asl, respectively, i.e. the ELA ascended to ~2040-2200 m asl. in this period (Ruszkiczay-Rüdiger et al., 2017; 2021). This also means that during these late phases the condition of glaciers affected only the top most region of the mountain range, thus melting could not significantly contribute to the high discharges experienced in terms of the palaeochannels on the alluvial fan (Fig. 5). Moreover, palaeochannel "C" with a bankfull discharge of ~2500 m^3/s was dated to GS-2 stadial, a cold period presumably resulting glacier advance anyway.

Although the activity of the now investigated palaeochannel "D" started during deglaciation phase M4, it also coincides with the GI-1 interstadial (Rasmussen et al., 2014), notable of large discharges on other Carpathian Basin rivers as a matter of precipitation increase (see e.g. Gábris, 1995, Gábris and Nádor, 2007).

At the same time, the braided pattern of palaeochannels from this period suggests a high availability of sediments on the catchment that can be partly caused by coarse grain sediments released from previously glaciated valleys on the upland catchment (Antoniazza and Lane, 2021), and the time lag between the adaptation of vegetation to climate change (Vandenberghe, 2008). Both leading to the initiation of sediment pulses towards the alluvial fan. Thus, due to the rapid warming (GI-1) and cooling (GS-1) of the climate, coarse grain sediments accumulated previously as a matter of limited runoff could be mobilised on the upper catchment. Consequently, deglaciation rather contributed to the changing sediment regime, the development of sediment pulses and the changing style of river channels on the alluvial fan.

CONCLUSIONS

The obtained ages pushed back the activity of the largest palaeochannel (palaeochannel "D") on the alluvial fan of River Maros/Mureş by approximately 1.0 ka compared to earlier studies. Still, the ages between 13.5±0.9 (this study) and 9.6±1.3 ka (Kiss et al., 2014), representing the channel forming period of the investigated palaeochannel, cannot be directly related to the major deglaciation phases of the Retezat Mts. Thus, the extremely high discharge inferred from the studied channel occurred as a matter of increased precipitation during the GI-1 interstadial and the delayed appearance of vegetation cover, both contributing to very high runoff values. Concerning other, relatively high discharge palaeochannels (A2, B, C) activity periods overlap with the final deglaciation phases of the Retezat Mts, but these final phases affected very limited areas on the upland catchment, and therefore, could not significantly contribute to increased runoff.

Though deglaciation did not affect significantly plaeodischarge values, sediment availability supposedly increased during the climatic amelioration. From upland sub-catchments a considerable amount of coarse grain sediment could be mobilised after the retreat of glaciers, and consequently shallow, braided channels could develop on the alluvial fan. Increased sediment delivery was also supported by the measured luminescence sensitivity values. Sediments associated with the fluvial activity of the investigated palaeochannel exhibit lower quartz luminescence sensitivity than any other previously investigated palaeochannels on the Maros/Mureş Alluvial Fan. Low values could be caused by 1) more active sediment supply from previously glaciated sub-catchments rich in low luminescence sensitivity quartz grains, and 2) faster delivery of grains towards the alluvial fan, whereby the grains were not subjected to several cycles of deposition which could enhance their sensitivity.

ACKNOWLEDGEMENTS

This work was supported by the Hungarian National Research, Development and Innovation Office (OTKA K119309 and K135793) and by the ÚNKP-21-4-SZTE-447 New National Excellence Program of the Ministry for Innovation and Technology from the source of the National Research, Development and Innovation Fund.

REFERENCES

Antoniazza, G., Lane, S.N. 2021. Sediment yield over glacial cycles: A conceptual model. *Progress in Physical Geography: Earth and Environment* (OnlineFirst), 1–24. DOI: 10.1177/0309133321997292

Arnold, L.J., Bailey, R.M., Tucker G.E. 2007. Statistical treatment of fluvial dose distributions from southern Colorado arroyo deposits. *Quaternary Geochronology* 2, 162–167. DOI: 10.1016/j.quageo.2006.05.003

Bartyik, T., Floca, C., Pál-Molnár, E., Urdea P., Hamed, E.D., Sipos, Gy. 2021a. The potential use of OSL properties of quartz in investigating fluvial processes on the catchment of river Mures, Romania. *Journal of Environmental Geography* 14(1-2), 58–67. DOI: 10.2478/jengeo-2021-0006

Bartyik, T., Magyar, G., Filyó, D., Tóth, O., Blanka-Végi, V., Kiss, T., Marković, S., Persoiu, I., Gavrilov, M., Mezősi, G., Sipos, G. 2021b. Spatial differences in the luminescence sensitivity of quartz extracted from Carpathian Basin fluvial sediments. *Quaternary Geochronology* 64, 101166. DOI: 10.1016/j.quageo.2021.101166

Fiala, K., Sipos, Gy., Kiss, T., Lázár, M. 2007. Morfológiai változások és a vízvezető képesség a Tisza és Maros makói szelvényében a 2000. évi árvíz kapcsán (Morphological changes and water conductivity in the Makó section of the Tisza and Maros rivers in relation to the 2000 flood). *Hidrológiai Közlöny* 87(5), 37–45. (in Hungarian)

Fitzsimmons, E. 2011. An assessment of the luminescence sensitivity of Australian quartz with respect to sediment history. *Geochronometria* 38(3), 199–208. DOI: 10.2478/s13386-011-0030-9

Galbraith, R.F., Roberts, R.G., Laslett, G.M., Yoshida, H., Olley, J.M. 1999. Optical dating of single and multiple grains of quartz from Jinmium Rock Shelter, northern Australia: Part 1, experimental design and statistical models. *Archaeometry* 41, 339–364. DOI: 10.1111/j.1475-4754.1999.tb00987.x

Gábris, Gy. 1995. A folyóvízi felszínalakítás módosulásai a hazai későglaciális-holocén őskörnyezet változásainak tükrében (River activity as a function of changing palaeoenvironmental conditions during the Late Glacial-Holocene, Hungary). *Földrajzi Közlemények* 119, 3–10. (in Hungarian)

Gábris, Gy., Nádor, A. 2007. Long-term fluvial archives in Hungary: response of the Danube and Tisza rivers to tectonic movements and climatic changes during the Quaternary: a review and new synthesis. *Quaternary Science Reviews* 26, 2758–2782. DOI: 10.1016/j.quascirev.2007.06.030

Gábris, Gy. 2013. A folyóvízi teraszok hazai kutatásának rövid áttekintése – A teraszok kialakulásának és korbeosztásának új magyarázata (A brief review of domestic research on river terraces - A new explanation of terrace formation and age distribution). *Földrajzi Közlemények* 137(3), 240–247. (in Hungarian)

Gray, H.J., Jain, M., Sawakuchi, A.O., Mahan, S.A., Tucker, G.E. 2019. Luminescence as a sediment tracer and provenance tool. *Reviews of Geophysics* 57(3), 987–1017. DOI: 10.1029/2019RG000646

Katona, O., Sipos, Gy., Onaca, A., Ardelean, F. 2012. Reconstruction of palaeo-hydrology and fluvial architerture at the Orosháza palaeochannel of River Maros, Hungary. *Journal of Environmental Geography* 5(1-2), 29–38.

Kiss, T., Sümeghy, B., Hernesz, P., Sipos, Gy., Mezősi, G. 2013. Az Alsó-Tisza menti ártér és a Maros hordalékkúp késő-pleisztocén és holocén fejlődéstörténete (The Late Pleistocene and Holocene evolution of the Lower Tisza floodplain and the Maros alluvial fan). *Földrajzi Közlemények* 137, 269–277. (in Hungarian)

Kiss, T., Sümeghy, B., Sipos, Gy. 2014. Late Quaternary paleo-drainage reconstruction of the Maros River Alluvial Fan. *Geomorphology* 204, 49–60. DOI: 10.1016/j.geomorph.2013.07.028

Kiss, T., Hernesz, P., Sümeghy, B., Györgyövics, K., Sipos, Gy. 2015. The evolution of the Great Hungarian Plain fluvial system - Fluvial processes in a subsiding area from the beginning of the Weichselian. *Quaternary International* 388, 142–155. DOI: 10.1016/j.quaint.2014.05.050

Lisiecki, E.L., Raymo, E.M. 2005. A Pliocene-Pleistocene stack of 57 globally distributed benthic $\delta^{18}O$ records. *Paleoceanography* 20(1), PA1003, 1–17. DOI: 10.1594/PANGAEA.704257

Mauz, B., Bode, T., Mainz, E., Blanchard, H., Hilger, W., Dikau, R., Zöller, L. 2002. The luminescence dating laboratory at the University of Bonn: Equipment and procedures. *Ancient TL* 20(2), 53–61.

Mezősi, G. 2011. Magyarország természetföldrajza (Physical Geography of Hungary). Akadémiai Kiadó, Budapest. 49–65. (in Hungarian)

Murray, A.S., Wintle, A.G. 2003. The single aliquot regenerative dose protocol: Potential for improvements in reliability. *Radiation Measurements* 37(4), 377–381. DOI: 10.1016/S1350-4487(03)00053-2

Nian, X., Zhang, W., Qiu, F., Qin, J., Wang, Z., Sun, Q., Chen, J., Chen, Z., Liu, N. 2019. Luminescence characteristics of quartz from Holocene delta deposits of the Yangtze River and their provenance implications. *Quaternary Geochronology* 49, 131–137. DOI: 10.1016/j.quageo.2018.04.010

Pietsch, T.J., Olley, J.M., Nanson, G.C. 2008. Fluvial transport as a natural luminescence sensitiser of quartz. *Quaternary Geochronology* 3(4), 365–376. DOI: 10.1016/j.quageo.2007.12.005

Prescott, J.R., Hutton, J.T. 1994. Cosmic ray contributions to dose rates for luminescence and ESR dating: large depths and long term variations. *Radiation Measurements* 23, 497–500. DOI: 10.1016/1350-4487(94)90086-8

Preusser, F., Ramseyer, K., Sclücheter, C. 2006. Characterisation of low OSL intensity quartz from New Zealand Alps. *Radiation Measurements* 41, 871–877. DOI: 10.1016/j.radmeas.2006.04.019

Rasmussen, S.O., Bigler, M., Blockley, S.P.E., Blunier, T., Buchardt, S.L., Clausen, H.B., Cvijanovic, I., Dahl-Jensen, D., Johnsen, S.J., Fischer, H., Gkinis, V., Guillevic, M., Hoek, W.Z., Lowe, J.J., Pedro, J., Popp, T., Seierstad, I.K., Steffensen, J.P., Svensson, A.M., Vallelonga, P., Vinther, B.M., Walker, M.J.C., Wheatley, J.J., Winstrup, M. 2014. A stratigraphic framework for naming and robust correlation of abrupt climatic changes during the last glacial period based on three synchronized Greenland ice core records. *Quaternary Science Review* 106, 14–28. DOI: 10.1016/j.quascirev.2014.09.007

Rittenour, T.M. 2008. Luminescence dating of fluvial deposits: applications to geomorphic, palaeoseismic and archeological research. *Boreas* 37(4), 613–635. DOI: 10.1111/j.1502-3885.2008.00056.x

Ruszkiczay-Rüdiger, Zs., Kern, Z., Urdea, P., Braucher, R., Madarász, B., Schimmelpfennig, I., ASTER TEAM 2016. Revised deglaciation history of the Pietrele-Stânişoara glacial complex, Retezat Mts, Southern Carpathians, Romania. *Quaternary International* 415, 216–229. DOI: 10.1016/j.quaint.2015.10.085

Ruszkiczay-Rüdiger, Zs., Madarász, B., Kern, Z., Urdea, P., Braucher, R., ASTER TEAM 2017. Late Pleistocene deglaciation and paleo-environment in the Retezat Mountains, Southern Carpathians, in*:* Geophysical Research Abstracts 18, EGU2017-2755.

Ruszkiczay-Rüdiger, Zs., Kern, Z., Urdea, P., Madarász, B., Braucher, R., ASTER TEAM 2021. Limited glacial erosion during the last glaciation in mid-latitude cirques (Retezat Mts, Souther Carpathians, Romania). *Geomorphology* 384, 107719, 1–19. DOI: 10.1016/j.geomorph.2021.107719

Sawakuchi, A.O., Blair, M.W., DeWitt, R., Faleiros, F.M., Hyppolito, T.N., Guedes, C.C.F. 2011. Thermal history versus sedimentary history: OSL sensitivity of quartz grains extracted from rocks and sediments. *Quaternary Geochronology* 6, 261–272. DOI: 10.1016/j.quageo.2010.11.002

Sawakuchi, A.O., Jain, M., Mineli, T.D., Nogueira, L., Bertassoli Jr., D.J., Häggi, C., Sawakuchi, H.O., Pupi, F.N., Grohmann, C.H., Chiessi, C.M., Zabel, M., Mulitza, S., Mazoca, C.E.M., Cunha, D.F. 2018. Luminescence of quartz and feldspar fingerprints provenance and correlates with the source area denudation in the Amazon River basin. *Earth and Planet Science Letters* 492, 152–162. DOI: 10.1016/j.epsl.2018.04.006

Sipos, Gy. (ed.) 2012. Past, Present and Future of the Maros/Mureş River. University of Szeged. p. 212.

Sipos, Gy., Kiss, T., Tóth, O. 2016. Constraining the age of floodplain levels along the lower section of river Tisza. Hungary. *Journal of Environmental Geography* 9(1-2), 39–44. DOI: 10.1515/jengeo-2016-0006

Starkel, L. 2002. Younger Dryas-Preboreal transition documented in the fluvial environment of Polis rivers. *Global and Planetary Change* 35, 157–167. DOI: 10.1016/S0921-8181(02)00133-9

Starkel, L., Gębica, P., Superson, J. 2007. Last Glacial–Interglacial cycle in the evolution of river valleys in southern and central Poland. *Quaternary Science Reviews* 26, 2924–2936. DOI: 10.1016/j.quascirev.2006.01.038

Sümeghy, B., Kiss, T., Sipos, Gy., Tóth, O. 2013. A Maros hordalékkúp felszíni képződményeinek geomorfológiája és kora (Geomorphology and age of the surface formations of the Maros alluvial fan). *Földtani Közlöny* 143/3, 265–278. (in Hungarian)

Sümeghy, B. 2014. A Maros hordalékkúp fejlődéstörténeti rekonstrukciója (Historical reconstruction of the evolution of the Maros alluvial fan). PhD dissertation, Szegedi Tudományegyetem. (in Hungarian)

Urdea, P. 2004. The Pleistocene glaciation of the Romanian Carpathians, in: Quaternary Glaciations – Extend chronology, Ehlers, J., Gibbard, P.L. (eds.), 2004 Elsevier B.V. 301–307.

Vandenberghe, J. 2008. The fluvial cycle at cold-warm-cold transitions in lowland regions: a refinement of theory. *Geomorphology* 98, 275–284. DOI: 10.1016/j.geomorph.2006.12.030

Wintle, A.G., Murray, A.S. 2006. A review of quartz optically stimulated luminescence characteristics and their relevance in single-aliquot regeneration dating protocols. *Radiation Measurements* 41, 369–391. DOI: 10.1016/j.radmeas.2005.11.001

sciendo

Journal of Environmental Geography 14 (3–4), 47–53.

DOI: 10.2478/jengeo-2021-0011
ISSN 2060-467X

STATISTICAL ANALYSIS OF WEATHER PARAMETERS FOR SUSTAINABLE FLIGHT OPERATION IN NIGERIA

Abiodun Daniel Olabode[1]

[1]Department of Geography and Planning Sciences, Adekunle Ajasin University, Akungba-Akoko, Ondo State, Nigeria
*Corresponding author, email: olabiodun4real@gmail.com

Research article, received 28 June 2021, accepted 20 October 2021

Abstract

The recent complications in the weather system, which oftentimes lead to flight cancellation, delay and diversion have become a critical issue in Nigeria. This study however considers the weather related parameters and their impacts on flight disruption in the country. Weather data (on thunderstorm, wind speed and direction, visibility and cloud cover) and flight data (delay, cancellation and diversion) were collected from Murtala International Airport, Ikeja-Lagos, Nigeria. The data covered the period between 2005 and 2020. However, Regional Climate Models (RCMs) were also used to run climate data projections between year 2020 and 2035 in the study region. The study employed Statistical Package for Social Sciences (SPSS) software for the descriptive and inferential analysis. Time series analysis, Pearson Moment Correlation for interrelationship among the weather parameters and the flight disruption data, and multiple linear regression analysis were applied to determine the influence of weather parameters on flight disruption data. Results show that cloud cover and high visibility are negatively correlated. Wind speed has positive relationship with wind direction; and an inverse relationship between visibility, thunderstorm, and fog. Direct relationship exists between highest visibility and thick dust, wind speed and cloud cover. Thick dust, wind speed and cloud cover indicate increased visibility level in the study area. Flight delay is prominent over flight diversion and cancellation, which indicates their relevance in air traffic of the study area. The prediction model indicates high degree of cloud cover at the beginning of every year and later declines sharply in 2035, the visibility flattens out by the year 2025, and low pattern of thick dust was calculated in the same pattern in 2011, 2016 and 2027. Based on this conclusion, the study recommends accurate weather reporting and strict compliance to safety regulations, and attention should be paid to changing pattern of weather parameters in order to minimize fight related disasters.

Keywords: weather parameters, air traffic, flight delay, flight diversion, flight cancellation

INTRODUCTION

Weather is extremely changeable because the atmosphere that constitute it is never static. Consequently, it is crucial to understand the mechanism of this variation to mitigate the negative effects on the society. The general public and the aviation industry in particular have become aware of this variability, and feel its negative impacts where they live. There has been an increasing awareness, concern and studies on weather parameters as one of the causes of air disasters over the years. The importance of such studies cannot be overemphasized if air safety must be achieved. However, there is still low level of recognition and research attention on some weather parameters in Nigeria.

Aviation is one of the critical parts of any national economy. It provides fastest means of moving people and goods among the world's nations for enabling economic growth (Waitz et al., 2004). The volume of air transportation is increasing rapidly; though the safety of aviation becomes an important problem over many countries. As noted by McFadden and Hosmane (2001), accident of an aircraft usually leads to human injury and loss of life. As noted by Nwaogbe et al. (2013), air transportation is a major industry in its own right and it also provides important inputs into wider economic, political, and social processes. The demand for its services, as with most transport, is a derived one that is driven by the needs and desires to attain some other final objective. Lack of air transport, as with any other input into the economic system, can prevent efficient growth.

The Nigerian aviation industry witnessed its darkest period between 2003 and 2010, when several aircraft accidents occurred, resulting in loss of lives. It was however observed that air crashes occurred between 2003 and 2006 mostly as a result of weather and wind shear anomalies. Knecht (2008) confirmed that most of the plane crashes could be associated with poor conditions of weather and some other factors. Similarly, flight delay, cancellation, diversion and air craft accidents affect the Nigerian Aviation Industry as Ayoade (2004) has earlier noted that "the vagaries of weather with references of the various meteorological parameters act malevolently against most of man's socio-economic activities". Consequently, flight delay, flight cancellation, and flight diversion were adopted as control measure of avoiding aircraft accidents.

Weather, which is defined as the snapshot of atmospheric conditions and a technical status report of the earth atmosphere heat energy budget or simply defined as an everyday experience (Stringer, 1989), can evolve at a

rapid rate over a wide spatial extent when compared with other factors that may affect the safe conduct of flight. Thus, the spectrum of weather information is an important component for flight safety and the efficient management of air transport in future (Mirza et al., 2009).

In some cases, weather is completely neglected. For instance, Arizona-Ogwu (2008), in a study on safety of air transport in Nigeria reported that experts attributed the causes of air disaster to pilot error (human related), pilot error (weather related), pilot error (mechanical related), other human error, weather, mechanical failure, sabotage etc. Nevertheless, he attributed it to out-dated air crafts being flown everywhere in Nigeria rather than what the experts revealed. He also reported that between 1988 and 2005 (in 17 years), the private airlines recorded 12 crashes, of which only one had no casualties, while the total deaths recorded was 762. There are three major weather phenomena, which pose severe threat to air transportation under the two distinct seasons observed in Nigeria. Thunderstorms occur within the wet/rainy season, while fog and dust haze (harmattan) are typical in the dry period of the year. This implies that the phenomenon of plane crash is tied to these two major seasons in Nigeria.

Thus, assessment of relevant weather parameters that include temperature, humidity, wind, cloud cover, visibility, fogs, thunderstorms, and dust haze is critical for aviation activities. This is more so considering aviation as one of the earliest industries involved in using weather as the basis for its operational decision making. Good knowledge of flight operation vis-à-vis operational weather situation is a precondition for passengers' safety and protection of goods. Riehl (1965) has shown that low ceilings and visibilities cause the major traffic disruptions at airport terminals, and the problem is said to remain unchanged over the years. In addition, Smith (1975) reports that despite increasing sophistication of automatic landing equipment, poor visibility from layer of fog, mist or thick haze and low cloud ceilings is probably the major impediment to airport operations throughout the world. The major challenges facing the aviation industry has been to adapt to the vigorous of an extreme and variable weather environment. In prospect of this fact, it becomes highly desirable to ascertain the nature of weather parameters in an area. This is because the safety of modern air communication is closely tied to accurate weather reports from the meteorological stations, and weather conditions influence the performance and durability of aircraft engines. More so, wind affects the degree of smoothness of the air and brings about changes in weather, which makes a difference between safe flight and disaster. The apprehension is that, the incessant flight cancellation, re-routing, delay, diversion of recent, mostly because of this natural factors (bad and inclement weather) may remain or even increase with the present concept of climate change and its resultant global warming if something is not done to mitigate the situation.

The focus of this study is on the statistical analysis of weather parameters for flight operation in Lagos, Ikeja, Nigeria; aiming to describe various parameters influencing flight operation, and relationship among weather parameters for supporting sustainable flight planning. Evaluating the effects of cloud cover, thunderstorm, visibility, wind speed and direction on flight operation and how weather conditions could be managed for sustainable flight operation in Murtala Mohammed International Airport is the prime focus of this study.

STUDY AREA

The Murtala Mohammed International Airport owned and operated by the Federal Airport Authority of Nigerian (FAAN) is situated in the suburb of Ikeja, 22 km northwest of Lagos. The coordinate of the airport is 06°34'39''N and 03°19'16''E (Fig. 1).

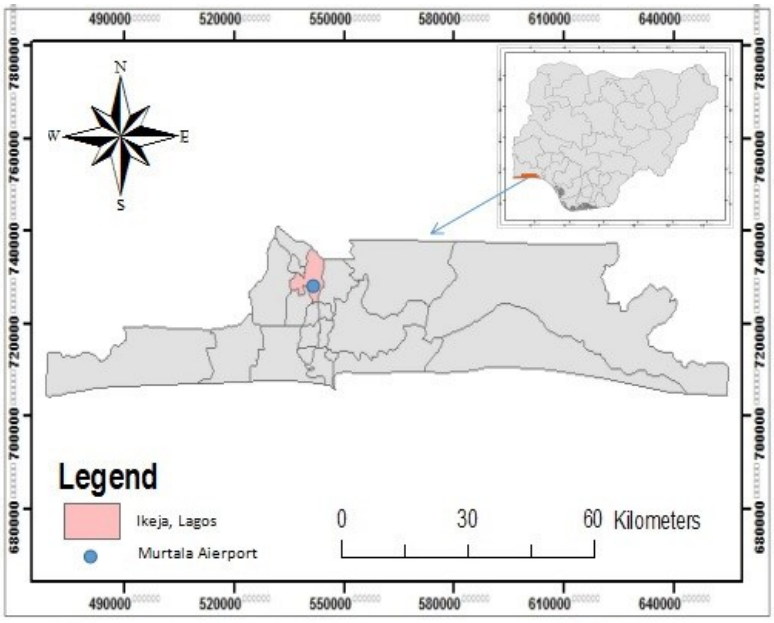

Fig. 1 Map of Lagos State showing study area at the Murtala Mohammed International Airport (source: Ministry of Lands and Housing, Ikeja, 2020)

Lagos experiences tropical wet and dry Savannah climate AW according to the Köppen climate classification. The heavy rainy season is between April and June, and the milder rainy season occurs between October and November. A very brief dry season is in August and September, whereas a long dry period occurs from December to March. The average rainfall between May and July is over 300 mm, while it is only 75 mm to 100 mm in August and September. In January, the average rainfall is only 35 mm (Fig. 2). The long dry season is followed by dry wind coming from the Sahara Desert, which is the most intense during the months from December to February (Pospichal, et al., 2010).

Temperature in Lagos does not vary greatly. March is generally the hottest month, with an average temperature reaching 29°C (Fig. 3). July is usually the coolest month, averaging 25°C. The average temperature in January is 27°C. Temperature in Lagos rarely gets colder than 20°C and rarely gets hotter than 30°C. The month with the highest average low temperature is March (23.8°C). The coldest month (with the lowest average low temperature) is August (21.7°C).

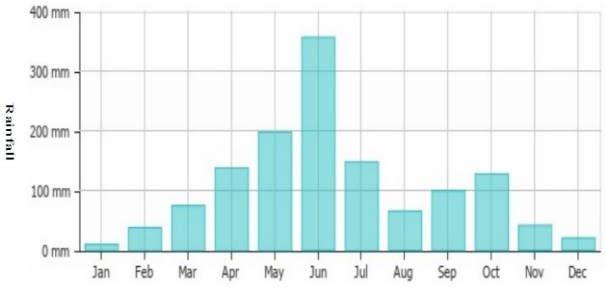

Fig. 2 Average monthly rainfall (mm) in Lagos (source: weather-and-climate.com)

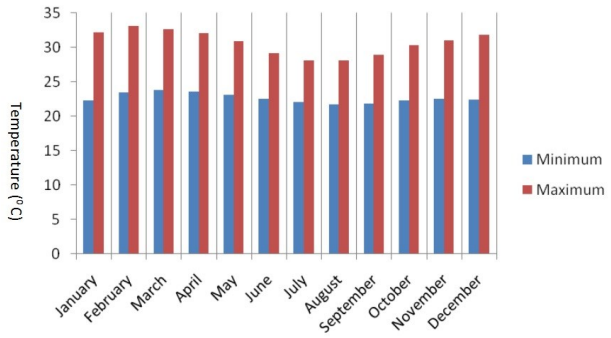

Fig. 3 Lagos average monthly temperature in Lagos (source: weather-and-climate.com)

Fig. 4 Average wind speed (m/s) in Lagos (source: weather-and-Climate.com)

Furthermore, Lagos state is under the influence of the south west trade wind at most times of the year, and this account for its moderate temperature throughout the year. The highest average wind speed recorded was between July and August, which is above 6 m/s (Fig. 4).

METHODS

In this study monthly mean temperature, wind, visibility, cloud cover, thunderstorm, fog, and dust data were used for the period of 2005–2020. These parameters were selected because they were available from ground measurements. The possibilities of these parameters are noticed in reduction of visibility, creation of turbulence, and general poor aircraft performance. The focus was on analysing wind speed and direction (knot), cloud cover (okta), thunderstorm, fog (mm), dust, visibility (mi) as they affect flight delay, cancellation, and diversion in the study area. The monthly data were obtained from the Nigerian Meteorological Agency (NIMET), and monthly flight disruption data on flight diversion, delay and cancellation were collected from Nigerian Civil Aviation Authority (NCAA), Oshodi, Lagos State, Nigeria. Regional Climate Models (RCMs) were used to run climate data projections between year 2020 and 2035 within the study region.

The study employed Statistical Package for Social Sciences (SPSS) software for the descriptive and inferential statistics that include, time series for trend analysis, Pearson Moment Correlation for interrelationship among the weather parameters and the flight disruption data, and multiple linear regression analysis to determine the influence of weather parameters on flight disruption data. The correlation was tested at 5% level of significance with Pearson Product Moment Correlation. The rational for the choice of the statistics is due to the fact that all the weather variables are metric. The OFD is a simple device suitable for the detection of fog and cloud. Calculations show that the OFD responds to visibility reductions by droplets in the size range of 2–20 mm. Fog is large density of small water droplets that are small enough to "float" in the air. The size of fog particles is typically 5–50 μm (0.005–0.05 mm). The dust measuring device PCE-MPC 20 was used to measure the particles in the atmosphere. The measurable particle sizes in the particle collector are 0.3, 2.5 and 10 μm.

RESULTS AND DISCUSSIONS

Relationship among weather parameters in the study area

Table 1 shows the correlation between all studied weather elements in the study area. The results of the analysis indicate that all the tested weather parameters have correlation coefficients that are far from the value of 1.0. However, there is an inverse relationship between highest visibility and visibility, thunderstorm, fog, and wind direction; while direct relationship exists between highest visibility and thick dust, wind speed and cloud cover.
Also, the correlation matrix (Table 1) indicates negative relationship between the highest visibility and thunderstorms, thick dust, fog, cloud cover and wind

Table 1 Correlation matrix of weather parameters in the study area.

Weather parameters	Highest visibility	Visibility	Thunder-storm	Thick dust	Fog	Wind speed	Cloud cover	Wind direction
Highest visibility	1.000							
Visibility	- 0.077	1.000						
Thunderstorm	-0.058	-0.108	1.000					
Thick dust	-0.076	-0.000	-0.031	1.000				
Fog	-0.117	0.016	-0.142	-0.004	1.000			
Wind speed	0.133	0.003	-0.157	0.028	-0.052	1.000		
Cloud cover	-0.029	-0.144	-0.109	0.073	0.027	0.058	1.000	
Wind direction	-0.072	0.085	-0.125	0.122	0.135	0.470	0.095	1.000

direction with -0,077, -0.58, -0.076, -0.117, -0.029 and - 0.072 respectively. This simply explained by the influence of these parameter on visibility. It is worthy to note that dust, wind speed and cloud cover could indicate increased visibility level as an environmental factor in the study area. However, wind speed has positive relationship with recorded highest visibility of the study area. Thunderstorm has negative relationship with highest visibility, visibility, dust, winds, fog and cloud cover. Further, it was established that cloud cover and highest visibility are positively correlated. This shows that the highest visibility experience in the study area depends on the level at which cloud cover is perceived. Wind direction (0.470) has positive relationship with wind speed.

There is negative relationship between thick dust and fog (r=0.00, p>0.05). However, all other weather elements show positive association with thick dust. The association is, also, not significant. There is no relationship between fog (r=0.00, p>0.05) and thick dust, whereas, wind speed (r=0.03, p>0.05), cloud cover (r=0.07, p>0.05), and wind direction (r=0.12, p>0.05) show direct correlation with thick dust but the relationships are not significant.

The relationship between fog and wind speed (r=-0.05, p>0.05) is negative; while cloud cover (r=0.03, P>0.05) and wind speed (r=0.14, p>0.05) show positive relationship with fog, although, the correlation is not significant in any of the cases. Both cloud cover (r=0.06, p>0.05) and wind direction (r=0.5, p<0.05) show positive relationship with wind speed but not significant. There is a significant moderate relationship between wind speed and wind direction. It is evident, that strong vertical wind shear is important to severe thunderstorm development. Wind shear influences a storm in potentially several ways of significant increase of wind speed with height will tilt a storm's updraft, strong upper tropospheric winds evacuates mass from the top of the updraft, directional shear in the lower troposphere helps initiate the development of a rotating updraft, and the shear environment important in determining the thunderstorm type. This relationship could mean that wind speed is propelled by the direction of increased wind pressure. The relationship between cloud cover and wind speed (r=0.01, p>0.05) is positive but weak and not significant.

Impact of weather parameters on flight disruption in the study area

The effect of weather elements on flight operations in the study area was presented in Table 2 with multiple linear regression output. Three approaches were designed to test the impacts of weather elements on flight disruption data. Flight disruptions were measured by numerically capturing number of flight delay, number of flight diversion, and number of flight cancellation over time. Table 2 presents statistics of recorded flight disruption parameters in the study area. It was revealed that flight delay has the mean of 44.06, flight diversion has 22.13, and flight cancellation has 19.19. Considering these calculated means, it is obvious that flight delay is prominent among other parameters of flight disruption in the study area. However, the results of mean on flight diversion and cancellation are not too far apart, which indicates their relevance in air traffic. To this, Rodenhuis (2004) submitted that critical weather phenomenon reduces the operational capacity of regions entire airspace through delays, diversion and flight cancellations.

In Table 3, the multiple linear regression model presents highest visibility, thunderstorm and dust, cloud

Table 2 Recorded annual flight disruptions between 2005 and 2020

Variables	N	Minimum	Maximum	Mean	Std. Deviation
Diversion	16	11.00	40.00	22.1250	8.77021
Delay	16	16.00	70.00	44.0625	17.22196
Cancellation	16	3.00	30.00	19.1875	6.77465

Table 3 Regression analysis of the effect of weather parameters on flight disruption in the study area

	Coefficient	p-value	Beta coefficient
Delay			
Highest Visibility	4.619	0.000	0.511
Visibility	-0.009	0.207	-0.159
Thunderstorm	3.328	0.001	0.434
Thick dust	0.876	0.616	0.051
Fog	-2.755	0.345	-0.118
Wind speed	-1.535	0.323	-0.140
Cloud cover	2.377	0.636	0.053
Wind direction	0.125	0.108	0.183
Constant	-243.132	0.577	
Diversion			
Highest Visibility	-0.067	0.936	-0.016
Visibility	-0.005	0.373	-0.178
Thunderstorm	0.339	0.640	0.093
Thick dust	0.957	0.471	0.125
Fog	-1.711	0.439	-0.154
Wind speed	-0.242	0.837	-0.046
Cloud cover	3.529	0.619	0.089
Wind direction	0.059	0.313	0.181
Constant	-152.595	0.645	
Cancellation			
Highest Visibility	0.567	0.156	0.155
Visibility	-0.001	0.760	-0.033
Thunderstorm	1.709	0.000	0.550
Thick dust	-0.965	0.125	-0.148
Fog	-0.854	0.409	-0.090
Wind speed	2.201	0.000	0.491
Cloud cover	-3.466	0.875	-0.015
Wind direction	0.033	0.223	0.120
Constant	6.774	0.965	

cover and wind direction with positive beta values of 0.511, 0.434, 0.051, 0.053, and 0.183 respectively. This result indicates that climate data (Coeff=4.62, $p<0.05$) and thunderstorm (Coeff=3.33, $p<0.05$) are significant predictor of flight delay relating to diversion indicates cloud cover with (Coeff=3.53, $p<0.05$). The beta coefficient has positive values on high visibility, thunderstorm, tick dust, cloud cover and wind. This indicates that for every 1-unit increase in the weather parameters that were positive, the delay in flight will increase by the beta coefficient values. However, the negative values explained 1-unit reduction by the beta coefficient values.

Further, it was indicated in Table 3 that cloud cover has significant impact on flight diversion. It was also revealed that thunderstorm (Coeff=1.71, $p<0.05$) and wind speed (Coeff=2.20, $p<0.05$) have significant influence on flight cancellation. The thunderstorm has highest beta coefficient being the prominent predictor of flight cancellation. It was observed that the faster the wind speed coupled with high degree of thunderstorm, more flight cancellations are usually recorded. The study of Weli and Ifediba (2014) confirmed that various weather hazards which include thunderstorm, fog, dust haze and line squall affect flight operation such as flight delays, diversion and cancellation. Also, the current study supports the findings of Schaefer and Millner (2001) who opined that weather is the single largest contributor to delays in the efficiency of flight operation. It is becoming the dominant cause of delay in Nigeria. Flights can incur delays while airborne or on the ground, for example, a late arrival of one flight may cause a late departure of the next flight on the itinerary of the aircraft.

Projection of weather parameters from 2005 to 2035

This study revealed how the studied weather parameters have contributed, and will contribute to disruption of aircraft operation between years 2005 and 2019 with projection from 2020 to 2035. The annual mean wind speed and direction, annual average of flight disruptions, horizontal visibility, annual total cloud cover, and annual average of fog, haze and thunderstorm were major parameters under consideration.

The highest visibility occurred as seasonal phenomenon from the year 2006 to the peak of year 2020 (Fig. 5). However, the highest visibility declines sharply with a rise in 2025. It was further observed that the visibility will flatten out beyond year 2025.

Thunderstorm shows a seasonal trend throughout 2005 to 2006 after which it reached its peak in 2020 with sharp upward increase in 2026, 2030 and 2034 (Fig. 6).

The thick dust had a very low abundance in 2005 and ceased to exist shortly after until 2008 when it peaked to its first highest point. It declined to zero level in 2011 till 2015 and peaks upward in 2019 (Fig. 7). This low pattern of thick dust was observed in the same configuration in 2011, 2016 and 2027.

Figure 8 shows that the trend of fog increases in 2015 and 2030 with possible sharp decline in 2035. Trend shows a regular short period of peak for fog. Almost every year is devoid of long period of fog. Fog continued to exist in short period from 2005 to 2013, however, it ceased to exist from 2015 to 2020. The observed trend further indicates visible pattern of fog between 2023 and 2028, which may not have regular trend until 2035.

In Figure 9, the trend of wind speed shows somewhat smooth directional pattern starting at a high level in 2005 and keeps declining gradually in each successive year till 2011. Later in 2013, the trend peaked to reach its highest point with downward trend till 2035.

The trend in Figure 10 shows high degree of cloud cover at the beginning of every year and later declines sharply. However, the trend further shows declining pattern in 2035. Figure 10 further indicates consistent declining pattern of cloud cover in 2035. However, the lowest downward trend would be observed in 2031. Cloud cover shows a seasonal pattern throughout the reviewed period and it is forecast that the trend will continue till 2034.

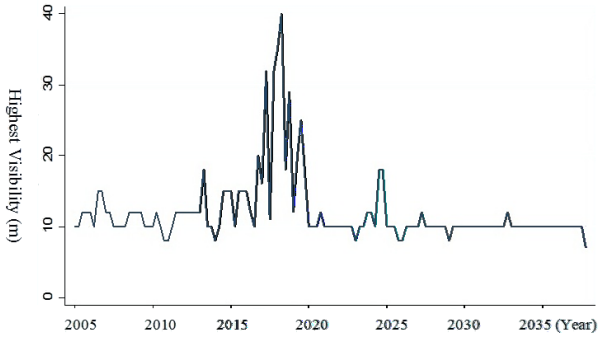

Fig. 5 Projected trend of the highest visibility from 2005 to 2035

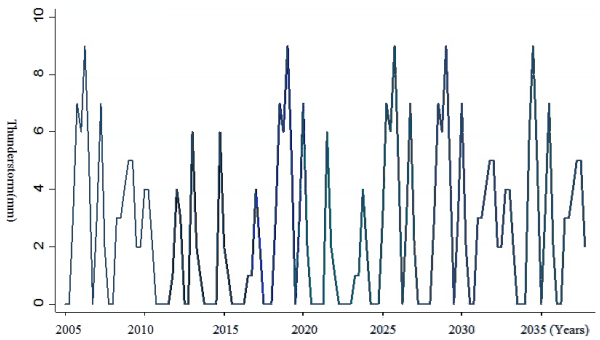

Fig. 6 Projected trend of thunderstorms from 2005 to 2035

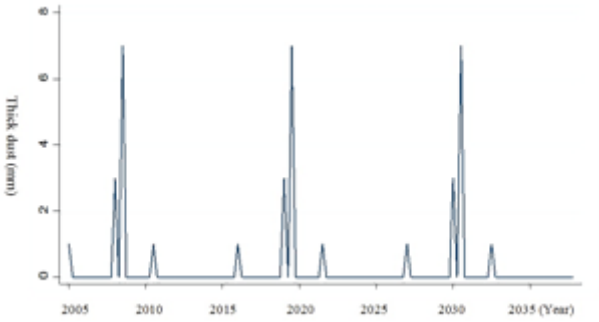

Fig. 7 Projected trend of thick dust from 2005 to 2035

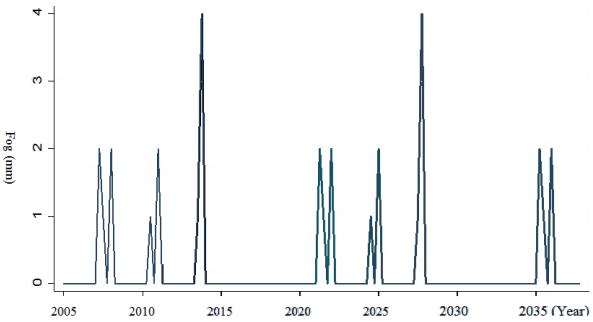

Fig. 8 Projected trend of fog from 2005 to 2035.

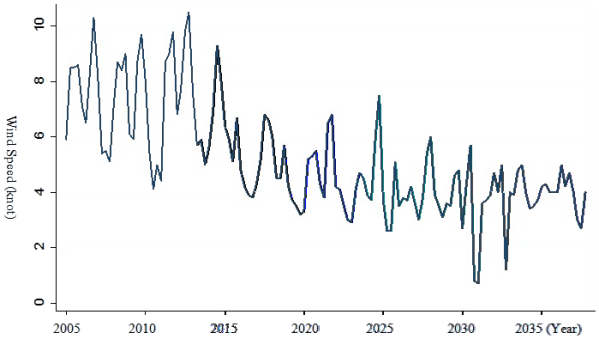

Fig. 9 Projected trend of wind speed from 2005 to 2035

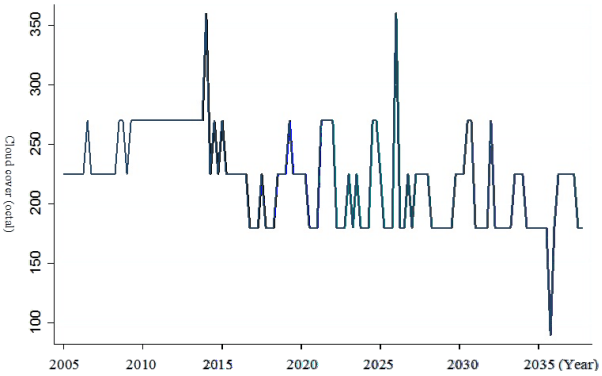

Fig. 10 Projected trend of cloud cover from 2005 to 2035

CONCLUSION

This study has analysed weather parameters along with identified cases of flight disruptions in Nigeria. It was established that cloud cover and highest visibility are negatively correlated. This shows that the highest visibility experienced in the study area depends on the level at which cloud cover is perceived. Wind direction has positive relationship with wind direction. It was established that there is an inverse relationship between visibility, thunderstorm, fog, and wind direction; while direct relationship exists between highest visibility and thick dust, wind speed and cloud cover. It is worth to note that dust, wind speed and cloud cover could indicate increased visibility level as an environmental factor in the study area.

Considering the calculated means for flight disruption parameters, it is obvious that flight delay is prominent over flight diversion and cancellation. However, the results of the mean on flight diversion and cancellation are not too far apart, which indicates their relevance in air traffic. The prediction model indicates; high degree of cloud cover at the beginning of every year and later declines sharply in 2035, regular short period of peak for fog, that the visibility will flatten out by the year 2025, and that low pattern of thick dust was observed in the same pattern in 2011, 2016 and 2027. Based on this conclusion, the study recommends accurate weather reporting and strict compliance to safety regulations, and attention should be paid to changing pattern of weather parameters in order to minimize fight related disaster.

REFERENCES

Arizona-Ogwu, L.C. 2008. Airports for Lease: Is FAAN a Fun? *NigeriaWorld*, March 4th.

Ayoade, J.F. 2004. Introduction to Climatology for the Tropics. Spectrum Books Ltd., Ibadan, XVII. 297 p.

Knecht, W.R. 2008. Use of weather information by general aviation pilots, Part II, Qualitative: Exploring factors involved in weather-related decision making. (Technical Report DOT/FAA/AM08/7). Washington, DC: Federal Aviation Administration, Office of Aerospace Medicine. 1–7.

McFadden, K. L., Hosmane B. S. 2001. Operations safety: an assessment of a commercial aviation safety program. *Journal of Operations Management* 19, 579–591. DOI: 10.1016/S0272-6963(01)00062-6

Mirza, A.K., Page, C., Geinde, S. 2009. An Approach to Flight Safe-Using GML/XML Objects to Define Hazardous Volume Space for Aviation, France. Retrieved September 25, 2020 from Flysafepaper.htm.1–14.

Nwaogbe, O. R., Wokili, H., Omoke, V., Asiegbu, B. 2013. An analysis of the impact of air transport sector to economic development in Nigeria. *IOSR Journal of Business and Management* 14(5), pp. 41–48. DOI: 10.9790/487X-1454148

Pospichal, B., Karam, D.B., Crewell, S., Flamant, C., Hünerbein, A., Bock, O., Saïd, F. 2010. Diurnal cycle of the inter tropical discontinuity over West Africa analysed by remote sensing and mesoscale modelling. *Quarterly Journal of the Royal Meteorological Society*,136(s1), 92–106. DOI: 10.1002/qj.435

Riehl, H. 1965. An Introduction to the Atmosphere (International Student ed.). McGrawHill Book Company Ltd., Tokyo

Rodenhuis, D. 2004. Adverse weather and air traffic delays.11th Conference on Aviation Range and aerospace. Online available at https://ams.confex.com/ams/pdfpapers/81938.pdf

Stringer, E.T. (ed) 1989. Foundations of Climatology. An Introduction to Physical, Dynamic Synoptic and Geographical Climatology. Surjeet Publications, Delhi

Schaefer, L.,Millner, D. 2001. Flight delay propagation analysis with the detailed policy assessment tool. *2001 IEEE International Conference on Systems, Man and Cybernetics. e-Systems and e-Man for Cybernetics in Cyberspace* (Cat.No.01CH37236) 2, 1299-1303. DOI: 10.1109/ICSMC.2001.973100.

Smith, K. 1975. Principle of Applied Climatology. McGraw Hill Company Ltd., UK

Waitz, I., Townsend,J., Cutcher-Gershenfeld,J., Greitzer,E., Kerrebrock, J. 2004. Aviation and the environment: A National Vision Statement, Framework for Goals and Recommended Actions, 55 p.

Weli, V.E., Ifediba, U.E. 2014. Poor Weather Conditions and Flight Operations: Implications for Air Transport Hazard Management in Nigeria. *Ethiopian Journal of Environmental Studies & Management* 7, 235–243. DOI: 10.4314/EJESM.V7I3.2